Understanding anthracycline action: molecular insights to improve cancer therapy

Gelder, M.A. van

Understanding Anthracycline Action

Molecular Insights to Improve Cancer Therapy

Merle Anne van Gelder

Understanding Anthracycline Action:
Molecular Insights to Improve Cancer Therapy

Merle Anne van Gelder

ISBN: 978-94-6510-618-2

Cover Design and Layout: Ilse Radstaat
Print: ProefschriftMaken | Proefschriftmaken.nl

The research described in this thesis was performed at the Department of Cell and Chemical Biology at Leiden University Medical Center in Leiden, the Netherlands.

Understanding Anthracycline Action:

Molecular Insights to Improve Cancer Therapy

Proefschrift

ter verkrijging van

de graad van doctor aan de Universiteit Leiden,

op gezag van rector magnificus prof.dr.ir. H. Bijl,

volgens besluit van het college voor promoties

te verdedigen op woensdag 21 mei 2025

klokke 13.00 uur

door

Merle Anne van Gelder

Promotores
Prof. dr. J.J.C. Neefjes
Prof. dr. H.S. Overkleeft

Copromotor
Dr. S. Y. van der Zanden

Promotie commissie
Prof. dr. M. van der Stelt
Leiden Institute of Chemistry, Leiden

Dr. H. van Ingen
Universiteit Utrecht, Utrecht

Prof. dr. M.J.T.H. Goumans

Prof. dr. C.C.D. van der Rijt
Erasmus MC, Rotterdam

Prof. dr. G.P. van Wezel
Institute of Biology Leiden, Leiden

"No kind action ever stops with itself. One kind action leads to another. Good example is followed. A single act of kindness throws out roots in all directions, and the roots spring up and make new trees. The greatest work that kindness does to others is that it makes them kind themselves."

Amelia Earhart

TABLE OF CONTENTS

CHAPTER 1

Introduction to Anthracycline Biology

Anthracyclines comprise a class of chemotherapeutics that are among the most effective antineoplastic agents currently in clinical use. Daunorubicin (originally named daunomycin) was first discovered as a natural compound produced by *Streptomyces peucitus* in 1960.[1,2] Shortly thereafter, doxorubicin (also known as adriamycin) was isolated from a randomly mutagenized strain of *S. peucitus*.[3] Daunorubicin is highly effective in treating leukemias[4], and doxorubicin exerts even broader anti-cancer activity that extends to lymphomas, sarcomas, and a wide range of solid tumors.[5] Although these anthracyclines were discovered decades ago, they remain among the most potent and widely used anticancer drugs and are therefore a cornerstone of cancer treatment today.

Anthracyclines are composed of a tetracyclic anthraquinone aglycone linked to a sugar moiety by a glycoside bond.[6] Daunorubicin and doxorubicin are the archetypal anthracycline drugs, and due to their remarkable effectivity thousands of analogues have been produced in attempt to discover equally or more effective compounds. Numerous anthracycline analogues have been generated using modified bacterial strains, of which aclarubicin (produced in *S. galilaeus*) is the only variant in current clinical use, although its application is limited to China and Japan.[7] Many other anthracyclines have been produced through semi-synthesis, notably epirubicin[8] and idarubicin[9] which are used

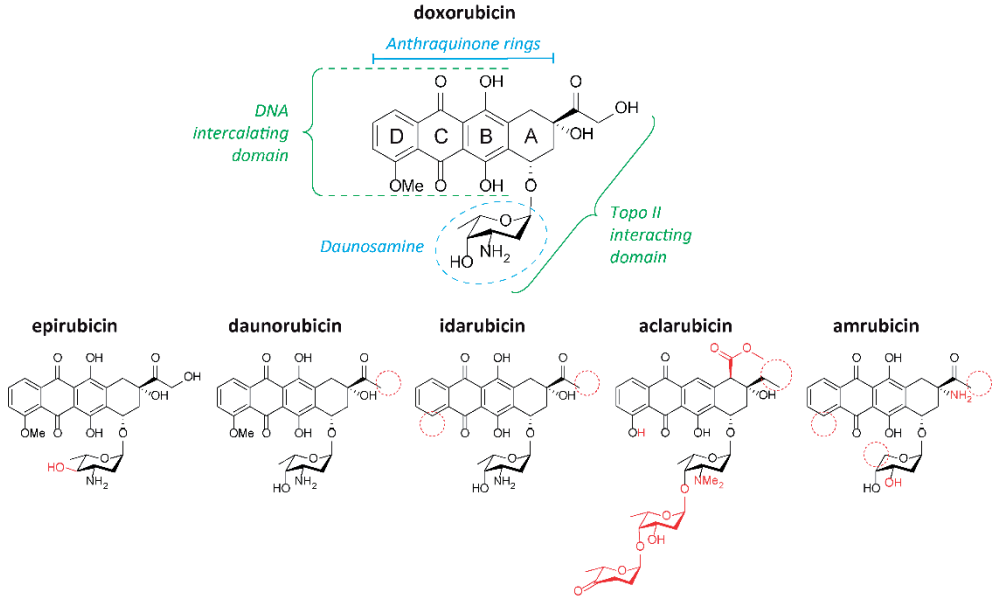

Figure 1 – Chemical structures of doxorubicin and related anthracyclines. The aglycone is numbered in accordance with Brockmann (1963).[6] The daunosamine is circled in blue. Anthracycline domains relevant for binding to DNA and topoisomerase II are indicated in green. Structural differences compared to doxorubicin are indicated in red. This figure is adapted from van der Zanden *et al.*, FEBS Journal (2020).

worldwide. Additionally, the completely synthetic anthracycline amrubicin is used for cancer treatment in Japan[10] (Figure 1).

Molecular mechanisms of action

Of all the anthracycline analogues discovered, synthesized and produced in the past decades, only six variants have made it into clinical practice[11] (Figure 1). One might wonder why we still dedicate research efforts to synthesizing more variants and improving our understanding of anthracycline biology. Interestingly, regardless of the decades of clinical use, new discoveries regarding the molecular mechanisms of these drugs still emerge to date.[12] Not all anthracyclines share the same modes of action, and our understanding of the different effects exerted by these structurally closely related drugs is still incomplete. Although the exact mechanisms through which anthracyclines exert their anti-cancer activity are not fully understood, it is generally accepted that multiple mechanisms and pathways are involved.[13]

Anthracyclines are mostly taken up by cells through passive diffusion, although ATP-dependent transporters can also contribute to drug uptake.[14] Once inside the cell, anthracyclines accumulate in many cellular compartments but most notably exert their cytotoxic effects in the nucleus and mitochondria. Their inherent capability to intercalate into double stranded DNA is at the basis of many modes of action. The anthraquinone aglycon intercalates between DNA base pairs while the sugar moiety is pointed into the DNA minor groove (Figure 1 and Figure 2A). Anthracycline intercalation is not mediated by active processes in the cell but happens because of affinity and occurs in the absence of the cellular context. DNA intercalation inhibits both DNA and RNA synthesis[15,16], thereby altering replication and transcription processes in the cell.

Inhibition of topoisomerase II (Topo II) is the best described molecular mechanism leading to anthracycline-induced cell death.[17] Topo II is an enzyme critical for managing torsional DNA stress and facilitating transcription, replication and repair. It creates transient double-stranded DNA breaks to release tension in the DNA created during replication and subsequently closes the initial break by re-ligating the DNA strands.[18] Most anthracyclines (such as doxorubicin, epirubicin, daunorubicin and idarubicin) intercalate into the DNA and form a stable anthracycline-DNA-Topo II ternary complex (Figure 2B). The enzyme is halted in its catalytic step after inducing the initial DNA breaks, which prevents Topo II from re-ligating the broken DNA strands. This leads to activation of the DNA damage response and p53 pathways. However, when the DNA repair process fails, the accumulation of lesions results in cell cycle arrest and cell death.[19]

Some anthracyclines (like aclarubicin) interrupt the binding of Topo II to DNA, and do not induce DNA double stranded breaks, despite inhibiting the enzymatic activity (Figure 2C).

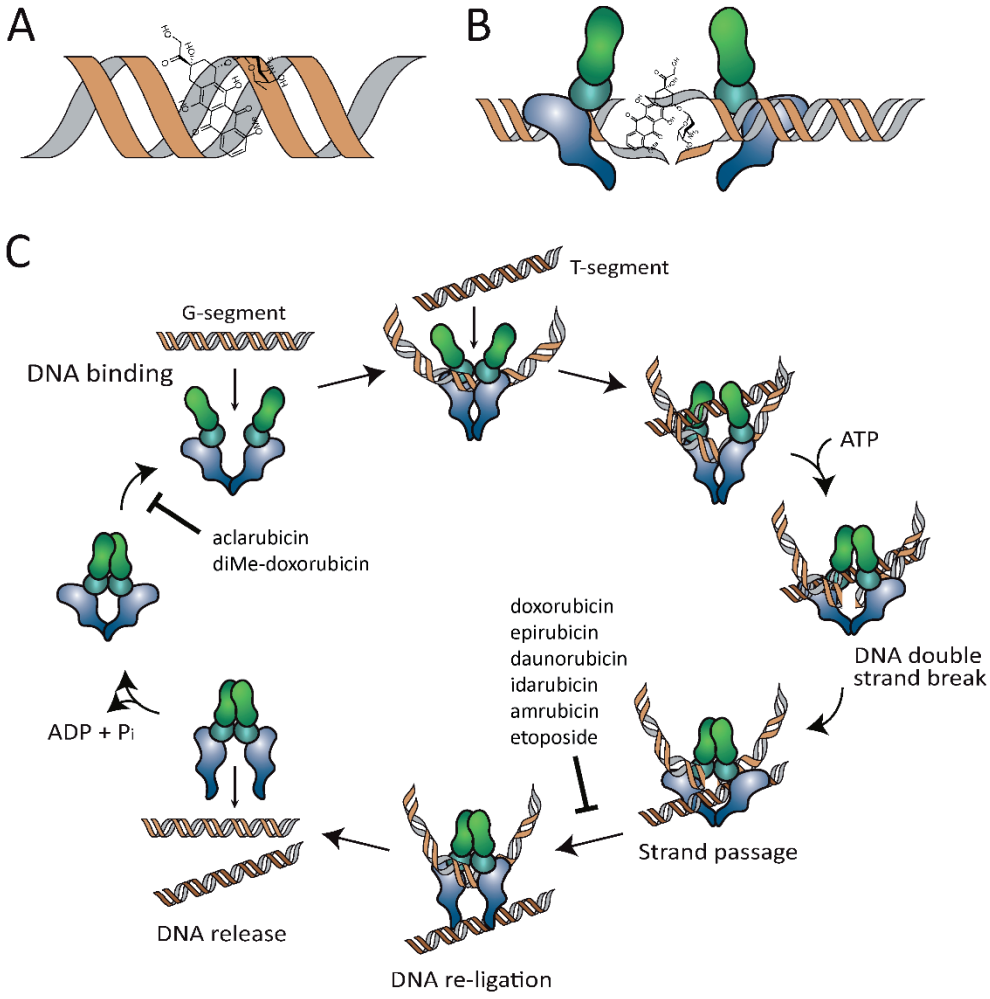

Figure 2- Schematic representation of the Topo II inhibition mechanism of anthracyclines. To release tension and DNA supercoils Topo II binds to the DNA and introduces a transient double strand break in one of the strands (the G-segment), allowing the second strand (the T-segment) to pass through. After religation of the DNA break, Topo II is released from the DNA. Most anthracyclines (doxorubicin, daunorubicin, epirubicin, idarubicin and amrubicin), as well as etoposide (having a chemotype distinct from the anthracyclines), stabilize the Topo II-DNA complex after the induction of double strand breaks and prevent the break from being resealed. The anthracycline variants aclarubicin and dimethyl-doxorubicin inhibit the enzymatic activity of Topo II by preventing its binding to DNA. This figure is adapted from van der Zanden *et al.*, FEBS Journal (2020).

Within the cell's nucleus, DNA is compacted at several levels. Genomic DNA is wrapped tightly around histones and the resulting DNA-protein complex is called chromatin. The repeating structural unit of chromatin is the nucleosome, which contains eight histone proteins.[20] One of the most recently discovered mode of action of anthracyclines involves the disruption of the chromatin structure. When anthracyclines intercalate into DNA the sugar moiety competes for space with histones, causing histones to dissociate from the DNA and nucleosomes to collapse.[21]

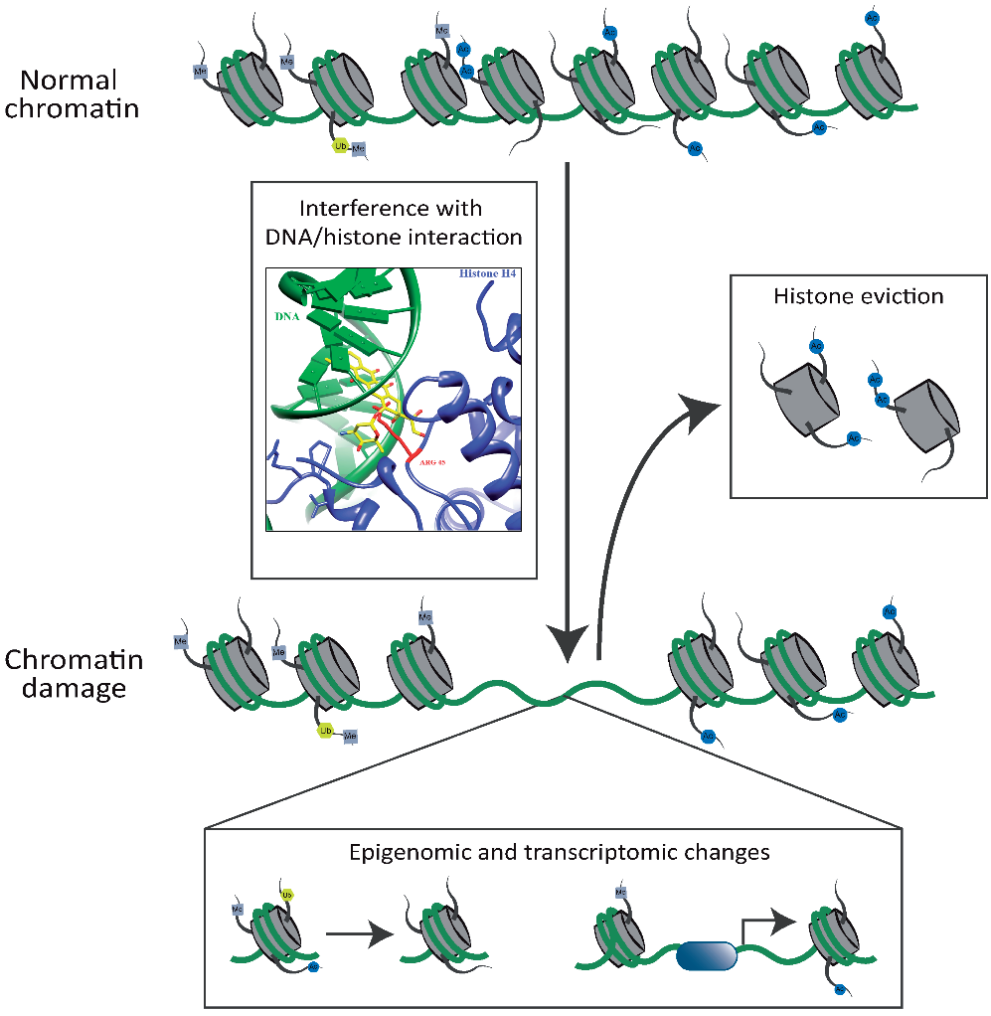

Figure 3 – Schematic representation of chromatin damage induced by doxorubicin. Doxorubicin intercalates into the DNA, where the sugar moiety destabilizes nucleosomes by competing for space with histones. Histone eviction results in epigenetic and transcriptomic alterations and altered DNA damage repair, collectively referred to as chromatin damage. This figure is adapted from van der Zanden *et al.*, FEBS Journal (2020).

This process has been shown to be independent of ATP, suggesting it is a drug-intrinsic action mediated by DNA intercalation of the anthraquinone aglycone and the competition for space between the sugar moiety and histones.[21] Histone eviction is not observed for all anthracycline variants[22–24], but this unique mode of action has only been observed for anthracyclines and one other class of compounds named curaxins.[25] Other DNA intercalating drugs (such as mitoxantrone) or non-intercalating Topo II poisons (for example etoposide) do not induce histone eviction.[26] The disruption of chromatin structures results in delayed DNA damage response and epigenetic and transcriptomic alterations, collectively referred to as chromatin damage (Figure 3). The molecular pathways that lead from histone eviction to programmed cell death are not known, but the capacity to evict histones appears to be a better indicator of the anticancer activity of anthracyclines than their DNA-damaging activity.[22]

The accumulation of anthracyclines in the cells mitochondria directly affects their energy management. Mitochondrial impairment is caused through direct interactions of anthracyclines with respiratory chain complexes and other proteins involved in oxidative phosphorylation[27], as well as through the generation of reactive oxygen species (ROS).[28] Extensive studies have shown that doxorubicin alters the respiratory chain in ways characteristic of chemicals that accept and redirect electrons, known as redox

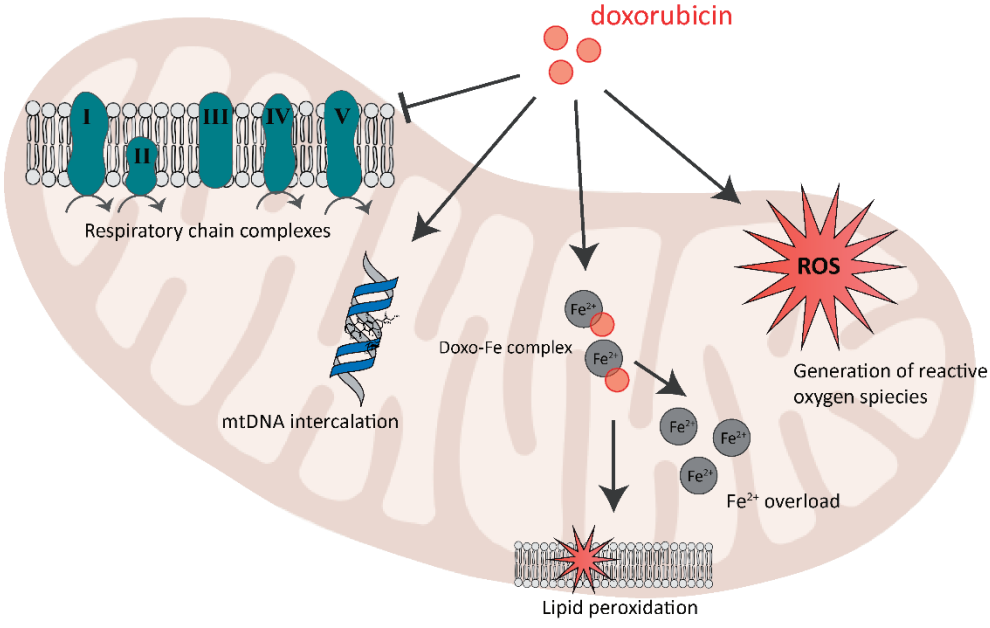

Figure 4 – Schematic representation of the mitochondrial processes that are that are disrupted by doxorubicin. Doxorubicin accumulates in the mitochondria, where it intercalates into mitochondrial DNA, disrupts oxidative phosphorylation and iron homeostasis, and induces an excessive production of reactive oxygen species.

cycling agents. The redox cycling capacity of anthracyclines is a major contributor to ROS generation.[29] Additionally, anthracyclines drive an iron overload in mitochondria which further contributes to excessive ROS production.[30] High levels of ROS can induce lipid peroxidation which results in damage to membranes and cellular structures, ultimately leading to cellular stress and apoptosis.[31] Another mechanism through which anthracyclines can induce mitochondrial damage is again linked to the inherent capacity to intercalate into DNA. Within the mitochondria the intercalation of anthracyclines leads to the formation of 8-hydroxydeoxyguanosine (8OHdG) adducts[32] (Figure 4). Similarly to genomic DNA lesions, these adducts affect the transcription and translation of mitochondrial genes. Lastly, mitochondrial dynamics are altered in response to anthracyclines, which are disrupting the balance between mitochondrial fusion and fission events.[33] This imbalance can lead to mitochondrial fragmentation and eventual cell death.

Side effects and toxicities

Tumor cells typically exhibit altered cellular features which make them distinct from healthy cells.[34] Some of these features contribute to anthracycline selectivity towards tumor cells, such as increased metabolism and rapid cell division. Anthracycline toxicity is however not limited to tumor cells, and the severe side effects that accompany anthracycline treatment can be both life threatening and treatment limiting. The difference in relative toxicity toward tumor cells versus healthy cells creates a therapeutic window, allowing for doses that effectively kill tumor cells while remaining within acceptable toxicity levels for normal cells. Still, anthracycline treatment is associated with various toxicities affecting normal cells. Anthracycline treatment induced-side effects include acute and reversible issues such as nausea, alopecia and leukopenia and long-term side effects such as cardiotoxicity, gonadotoxicity and therapy-related tumorigenesis. Overall, anthracycline treatment has a significant impact on patients' quality of life, and the associated adverse events restrict the clinical use of anthracyclines. The emergence of side effects is difficult to predict for individual patients and depends on multiple variables such as chemotherapeutic dose, the number of treatment cycles and individual risk factors.

Anthracycline-induced cardiotoxicity is one of the most severe side effects, encompassing a wide array of symptoms including contractile dysfunction, ventricular dysfunction, cardiomyopathy, arrythmias and heart failure.[35] Currently, no treatment exists for anthracycline-induced cardiotoxicity, leading to the exclusion of patients at higher risk such as the elderly or those with existing cardiac issues. The onset of anthracycline-induced cardiotoxicity is dose-dependent, irreversible and may occur early or late during

treatment. Although it is one of the best-studied side effects of anthracycline treatment, the underlying molecular mechanisms remain incompletely understood. They are likely to overlap with those underlying toxicity towards tumor cells, such as DNA intercalation, Topo II inhibition, and disruption of the respiratory chain and mitochondrial function. Previous studies have demonstrated that the combination of DNA damage and chromatin damage, as exerted by doxorubicin, may drive its cardiotoxicity.[26] Clinical observations reveal that aclarubicin, which only induces chromatin damage, is less cardiotoxic for cancer patients than doxorubicin treatment.[36,37] Specific characteristics of heart tissue may also increase its sensitivity for anthracycline-induced toxicity compared to other tissues. Due to their high energy demands, cardiac cells contain a large number of mitochondria and have a high respiratory rate. Previous studies suggest that the effects of anthracyclines on cardiac mitochondrial function may underlie cardiac dysfunction. Various strategies have been attempted to manage anthracycline-induced cardiotoxicity, including counteracting excessive levels of ROS[38], novel delivery methods[39,40] and the synthesis of less cardiotoxic anthracycline variants.[26,41]

Another drawback of anthracycline treatment resides in the toxicity towards rapidly dividing normal cells, such as those found in gonadal tissues. Damage to gonadal tissue can lead to a shortened reproductive lifespan and infertility, which are associated with significant psychosocial stress. For patients of reproductive age, fertility preservation can be achieved by cryopreserving gametes or embryos before anthracycline treatment.[42] However, this method is not applicable for prepubescent patients, even though doxorubicin treatment during childhood is known to affect adult fertility.[43] Several compounds have been proposed to be combined with anthracycline treatment to limit gonadotoxicity, including hormone agonists[44], antioxidants[45,46], proteasome inhibitors[47] and DNA damage repair inhibitors.[48] However, no clinical studies have yet validated the effects of these combination treatments on gonadal function and anthracycline efficacy. A preferable approach would be to develop anthracyclines that are less toxic to normal cells while retaining their antitumor effectivity. Previous studies have indicated that gonadotoxicity is largely attributable to the anthracycline-induced generation of DNA double-strand breaks.[48–53] Therefore, the development of anthracyclines with reduced DNA-damaging activity could offer more tolerable treatment options.

Among all long-term side effects, anthracycline-dependent tumorigenesis is considered one of the most detrimental due to the associated morbidity and mortality. Currently, 17-19% of all newly diagnosed primary tumors occur in cancer survivors.[54] Anthracycline treatment can cause transformation and mutagenesis in healthy cells[55], increasing the risk of secondary tumor formation. The susceptibility of cancer survivors to develop therapy-related malignancies depends on various risk factors, including genetic predisposition, carcinogenic exposures (such as tobacco and alcohol use), host effects

(like age, gender, immunodeficiency or obesity), and combination therapies with other mutagenic chemotherapeutics (such as alkylating agents, etoposide, or radiotherapy).[56–59] Consequently, the exact molecular mechanisms through which anthracyclines contribute to the development of therapy-related malignancies remain unclear. However, previous studies suggest that the generation of DNA double-strand breaks by anthracyclines may significantly contribute to the development of these malignancies. A better understanding of the structure-activity relationship of anthracyclines is required to eliminate their DNA-damaging activity and possibly prevent associated toxicities.

Resistance to anthracycline treatment

Resistance to chemotherapeutics poses a critical barrier to treatment and is one of the leading causes of chemotherapy failure. Several mechanisms contribute to anthracyclines resistance, and not all are fully understood. One key mechanism is mediated by ATP-binding cassette (ABC) transporters. These membrane transporters are responsible for the efflux of a wide range of chemotherapeutics across the plasma membrane, leading to decreased intracellular drug levels and treatment resistance.[60] ABCB1 is the best studied ABC transporter in the context of anthracycline resistance, and all anthracycline variants currently in clinical use are known substrates for ABCB1.[61] Numerous studies have observed increased ABCB1 expression in tumor cells in response to anthracycline chemotherapy, and correlations between ABCB1 expression levels, drug resistance, and poor prognosis have been reported for many tumor types.[62] Significant research efforts have focused on blocking ABC transporters with small molecule inhibitors to enhance chemotherapy efficacy.[63] However, none have made it to clinical practice due to off-target toxicities.[64] A more straightforward approach may be the development of anthracyclines which are not transported by ABC-transporters, but despite previous efforts such anthracyclines have not made it into clinical practice either.

The results of research on other cellular mechanisms regulating anthracycline resistance are more ambiguous. Early research suggested that Topo II expression might play an important role in anthracycline resistance, but the correlation between anthracycline sensitivity and Topo II expression is supported by conflicting evidence. Since the most widely used anthracyclines (doxorubicin, daunorubicin, epirubicin and idarubicin) induce DNA damage, it has been proposed that regulators and effectors of the DNA damage response may also be involved in anthracycline resistance. Genome-wide screening for factors driving resistance to doxorubicin revealed not only the expected involvement of ABCB1, but also multiple proteins associated with the DNA damage response.[65] Alterations in the expression and activity of DNA damage response regulators may alter the pathways leading to cell death, allowing tumor cells to continue proliferating. There

may be potential value in combining inhibitors of DNA damage repair kinases with anthracycline treatment.[66] But to date, such combinations have only been tested in pre-clinical settings and the development of anthracycline variants that do not cause DNA damage could potentially bypass the resistance mechanisms related to the DNA damage response altogether.

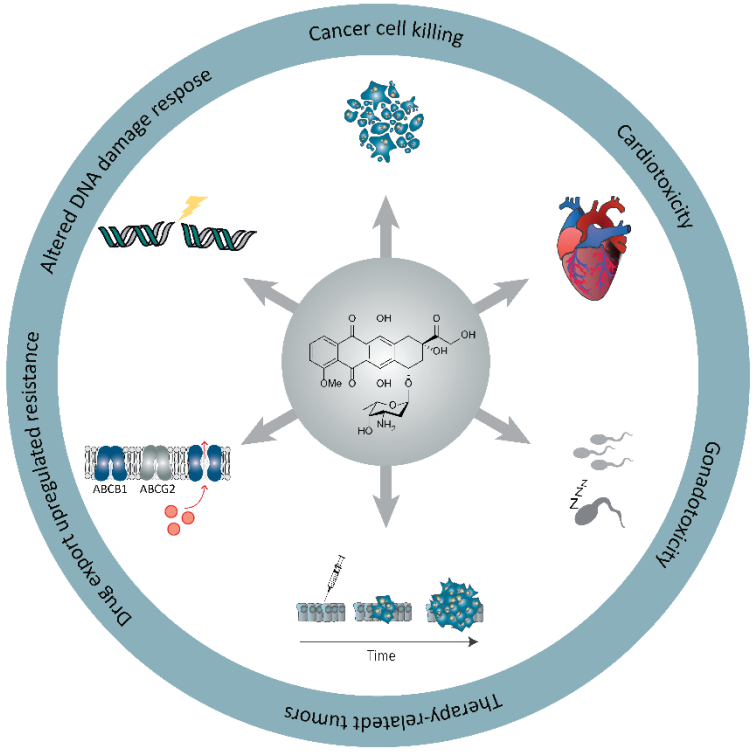

Figure 5 – Schematic overview of the different activities and toxicities of doxorubicin. The different activities and toxicities play a crucial role in identifying future limitations and opportunities of anthracycline development.

From past achievements to new developments

Anthracyclines have been in clinical use for decades, and their effectiveness against many tumor types has outweighed their limitations. However, it remains crucial to address these limitations because of significant impact on the quality of life for cancer patients. The use of anthracyclines is hindered by severe side effects and toxicities that occur during or after treatment. Additionally, the development of resistance poses a major

barrier to successful anthracycline treatment (Figure 5). Various approaches have been explored to improve the efficacy and reduce the toxicity of anthracyclines, but none have established a permanent position in cancer treatment.

In this thesis, we focus on one strategy to improve the efficacy of anthracyclines and overcome resistance. We report the design, synthesis and biological evaluation of structural variations of the archetypical anthracyclines (doxorubicin, daunorubicin, epirubicin, idarubicin and aclarubicin). The aim of this work is to gain a better understanding of the structure-activity relationships of anthracyclines, with the ultimate goals of identifying anthracycline variants that may elicit fewer adverse events and circumvent the molecular mechanisms underlying drug resistance.

In **chapter 2**, we demonstrate that different anthracycline variants have distinct molecular mechanisms. In this extensive structure-activity relationship study we show that small chemical modifications can significantly impact the cytotoxicity and biological activities of these drugs. In addition, we determined the ability of novel anthracycline variants to induce both DNA- and chromatin damage. To gain a better understanding of the molecular pathways leading to chromatin damage-induced cell death, we performed a genome-wide CRISPR screen in **chapter 3**. Here, we identified p53 as an important regulator of cell death in response to aclarubicin. We show that aclarubicin activates a p53-dependent transcriptional program that leads to apoptosis, like traditional DNA-damaging anthracyclines, but in the absence of DNA lesions. In **chapter 4**, we identified several anthracycline variants that are still effective in drug transporter overexpressing, doxorubicin-resistant cells. These variants exhibit improved cytotoxicity and enhanced nuclear localization compared to their clinically used counterparts, while retaining their canonical anthracycline functions of DNA intercalation and Topo II targeting. In **chapter 5**, we further explored anthracycline function by comparing the effects of different anthracycline variants on mitochondrial DNA intercalation, transcription and translation. Finally, we present some directions for future research regarding the development of effective but less toxic anthracycline variants.

In conclusion, the extensive structure-activity relationship studies on novel anthracycline variants presented in this thesis enhance our understanding of the molecular mechanisms involved in anthracycline activity and resistance and may aid in the development of more effective and more tolerable anthracyclines in the future.

References

(1) Camerino B; Palamidessi G. Derivati Della Parazina II. Sulfonamdopir (in Italian). *Gazz Chim Ital*. **1960**, *90*.

(2) di Marco, A.; Cassinelli, G.; Arcamone. The Discovery of Daunorubicin. *Cancer Treatment Reports*. **1981**, *65*.

(3) Arcamone, F.; Cassinelli, G.; Fantini, G.; Grein, A.; Orezzi, P.; Pol, C.; Spalla, C. Adriamycin, 14-Hydroxydaunomycin, a New Antitumor Antibiotic from S. Peucetius Var. Caesius. *Biotechnology and bioengineering*. **1969**, *11*, 1101–1110.

(4) Tan, C.; Tasaka, H.; Yu, K.-P.; Murphy, M. L.; Karnofsky, D. A. Daunomycin, an Antitumor Antibiotic, in the Treatment of Neoplastic Disease. Clinical Evaluation with Special Reference to Childhood Leukemia. *Cancer*. **1967**, *20*.

(5) Weiss, R. B.; Sarosy, G.; Clagett-Carr, K.; Russo, M.; Leyland-Jones, B. Anthracycline Analogs The Past, Present, and Future. *Cancer Chemotherapy and Pharmacology*. **1986**, *18*, 185–197.

(6) Brockmann, H. Anthracyclinones and Anthracyclines. (Rhodomycinone, Pyrromycinone and Their Glycosides). *Fortschritte der Chemie organischer Naturstoffe*. **1963**, *21*.

(7) Oki, T.; Matsuzawa, Y.; Yoshimoto, A.; Numata, K.; Kitamura, I.; Umezawa, H.; Ishizuka, M.; Naganawa, H.; Suda, H.; Hamada, M.; Takeuchi, T. New Antitumor Antibiotics Aclacinomycins A and B. *The Journal of Antibiotics*. **1975**, *28*, 830–834.

(8) Bonfante, V.; Bonadonna, G.; Villani, F.; Martini, A. Preliminary Clinical Experience with 4-Epidoxorubicin in Advanced Human Neoplasia. *Recent results in cancer research. Fortschritte der Krebsforschung. Progres dans les recherches sur le cancer*. **1980**, *74*, 192–199.

(9) Umezawa, H.; Kinoshita, M.; Takahashi, Y.; Tatsuta, K.; Naganawa, H.; Takeuchi, T. Synthesis of 4-Demethoxy-11-Deoxy-Analogs of Daunomycin and Adriamycin. *The Journal of antibiotics*. **1980**, *33*, 1581–1585.

(10) Kurata, T.; Okamoto, I.; Tamura, K.; Fukuoka, M. Amrubicin for Non-Small-Cell Lung Cancer and Small-Cell Lung Cancer. *Investigational New Drugs*. **2007**, *25*, 499–504.

(11) Weiss, R. B. The Anthracyclines: Will We Ever Find a Better Doxorubicin? *Seminars in oncology*. **1992**, *19*, 670–686.

(12) van der Zanden, S. Y.; Qiao, X.; Neefjes, J. New Insights into the Activities and Toxicities of the Old Anticancer Drug Doxorubicin. *FEBS Journal*. **2021**, *288*, 6095–6111.

(13) Mattioli, R.; Ilari, A.; Colotti, B.; Mosca, L.; Fazi, F.; Colotti, G. Doxorubicin and Other Anthracyclines in Cancers: Activity, Chemoresistance and Its Overcoming. *Molecular Aspects of Medicine*. **2023**, *93*, 101205.

(14) Karim, H.; Bogason, A.; Bhuiyan, H.; Fotoohi, A.; Lafolie, P.; Vitols, S. Comparison of Uptake Mechanisms for Anthracyclines in Human Leukemic Cells. *Current drug delivery*. **2013**, *10*, 404–412.

(15) Munger, C.; Ellis, A.; Woods, K.; Randolph, J.; Yanovich, S.; Gewirtz, D. Evidence for Inhibition of Growth Related to Compromised DNA Synthesis in the Interaction of Daunorubicin with H-35 Rat Hepatoma. *Cancer research*. **1988**, *48*, 2404–2411.

(16) Di Marco, A.; Silvestrini, R.; Di Marco, S.; Dasdia, T. Inhibiting Effect of the New Cytotoxic Antibiotic Daunomycin on Nucleic Acids and Mitotic Activity of HeLa Cells. *The Journal of cell biology*. **1965**, *27*, 545–550.

(17) Tewey, K. M.; Rowe, T. C.; Yang, L.; Halligan, B. D.; Liu, L. F. Adriamycin-Induced DNA Damage Mediated by Mammalian DNA Topoisomerase II. *Science (New York, N.Y.)*. **1984**, *226*, 466–468.

(18) Nitiss, J. L. DNA Topoisomerase II and Its Growing Repertoire of Biological Functions. *Nature reviews. Cancer*. **2009**, *9*, 327–337.

(19) Perego, P.; Corna, E.; De Cesare, M.; Gatti, L.; Polizzi, D.; Pratesi, G.; Supino, R.; Zunino, F. Role of Apoptosis and Apoptosis-Related Genes in Cellular Response and Antitumor Efficacy of Anthracyclines. *Current medicinal chemistry*. **2001**, *8*, 31–37.

(20) Alberts, B.; Johnson, A.; Lewis, J.; Raff, M.; Roberts, K.; Walter, P. Chromosomal DNA and Its Packaging in the Chromatin Fiber. **2002**.

(21) Pang, B.; Qiao, X.; Janssen, L.; Velds, A.; Groothuis, T.; Kerkhoven, R.; Nieuwland, M.; Ovaa, H.; Rottenberg, S.; Van Tellingen, O.; Janssen, J.; Huijgens, P.; Zwart, W.; Neefjes, J. Drug-Induced Histone Eviction from Open Chromatin Contributes to the Chemotherapeutic Effects of Doxorubicin. *Nature Communications 2013 4:1*. **2013**, *4*, 1–13.

(22) van Gelder, M. A.; van der Zanden, S. Y.; Vriends, M. B. L.; Wagensveld, R. A.; van der Marel, G. A.; Codée, J. D. C.; Overkleeft, H. S.; Wander, D. P. A.; Neefjes, J. J. C. Re-Exploring the Anthracycline Chemical Space for Better Anti-Cancer Compounds. *Journal of Medicinal Chemistry*. **2023**, *66*, 11390–11398.

(23) Wander, D. P. A.; Van Der Zanden, S. Y.; Van Der Marel, G. A.; Overkleeft, H. S.; Neefjes, J.; Codée, J. D. C. Doxorubicin and Aclarubicin: Shuffling Anthracycline Glycans for Improved Anticancer Agents. *Journal of Medicinal Chemistry*. **2020**, *63*, 12814–12829.

(24) Wander, D. P. A.; van der Zanden, S. Y.; Vriends, M. B. L.; van Veen, B. C.; Vlaming, J. G. C.; Bruyning, T.; Hansen, T.; van der Marel, G. A.; Overkleeft, H. S.; Neefjes, J. J. C.; Codée, J. D. C. Synthetic (N , N -Dimethyl)Doxorubicin Glycosyl Diastereomers to Dissect Modes of Action of Anthracycline Anticancer Drugs. *The Journal of Organic Chemistry*. **2021**, *86*, 5757–5770.

(25) Nesher, E.; Safina, A.; Aljahdali, I.; Portwood, S.; Wang, E. S.; Koman, I.; Wang, J.; Gurova, K. V. Role of Chromatin Damage and Chromatin Trapping of FACT in Mediating the Anticancer Cytotoxicity of DNA-Binding Small Molecule Drugs. *Cancer research*. **2018**, *78*, 1431.

(26) Qiao, X.; Van Der Zanden, S. Y.; Wander, D. P. A.; Borràs, D. M.; Song, J. Y.; Li, X.; Duikeren, S. Van; Gils, N. Van; Rutten, A.; Herwaarden, T. Van; Tellingen, O. Van; Giacomelli, E.; Bellin, M.; Orlova, V.; Tertoolen, L. G. J.; Gerhardt, S.; Akkermans, J. J.; Bakker, J. M.; Zuur, C. L.; Pang, B.; Smits, A. M.; Mummery, C. L.; Smit, L.; Arens, R.; Li, J.; Overkleeft, H. S.; Neefj, J. Uncoupling DNA Damage from Chromatin Damage to Detoxify Doxorubicin. *Proceedings of the National Academy of Sciences of the United States of America*. **2020**, *117*, 15182–15192.

(27) Tokarska-Schlattner, M.; Zaugg, M.; Zuppinger, C.; Wallimann, T.; Schlattner, U. New Insights into Doxorubicin-Induced Cardiotoxicity: The Critical Role of Cellular Energetics. *Journal of molecular and cellular cardiology*. **2006**, *41*, 389–405.

(28) Keizer, H. G.; Pinedo, H. M.; Schuurhuis, G. J.; Joenje, H. Doxorubicin (Adriamycin): A Critical Review of Free Radical-Dependent Mechanisms of Cytotoxicity. *Pharmacology & therapeutics*. **1990**, *47*, 219–231.

(29) Davies, K.; Chemistry, J. Redox Cycling of Anthracyclines by Cardiac Mitochondria. I. Anthracycline Radical Formation by NADH Dehydrogenase. *Journal of Biological Chemistry*. **1986**, *261*, 3060–3067.

(30) Xu, X.; Persson, H. L.; Richardson, D. R. Molecular Pharmacology of the Interaction of Anthracyclines with Iron. *Molecular pharmacology*. **2005**, *68*, 261–271.

(31) Li, H.; Wang, M.; Huang, Y. Anthracycline-Induced Cardiotoxicity: An Overview from Cellular Structural Perspective. *Biomedicine & Pharmacotherapy*. **2024**, *179*, 117312.

(32) Serrano, J.; Palmeira, C.; Kuehl, D.; Wallace, K. Cardioselective and Cumulative Oxidation of Mitochondrial DNA Following Subchronic Doxorubicin Administration. *Biochimica et Biophysica Acta*. **1999**, *1411*.

(33) Dirks-Naylor, A. J.; Kouzi, S. A.; Bero, J. D.; Phan, D. T.; Taylor, H. N.; Whitt, S. D.; Mabolo, R. Doxorubicin Alters the Mitochondrial Dynamics Machinery and Mitophagy in the Liver of Treated Animals. *Fundamental and Clinical Pharmacology*. **2014**, *28*, 633–642.

(34) Hanahan, D.; Weinberg, R. Hallmarks of Cancer: The next Generation. *Cell*. **2011**, *144*, 646–674.

(35) Qiu, Y.; Jiang, P.; Huang, Y. Anthracycline-Induced Cardiotoxicity: Mechanisms, Monitoring, and Prevention. *Frontiers in cardiovascular medicine*. **2023**, *10*.

(36) Rothig, H. J.; Kraemer, H. P.; Sedlacek, H. H. Aclarubicin: Experimental and Clinical Experience. *Drugs under experimental and clinical research*. **1985**, *11*, 123–125.

(37) Mortensen, S. A. Aclarubicin: Preclinical and Clinical Data Suggesting Less Chronic Cardiotoxicity Compared with Conventional Anthracyclines. *European Journal of Haematology*. **1987**, *38*, 21–31.

(38) Legha, S.; Wang, Y.; Mackay, B.; Ewer, M.; Hortobagyi, G.; Benjamin, R.; Ali, M. Clinical and Pharmacologic Investigation of the Effects of Alpha-Tocopherol on Adriamycin Cardiotoxicity. *Annals of the New York Academy of Sciences*. **1982**, *393*.

(39) Harris, L.; Batist, G.; Belt, R.; Rovira, D.; Navari, R.; Azarnia, N.; Welles, L.; Winer, E.; Garrett, T.; Blayney, D.; Elias, L.; Mortimer, J.; Needles, B.; Webb, T.; Atiba, J.; Bickers, J.; Godfrey, T.; Love, R.; Osborn, D.; Aisner, J.; Anderson, T.; Butler, D.; Calabresi, P.; Feldman, L.; Kerr, R.; Nevinny, H.; Reynolds, C.; Schneider, A.; Tweedy, C.; Whaley, W.; Demattia, M.; Harper, G.; Moroose, R.; Staszewski, H.; Begas, A.; Dutcher, J.; Ellis, R.; Fleming, G.; Garcia, M.; Granick, J.; Kloss, J.; Roberts, M.; Sanchez, F.; Silver, R.; Taylor, H. Liposome-Encapsulated Doxorubicin Compared with Conventional Doxorubicin in a Randomized Multicenter Trial as First-Line Therapy of Metastatic Breast Carcinoma. *Cancer*. **2002**, *94*, 25–36.

(40) Batist, G.; Ramakrishnan, G.; Rao, C. S.; Chandrasekharan, A.; Gutheil, J.; Guthrie, T.; Shah, P.; Khojasteh, A.; Nair, M. K.; Hoelzer, K.; Tkaczuk, K.; Youn Choi Park; Lee, L. W. Reduced Cardiotoxicity and Preserved Antitumor Efficacy of Liposome-Encapsulated Doxorubicin and Cyclophosphamide Compared with Conventional Doxorubicin and Cyclophosphamide in a Randomized, Multicenter Trial of Metastatic Breast Cancer. *Journal of Clinical Oncology*. **2001**, *19*, 1444–1454.

(41) Dempke, W. C. M.; Zielinski, R.; Winkler, C.; Silberman, S.; Reuther, S.; Priebe, W. Anthracycline-Induced Cardiotoxicity — Are We about to Clear This Hurdle? *European Journal of Cancer*. **2023**, *185*, 94–104.

(42) Anderson, R. A.; Mitchell, R. T.; Kelsey, T. W.; Spears, N.; Telfer, E. E.; Wallace, W. H. B. Cancer Treatment and Gonadal Function: Experimental and Established Strategies for Fertility Preservation in Children and Young Adults. *The Lancet Diabetes and Endocrinology*. **2015**, *3*, 556–567.

(43) Brilhante, O.; Stumpp, T.; Miraglia, S. Long-Term Testicular Toxicity Caused by Doxorubicin Treatment during Pre-Pubertal Phase. *Int J Med Sci*. **2011**, *3*.

(44) Endo, F.; Manabe, F.; Takeshima, H.; Akaza, H. Protecting Spermatogonia from Apoptosis Induced by Doxorubicin Using the Luteinizing Hormone-Releasing Hormone Analog Leuprorelin. *International Journal of Urology*. **2003**, *10*, 72–77.

(45) Kropp, J.; Roti Roti, E. C.; Ringelstetter, A.; Khatib, H.; Abbott, D. H.; Salih, S. M. Dexrazoxane Diminishes Doxorubicin-Induced Acute Ovarian Damage and Preserves Ovarian Function and Fecundity in Mice. *PloS one*. **2015**, *10*.

(46) Levi, M.; Tzabari, M.; Savion, N.; Stemmer, S. M.; Shalgi, R.; Ben-Aharon, I. Dexrazoxane Exacerbates Doxorubicin-Induced Testicular Toxicity. *Reproduction (Cambridge, England)*. **2015**, *150*, 357–366.

(47) Roti Roti, E. C.; Ringelstetter, A. K.; Kropp, J.; Abbott, D. H.; Salih, S. M. Bortezomib Prevents Acute Doxorubicin Ovarian Insult and Follicle Demise, Improving the Fertility Window and Pup Birth Weight in Mice. *PloS one*. **2014**, *9*.

(48) Tuppi, M.; Kehrloesser, S.; Coutandin, D. W.; Rossi, V.; Luh, L. M.; Strubel, A.; Hötte, K.; Hoffmeister, M.; Schäfer, B.; De Oliveira, T.; Greten, F.; Stelzer, E. H. K.; Knapp, S.; De Felici, M.; Behrends, C.; Klinger, F. G.; Dötsch, V. Oocyte DNA Damage Quality Control Requires Consecutive Interplay of CHK2 and CK1 to Activate P63. *Nature structural & molecular biology*. **2018**, *25*, 261–269.

(49) Smart, E.; Lopes, F.; Rice, S.; Nagy, B.; Anderson, R. A.; Mitchell, R. T.; Spears, N. Chemotherapy Drugs Cyclophosphamide, Cisplatin and Doxorubicin Induce Germ Cell Loss in an in Vitro Model of the Prepubertal Testis. *Scientific Reports 2018 8:1*. **2018**, *8*, 1–15.

(50) Mohan, U. P.; Tirupathi Pichiah, P. B.; Iqbal, S. T. A.; Arunachalam, S. Mechanisms of Doxorubicin-Mediated Reproductive Toxicity – A Review. *Reproductive Toxicology*. **2021**, *102*, 80–89.

(51) Roti Roti, E. C.; Leisman, S. K.; Abbott, D. H.; Salih, S. M. Acute Doxorubicin Insult in the Mouse Ovary Is Cell- and Follicle-Type Dependent. *PloS one*. **2012**, *7*.

(52) Perez, G. I.; Knudson, C. M.; Leykin, L.; Korsmeyer, S. J.; Tilly, J. L. Apoptosis-Associated Signaling Pathways Are Required for Chemotherapy-Mediated Female Germ Cell Destruction. *Nature medicine*. **1997**, *3*, 1228–1232.

(53) Ben-Aharon, I.; Bar-Joseph, H.; Tzarfaty, G.; Kuchinsky, L.; Rizel, S.; Stemmer, S. M.; Shalgi, R. Doxorubicin-Induced Ovarian Toxicity. *Reproductive biology and endocrinology : RB&E*. **2010**, *8*.

(54) Travis, L. B.; Wahnefried, W. D.; Allan, J. M.; Wood, M. E.; Ng, A. K. Aetiology, Genetics and Prevention of Secondary Neoplasms in Adult Cancer Survivors. *Nature Reviews Clinical Oncology*. **2013**, *10*, 289–301.

(55) Marquardt, H.; Philips, F.; Sternberg, S. Tumorigenicity in Vivo and Induction of Malignant Transformation and Mutagenesis in Cell Cultures by Adriamycin and Daunomycin. *Cancer Research*. **1976**, *36*.

(56) Teepen, J. C.; Kremer, L. C. M.; Ronckers, C. M.; Van Leeuwen, F. E.; Hauptmann, M.; Van Dulmen-Den Broeder, E.; Van Der Pal, H. J.; Jaspers, M. W. M.; Tissing, W. J.; Van Den Heuvel-Eibrink, M. M.; Loonen, J. J.; Bresters, D.; Versluys, B.; Visser, O.; Neggers, S. J. C. M. M.; Van Der Heiden-Van Der Loo, M. Long-Term Risk of Subsequent Malignant Neoplasms After Treatment of Childhood Cancer in the DCOG LATER Study Cohort: Role of Chemotherapy. *Journal of clinical oncology : official journal of the American Society of Clinical Oncology*. **2017**, *35*, 2288–2298.

(57) Travis, L. B.; Wahnefried, W. D.; Allan, J. M.; Wood, M. E.; Ng, A. K. Aetiology, Genetics and Prevention of Secondary Neoplasms in Adult Cancer Survivors. *Nature reviews. Clinical oncology*. **2013**, *10*, 289–301.

(58) Henderson, T. O.; Rajaraman, P.; Stovall, M.; Constine, L. S.; Olive, A.; Smith, S. A.; Mertens, A.; Meadows, A.; Neglia, J. P.; Hammond, S.; Whitton, J.; Inskip, P. D.; Robison, L. L.; Diller, L. Risk Factors Associated with Secondary Sarcomas in Childhood Cancer Survivors: A Report from the Childhood Cancer Survivor Study. *International journal of radiation oncology, biology, physics*. **2012**, *84*, 224–230.

(59) Morton, L. M.; Swerdlow, A. J.; Schaapveld, M.; Ramadan, S.; Hodgson, D. C.; Radford, J.; van Leeuwen, F. E. Current Knowledge and Future Research Directions in Treatment-Related Second Primary Malignancies. *EJC supplements : EJC : official journal of EORTC, European Organization for Research and Treatment of Cancer ... [et al.]*. **2014**, *12*, 5–17.

(60) Pote, M. S.; Gacche, R. N. ATP-Binding Cassette Efflux Transporters and MDR in Cancer. *Drug Discovery Today*. **2023**, *28*, 103537.

(61) Hodges, L. M.; Markova, S. M.; Chinn, L. W.; Gow, J. M.; Kroetz, D. L.; Klein, T. E.; Altman, R. B. Very Important Pharmacogene Summary: ABCB1 (MDR1, P-Glycoprotein). *Pharmacogenetics and Genomics*. **2011**, *21*, 152.

(62) Mattioli, R.; Ilari, A.; Colotti, B.; Mosca, L.; Fazi, F.; Colotti, G. Doxorubicin and Other Anthracyclines in Cancers: Activity, Chemoresistance and Its Overcoming. *Molecular Aspects of Medicine*. **2023**, *93*, 101205.

(63) Dong, J.; Yuan, L.; Hu, C.; Cheng, X.; Qin, J. J. Strategies to Overcome Cancer Multidrug Resistance (MDR) through Targeting P-Glycoprotein (ABCB1): An Updated Review. *Pharmacology & therapeutics*. **2023**, *249*.

(64) Robey, R. W.; Pluchino, K. M.; Hall, M. D.; Fojo, A. T.; Bates, S. E.; Gottesman, M. M. Revisiting the Role of Efflux Pumps in Multidrug-Resistant Cancer. *Nature reviews. Cancer*. **2018**, *18*, 452.

(65) Wijdeven, R. H.; Pang, B.; Van Der Zanden, S. Y.; Qiao, X.; Blomen, V.; Hoogstraat, M.; Lips, E. H.; Janssen, L.; Wessels, L.; Brummelkamp, T. R.; Neefjes, J. Genome-Wide Identification and Characterization of Novel Factors Conferring Resistance to Topoisomerase II Poisons in Cancer. *Cancer Research*. **2015**, *75*, 4176–4187.

(66) Stefanski, C. D.; Keffler, K.; McClintock, S.; Milac, L.; Prosperi, J. R. APC Loss Affects DNA Damage Repair Causing Doxorubicin Resistance in Breast Cancer Cells. *Neoplasia*. **2019**, *21*, 1143–1150.

CHAPTER 2

2

Re-Exploring the Anthracycline Chemical Space for Better Anti-Cancer Compounds

Merle A. van Gelder[#,1], Sabina Y. van der Zanden[#,1], Merijn B. L. Vriends[2], Roos A. Wagensveld[1], Gijsbert A. van der Marel[2], Jeroen D. C. Codée[2], Herman S. Overkleeft[2], Dennis P. A. Wander[*,1] & Jacques Neefjes[*,1]

[1]Department of Cell and Chemical Biology, ONCODE Institute, Leiden University Medical Center, Einthovenweg 20, 2333 CZ Leiden, The Netherlands

[2]Leiden Institute of Chemistry, Leiden University, Einsteinweg 55, 2333 CC Leiden, The Netherlands

[#]These authors contributed equally

Journal of Medicinal Chemistry, **2023**

Abstract

The anthracycline anti-cancer drugs are intensely used in the clinic to treat a wide variety of cancers. They generate DNA double strand breaks, but recently the induction of chromatin damage was introduced as another major determinant of anti-cancer activity. The combination of these two events results in their reported side effects. While our knowledge on the structure-activity relationship of anthracyclines has improved, many structural variations remain poorly explored. Therefore, we here report on the preparation of a diverse set of anthracyclines with variations within the sugar moiety, amine alkylation pattern, saccharide chain and aglycone. We assessed the cytotoxicity in vitro in relevant human cancer cell lines, and the capacity to induce DNA- and chromatin damage. This coherent set of data allowed us to deduce a few guidelines on anthracycline design, as well as discover novel, highly potent anthracyclines that may be better tolerated by patients.

Introduction

Anthracyclines are extensively used as chemotherapeutics in the treatment of various hematological cancers and solid tumors since their discovery in the 1960s.[1] Because of their broad anti-cancer effectivity they are considered 'essential medicines' by the WHO[2], and their remarkable potency has inspired the development of thousands of variants.[3] Only few of these analogues have been approved for clinical use[4], of which only doxorubicin, daunorubicin, epirubicin and idarubicin have been adopted for worldwide use. While these anthracyclines are among the most effective anti-cancer drugs, their clinical application is hampered by treatment-limiting side effects and drug resistance.[5,6] The side effects of anthracycline treatment are severe: cardiotoxicity, secondary tumor formation and infertility affect the quality of life and survival of patients, regardless of the cancer prognosis.[7–10] Of these, cardiotoxicity is the main adverse effect which emerges in a cumulative manner and is restricting treatment regimens as a consequence.[8]

It has long been appreciated that anthracycline drugs cause DNA double-strand breaks by inhibition or poisoning of topoisomerase II.[11] For decades, this mode of action was thought to be the main reason for the remarkable effectiveness of these drugs. However, we revealed that DNA damage is not the only mode of action for most anthracycline variants. All clinically used anthracyclines induce chromatin damage upon DNA intercalation and subsequent eviction of histones.[12,13] Furthermore, we recently showed that the combination of DNA damage and chromatin damage, as exerted by doxorubicin, results in the major side effects reported for this compound.[13] In contrast, aclarubicin solely induces chromatin damage and is neither cardiotoxic nor induces therapy-related malignancies. Comparison of the structural similarities and differences of doxorubicin and aclarubicin inspired the design of *N,N*-dimethyldoxorubicin (**3**, Figure 1). This variant showed adequate anticancer effectivity in vitro and in various *in vivo* models, without accompanying (cardio)toxicity.[13] These results suggest that separating DNA damage from chromatin damage activities may guide the development of novel variants lacking the major long-term side effects that are associated with the anthracycline variants currently in clinical use.

In a follow-up study with the aim to better understand the molecular mode of action of these anthracycline drugs we synthesized a focused library of diastereomers of doxorubicin in the 1,2-amino alcohol arrangement of the 2,3-dideoxy-3-amino-L-fucoside. This yielded *N,N*-dimethylepirubicin (**4**, Figure 1), a compound slightly more potent than *N,N*-dimethyldoxorubicin.[14] In addition, the evaluation of doxorubicin/aclarubicin hybrid structures, varying in the tetracyclic aglycone, the sugar moiety and the N-alkylation pattern generated the doxorubicin trisaccharide (**5**, Figure 1) that is nearly 20-fold more cytotoxic than doxorubicin.[15] Building onto these studies, we here present

a further systematic expansion of our anthracycline library through the synthesis and evaluation of 19 additional anthracyclines. These constitute variations in amine alkylation (**6**-**9**), replacement/removal of the basic amine (**10**-**12**) and in regio-isomery (**13** and **14**). Additionally, exploration of the chemical space in the aglycone yielded (*N,N*-dimethyl-) amine bearing monosaccharides **15**-**24** and trisaccharides **25** and **26**. We determined the cytotoxic potency of these new variants in relevant cancer cell line models as well as their ability to induce both DNA and chromatin damage, in comparison to the clinically used variants doxorubicin (**1**), aclarubicin (**2**), daunorubicin (**15**) and idarubicin (**17**) and our most effective variants from previous studies (**3**-**5**).[13–15] Small modifications in the aglycone markedly changed the cytotoxicity of our compounds. Furthermore, our results underline our earlier findings that a tertiary amine on the first saccharide commonly improves the cytotoxicity of the compounds.

In summary, our endeavors to explore the chemical space of anthracycline variants resulted in a total of ten compounds that were more effective in K562 cells than doxorubicin (**1**), the foremost used clinical anthracycline. Of this list, compound **26**, composed of the idarubicin aglycone and the aclarubicin trisaccharide proved to be the most cytotoxic agent of the series with an IC_{50} towards K562 tumor cells in the low nanomolar range. This analogue does not induce DNA damage and is the fastest histone evictor we have identified to date. As a consequence, this compound is likely to have a favorable toxicity profile, similar to aclarubicin (**2**) and *N,N*-dimethyl doxorubicin (**3**), and would therefore be of high interest for further evaluation.

Results and discussion

The 26-compound anthracycline library subject of the here-presented studies is depicted in Figure 1. It is comprised of five compounds (**1**-**5**) reported on earlier[13–15], which we compare to 21 structural analogues (**6**-**26**). One distinguishing feature that determined (lack of) DNA damage induction in our previously reported studies on doxorubicin analogues is the addition of two methyl groups to the amine group in the daunosamine moiety: while doxo-rubicin (**1**) induces DNA double strand breaks, its *N,N*-dimethylated analogue **3** does not.[13] To further probe the relevance of the tertiary amine in the daunosamine moiety of these structures on DNA damage efficiency (and by extension, on toxic side effects) we prepared tertiary amines **6**-**9** featuring a cyclic azetidine (**6**), a pyrrolidine (**7**), a piperidine (**8**) and a morpholine moiety (**9**), respectively. Compounds **10**-**12** are included to examine whether the basic amine is required at all for any of the three biological activities (DNA damage, chromatin damage and cytotoxicity), with the amine either masked as an azide (**10**), substituted for an alcohol (**11**) or removed altogether (**12**). Compounds **13** and **14** are regio-isomers of doxorubicin (**1**) and *N,N*-

dimethyldoxorubicin (**3**), respectively, featuring a 2,3-dideoxy-3-aminofucose (*N,N*-dimethylated in **14**) and have been designed to establish the relevance of the location of the basic (alkylated) amine within the glycan moiety of doxorubicin (**1**). The clinically used drugs daunorubicin (**15**) and idarubicin (**17**), differ from doxorubicin (**1**) in the nature of the aglycone and feature the same daunosamine sugar moiety. To establish whether dimethylation of the amine removes DNA damaging activity, we included their

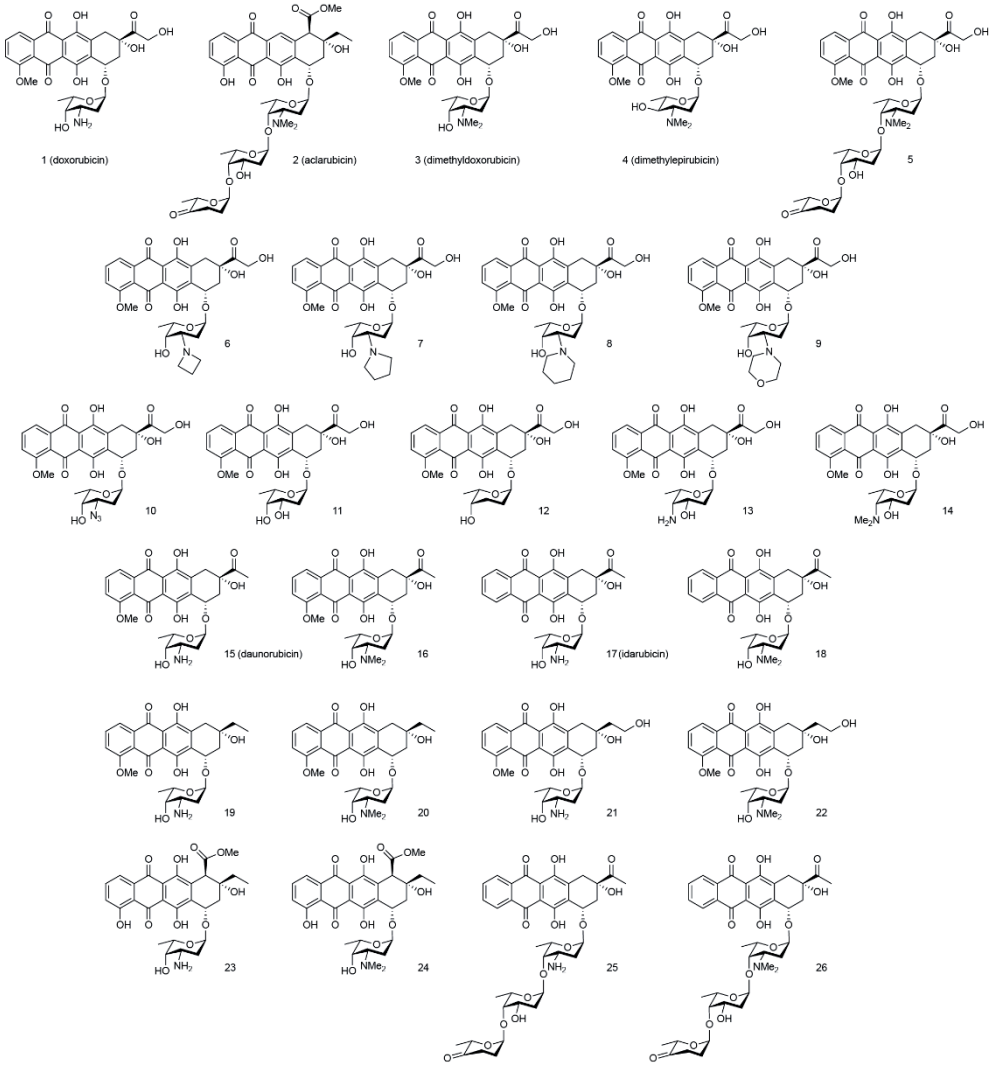

Figure 1. Chemical structures of compounds **1**-**26**, evaluated in this study. These contain the clinically used anthracyclines doxorubicin (**1**), aclarubicin (**2**), daunorubicin (**15**), idarubicin (**17**); the most potent anthracyclines from our previous work (**3**-**5**); doxorubicin derivatives differing in the sugar moiety (**6**-**14**, **25** and **26**) and (*N,N*-dimethyl) derivatives differing in the aglycone part (**16**, **18**-**24**).

respective *N,N*-dimethyl analogues **16** and **18** in this work. Compounds **19**-**24** comprise daunosamine/rhodosamine pairs featuring a number of alternative tetracyclic aglycones. Compounds **25** and **26** are composed of the idarubicin aglycone and the aclarubicin trisaccharide, with the latter again dimethylated at the daunosamine nitrogen.

Compounds **8**[16], **9**[17], **10**[18], **11**[19], **13**[20], **16**[16], **21**[21], **23**[22,23] and **24**[24] have been described previously; **1**, **2**, **15** and **17** are commercially available and **6**, **7**, **12**, **14**, **18**, **19**, **20**, **22**, **25** and **26** were newly synthesized (syntheses are detailed in the Supporting Information). Many of these compounds have had their cytotoxicity evaluated in past studies, and at times the DNA damage capacity has been included. However, this data is fragmented, because of the use of different methods, cell lines or (animal) models. Additionally, the induction of histone eviction has been shown by us to be a better determinant of cytotoxicity than DNA damage, and this had not yet been evaluated for **6**-**14**, **16** and **18**-**26**. As such, this work presents the assessment of compounds **1**-**26** for their potency to effect three biological processes: the cytotoxicity in three relevant cancer cell lines, DNA double strand break formation and chromatin damage via histone eviction.

Cytotoxicity of anthracycline derivatives

Anthracyclines are often used in the treatment of acute myeloid leukemia and other hematological malignancies. Therefore, the human myelogenous leukemia cell line K562 was used to determine the cytotoxicity of our set of anthracycline variants *in vitro*. The cytotoxicity of all variants (**1**-**26**) was tested using a short-term cell viability assay. In short, cells were treated for 2 hours with the different anthracycline variants at the indicated concentrations, and cell viability was determined 72 hours after treatment. The IC_{50} values for all analogues are plotted (Figure 2A). Within the set of cyclic (tertiary) amines, azetidine (**6**) proved equally effective when compared to the parental drug (**1**). The other three cyclic amines (**7**-**9**) were more effective than doxorubicin (**1**), with an IC_{50} similar to *N,N*-dimethyldoxorubicin (**3**). This is in line with our earlier observation that *N,N*-dimethylated anthracyclines, such as **3** and **4,** are more cytotoxic than their free-amine counterparts.[14,25] Of the three doxorubicin derivates not containing a basic amine, variants **11** and **12** are considerably less cytotoxic than doxorubicin (**1**), while azido-doxorubicin (**10**) proved to be almost 4-fold more potent. Relocation of the amine moiety from the 3'- to the 4'-position in the sugar, as in **13** and **14**, did not markedly change the IC_{50} for these compounds compared to their original counterparts **1** and **3**, respectively. Removal of the aglycone carbonyl function (as in **19**-**22**) generally did not improve cytotoxicity when compared to the parent compounds. A notable exception is 13-deoxydaunorubicin (**19**), which is nearly equipotent to the most cytotoxic free amine anthracycline in our hands – idarubicin (**17**). Compounds bearing an aglycone with three phenol groups (**23** and **24**) turned out to be poorly cytotoxic. However, they were both more cytotoxic than their aclarubicin-aglycone bearing counterparts described before.[15] The idarubicin-derived

trisaccharides in this set (**25** and **26**) were significantly more cytotoxic than doxorubicin (**1**), and *N,N*-dimethylated-idarubicin trisaccharide (**26**) was the most effective compound of this set; active at low nanomolar concentrations. In fact, with an IC_{50} of 20 nM in K562 cells this variant is 16 times more cytotoxic than doxorubicin (**1**). In general, the observed cytotoxic activity appeared consistent across cell types, since similar cytotoxicity profiles were observed in cell lines from different cancer origins (Figure 2B), however with some exceptions (for instance, **3**, **10**-**12** and **21**-**23**).

A

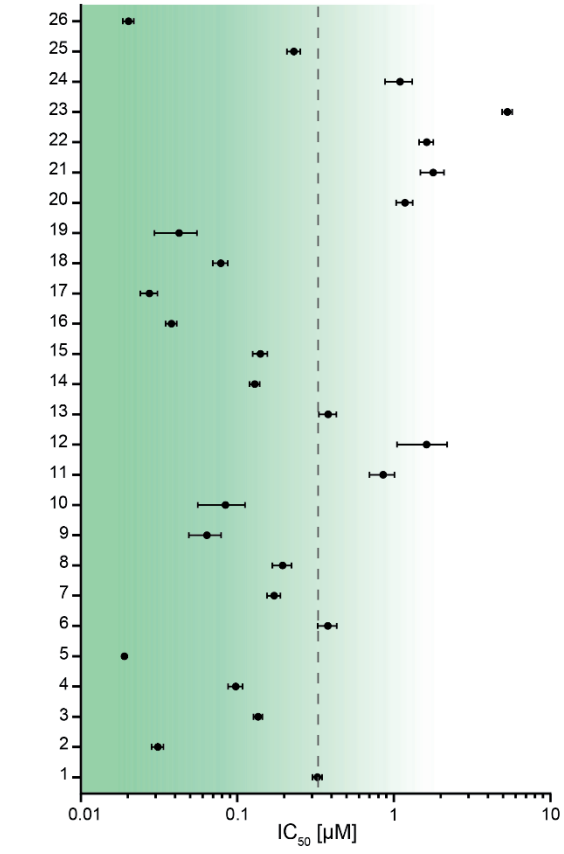

B

IC_{50} [μM] / cell line

	K562	MelJuSo	U2Os
26	0.020	0.008	0.012
25	0.230	0.680	0.376
24	1.098	0.835	1.126
23	5.320	4.292	10.000
22	1.623	2.867	4.208
21	1.788	1.151	0.891
20	1.180	1.810	1.362
19	0.042	0.372	0.237
18	0.078	0.111	0.118
17	0.027	0.069	0.024
16	0.038	0.078	0.068
15	0.141	0.286	0.061
14	0.129	0.433	0.285
13	0.381	0.998	1.121
12	1.622	2.430	10.000
11	0.856	1.904	6.793
10	0.084	1.224	10.000
9	0.064	0.051	0.077
8	0.195	0.078	0.105
7	0.172	0.073	0.122
6	0.379	0.297	0.159
5	0.019	0.007	0.011
4	0.098	0.136	0.095
3	0.136	0.073	0.056
2	0.031	0.099	0.209
1	0.325	0.523	0.339

Figure 2. Cytotoxic potency of anthracycline derivatives 1-26 to three different tumor cell lines. (A) IC_{50} values are plotted for all derivatives tested in the human myelogenous leukemia cell line K562. Dotted line indicated the IC_{50} of doxorubicin (1). The Y axis shows the number of the structures shown in Figure 1. The dotted line indicates the IC_{50} for doxorubicin. (B) IC_{50} values for the 26 anthracycline variants tested in human myelogenous leukemia cell line K562, human melanoma cell line MelJuSo and human osteosarcoma cell line U2OS.

Overall, evaluation of the cytotoxic activity of the full set of new anthracycline derivatives produced seven compounds that were less effective (**11**, **12**, and **20**-**24**) than doxorubicin (**1**), and two compounds (**6** and **13**) with a similar IC_{50} as doxorubicin (**1**). Interestingly, ten newly synthesized compounds showed to be (far) more effective than doxorubicin in the three tested cell lines.

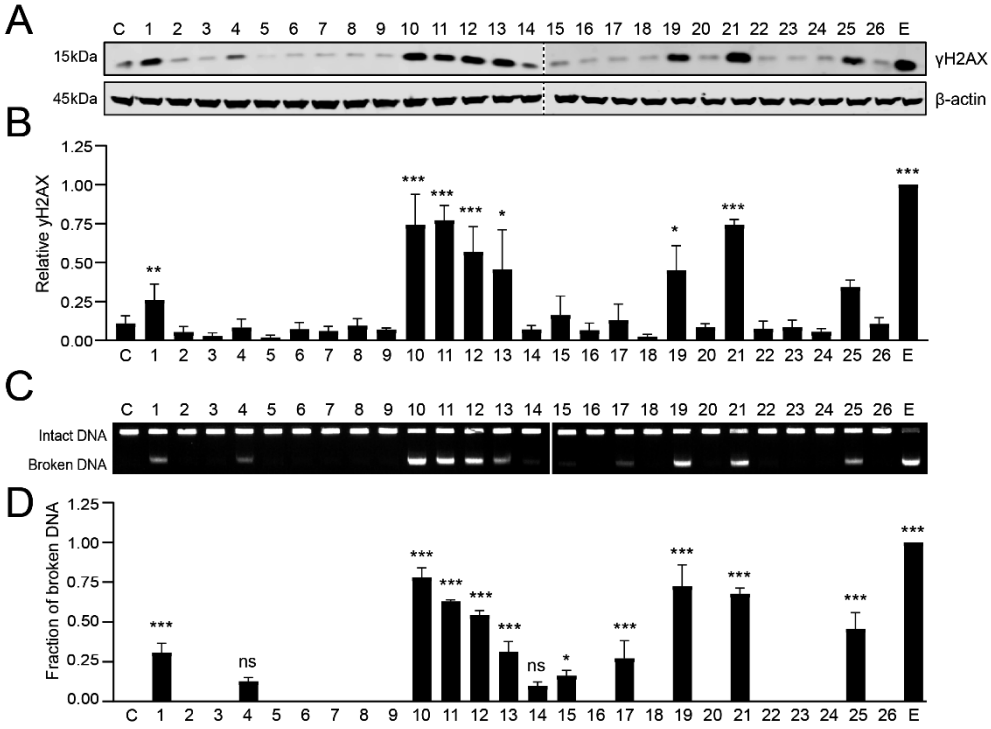

Figure 3. DNA damage capacity of the full set of anthracycline derivatives **1**-**26**. Numbers correspond to the structures in Figure 1, C; unmanipulated control. (A) K562 cells were treated for 2 h with 10 μM of the indicated compounds, etoposide [E] was used as positive control. γH2AX levels were examined by Western blot. Actin was used as a loading control, and molecular weight markers are indicated. (B) Quantification of γH2AX signal normalized to the loading control. Results are presented as mean ± SD of three independent experiments. Ordinary one-way ANOVA with Dunnett's multiple comparison test. *P < 0.05, **P < 0.01, ***P < 0.001. (C) DNA double strand breaks were directly visualized by CFGE. The position of intact and broken DNA is indicated. (D) Quantification of broken DNA relative to total DNA as analyzed by CFGE. Etoposide [E] was used as positive control. Results are presented as mean ± SD of three independent experiments. Ordinary one-way ANOVA with Dunnett's multiple comparison test. *P < 0.05, ***P < 0.001.

Evaluation of DNA damaging activity

Anthracycline variants that are used in the clinic display two modes of action: the induction of DNA damage via targeting of topoisomerase II and/or chromatin damage through eviction of histones.[25] DNA damage activity does contribute to the cytotoxicity of these (and other chemotherapeutics), however, we have shown that DNA damage conspires with chromatin damage to induce the severe therapy limiting side effects of this class of drugs.[13] Therefore, it is imperative to assess the different mechanism of action of each of the new variants.

In response to DNA double strand break formation, histone H2AX becomes phosphorylated, then called γH2AX[26]. The levels of gH2AX thus reflect the presence of DNA double strand breaks. Therefore we determined the DNA damaging capacity of this set of anthracyclines by assessing gH2AX protein levels using Western blot analysis. K562 cells were treated with the indicated compounds (**1**-**26**) at a concentration of 10μM, corresponding to serum peak levels for doxorubicin in cancer patients at standard treatment.[27] Etoposide (a podophyllotoxin based topoisomerase II inhibitor) was included as positive control for DNA break formation (Figure 3A and B). Variants with a tertiary amine on the reducing fucose (**2**-**9**, **16**, **18**, **20**, **22**, **24** and **26**) did not induce DNA damage, in line with results obtained previously for aclarubicin (**2**) and *N,N*-dimethyldoxorubicin (**3**).[13] Compound **4** and **14** may be exceptions as these compounds induce a slight increase in γH2AX level, similar to earlier observations.[14] On the other hand, (almost) all compounds with a primary amine at this position are able to induce DNA double strand breaks. Specifically, the non-basic doxorubicin variants lacking the amine (**10**-**12**), doxorubicin regio-isomer **13**, deoxy-daunorubicin (**19**), deoxy-doxorubicin (**21**) and non-methylated idarubicin-aclarubicin hybrid (**25**) all proved to be very potent DNA damage inducers. Here, the poorly cytotoxic compound **23**, deviated from the rule lacking DNA damage activity, despite its primary amine. A similar trend in γH2AX protein levels was observed for all compounds (**1**-**26**) at lower drug concentrations (1μM and 5μM, Figure S1 and S2).

Some anthracycline variants also cause dissociation of histones from chromatin upon intercalation into DNA including the histone variant H2AX. Therefore, the levels of γH2AX might not accurately represent DNA damage when compounds are efficient histone evictors. To determine DNA double strand break induction by the different anthracycline variants at the DNA level, we assessed the DNA damage capacity of our compounds using constant field gel electrophoresis (CFGE)[28] a direct method to visualize intact and broken DNA (Figure 3C and D). This complementary assay to study DNA damage confirmed the observations on γH2AX protein levels, showing the same trend in the DNA damaging capacity of our series of compounds.

Evaluation of chromatin damage activity

For previously reported anthracycline variants we have shown that chromatin damage following histone eviction is strongly correlating with cytotoxicity.[14,29] To visualize histone eviction, part of the nucleus of MelJuSo cells stably expressing PAGFP-H2A was

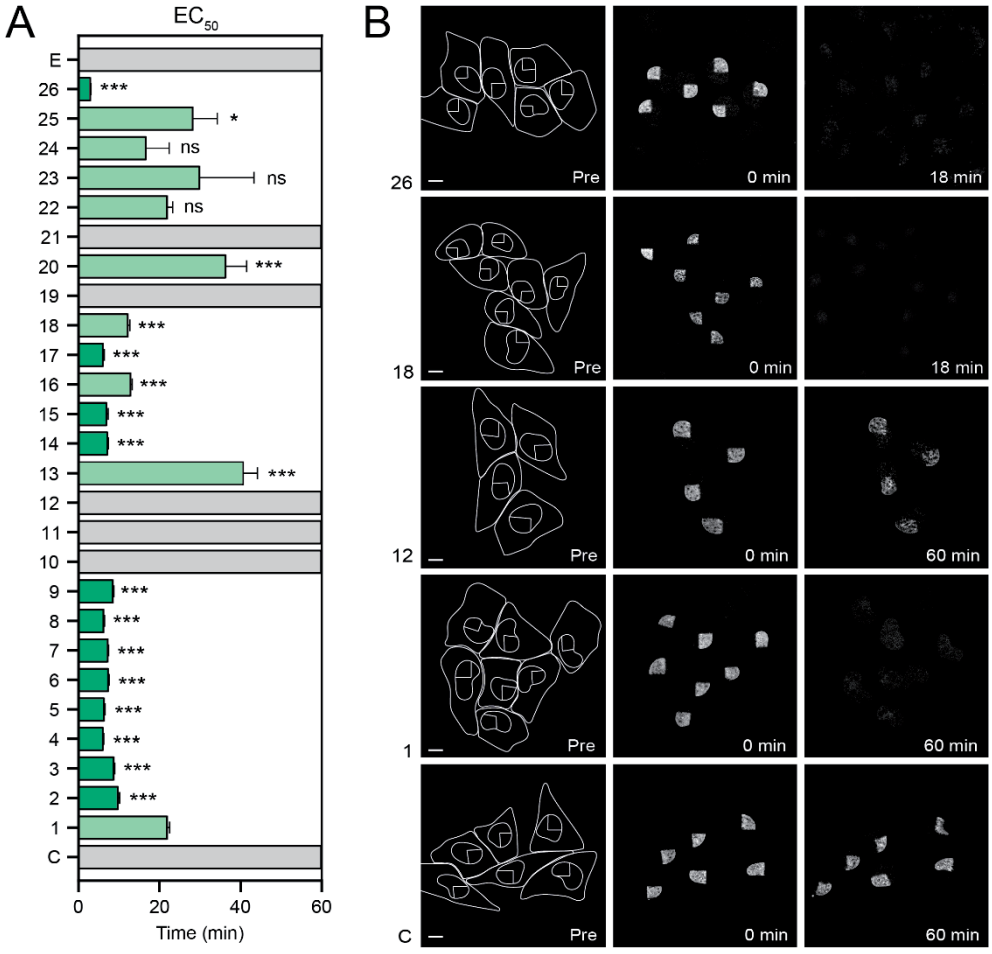

Figure 4. Efficacy of chromatin damage of the set of anthracycline derivatives **1**-**26**. (A) The rate of histone eviction for all derivatives is plotted as EC_{50} (time at which 50% of the initial signal in the photoactivated spot is reduced). Etoposide [E] was used as negative control. Nonlinear regression with sum-of-squares F test. *P < 0.05, ***P < 0.001, ns = not significant. (B) Illustration of the effects of indicated compounds (numbers on left side indicate the drug in Figure 1) on eviction of the photoactivated histones. Left panel: drawn cell out line and nucleus with the photoactivated part of the nucleus in living MelJuSo-PAGFP-H2A cells. Middle panel shows the photoactivated histones at the onset of the experiment after compound addition. Photo-activation was monitored by time-lapse confocal microscopy for 1 hour in the presence of the indicated compounds at 10 μM. Stills made at 60 min are shown in the right panel. Scale bar, 10 μm.

photoactivated. Subsequently, the fluorescence intensity was measured directly after addition of the indicated compounds using timelapse confocal microscopy, as previously described.[12] For all tested derivatives the rate of histone eviction (EC_{50}, the time at which 50% of the initial signal is reduced) was plotted (Figure 4A). Whereas compounds **10**, **11** and **12** are proven effective DNA damage inducers, removal and/or replacing the amine abolished the capacity to evict histones (Figure 4A and B). Furthermore, analogues lacking the aglycone-carbonyl characteristic for both daunorubicin and doxorubicin (**19**, 2**1**) are poor histone evictors. Likewise, for their *N,N*-dimethylated counterparts (**20** and **22**), the rate of histone eviction was markedly reduced when comparing the deoxy variants to those bearing the original aglycones (**20** versus **16** and **22** versus **3**). In general, variants containing a tertiary amine at the 3'-and 4'-position in the carbohydrate attached to the doxorubicin tetracyclin were effective histone evicting compounds (**3**-**9** and **14**), with strong eviction capacity and outperformed doxorubicin (**1**). The derivative with the fastest histone eviction activity was compound **26**. Combining the aclarubicin trisaccharide with the idarubicin aglycone, resulted in variant **26** that outperformed both aclarubicin (**2**) and idarubicin (**17**) in terms of the rate of histone eviction (Figure 4A and B). The aclarubicin/idarubicin hybrid structure (**26**) proved to be the most effective anthracycline variant with respect to histone eviction and this markedly improved chromatin damage activity may explain its superior cytotoxicity. This hypothesis is strengthened by the significant correlation of histone eviction rate and cytotoxicity when evaluating the compounds tested here (Supporting information, Figure S3).

While the alterations on the aglycones in this set of compounds failed to improve the chromatin damage activity of these compounds, shuffling the aglycone and saccharide moiety of proven effective anthracyclines (as for **5** and **26**) was effective in improving the histone eviction capacity of these compounds.

Conclusions

Anthracyclines have been extensively used in the past decades to treat various types of cancer. Despite their effectivity, the use of anthracyclines in clinical practice is restricted by their severe side effects, and functional understanding of the mechanisms underlying the manifestation of off-target toxicities is still incomplete. Therefore, studying the consequences of small systematic modifications can be valuable in understanding the biological activities of anthracyclines. To do so, we synthesized a diverse set of anthracycline variants with alterations in amine alkylation, replacement/removal of the basic amine and in regio-isomery. Additionally, exploration of the chemical space in the aglycone yielded novel (dimethyl)amine monosaccharides and trisaccharides with strong cytotoxicity profiles. In total, 10 out of 19 new anthracycline derivatives were more

cytotoxic than doxorubicin (**1**). Most notably, structures containing alkylated amines were particularly cytotoxic, while most of the variations on the tetracyclic aglycone did not typically yield more potent analogues. Exceptions are compound **19** and structures containing the idarubicin aglycone present in **17**, **18**, **25** and **26**. Especially the latter *N,N*-dimethylidarubicin-trisaccharide **26** has strong cytotoxicity, with IC_{50} values in the low nanomolar range in three cancer cell lines.

We have shown before that anthracycline variants that solely induce chromatin damage but not DNA double strand breaks still have excellent cytotoxic activity.[14,15] In line with these results, we now report a significant correlation between the rate of histone eviction and cytotoxicity. The extent to which anthracyclines induce DNA double strand breaks, on the other hand, does not correlate with their cytotoxicity. This was also noted in the clinic, as etoposide (that only induces DNA breaks) is a considerably less potent anti-cancer drug. Interestingly, etoposide also displays milder side effects compared to doxorubicin. This finding is strengthened by the additional biological data presented for deoxy-doxorubicin (**21**). While unable to evict histones, **21** is a very efficient DNA damaging agent. This variant entered phase I/II clinical trials but was never developed further.[30,31] These observations show that it is imperative to understand the biological consequences of structural variations for rational design of novel anthracyclines. In the development of annamycin, another anthracycline variant that entered phase I/II clinical trials[32], several important structural modifications were incorporated.[33] This analogue is characterized by the absence of the aglycone methoxy group, the introduction of an iodine at the 2'-position of the sugar and the replacement of the primary amine at the 3'-position with an OH group. The absence of the amino group results in reduced basicity, which appears to be at the cost of potency, as is also seen for the cytotoxicity profile of hydroxydoxorubicin (**11**). Therefore, removal of the methoxy on the aglycone seems to be important to increase cytotoxicity, which correlates with our findings on the structural variants with the idarubicin aglycone (**17**, **18**, **25** and **26**) that proved to be very potent.

From the set of anthracycline variants harboring cyclic (tertiary) amines, azetidine (**6**) proved equally effective to doxorubicin, whereas the other three cyclic amines (**7**-**9**) were more cytotoxic. These results are comparable to previous described cytotoxicity profiles in cell lines of different cancer origin.[34,35] Of the three doxorubicin derivates where the primary amine was either replaced (**10**, **11**) or removed (**12**), only azido-doxorubicin (**10**) was significantly cytotoxic to K562 cells. However, the cytotoxicity of this variant in MelJuSo and U2OS cell lines was considerably lower. Another study in which the amino group of daunorubicin was substituted for an azide showed that this variant is also particularly toxic for K562 cells.[36] This suggests that the improved toxicity seen for this modification might be cell-type specific.

Based on these and earlier data, we may deduce five guidelines related to the potency of anthracyclines.

1. The main cytotoxic activity of these compounds is associated with histone eviction activity rather than DNA double strand break induction;
2. Usually, *N,N*-dimethylation eliminates DNA double strand break formation at no cost to cytotoxicity;
3. Small differences in the tetracyclin aglycone structure further contribute to cytotoxicity, as illustrated by the difference in cytotoxicity between doxorubicin (**1**), 13-deoxydoxorubicin (**21**) and idarubicin (**4**);
4. The position of the amine in the sugar has minor effects, since placing the amine on either the 3'- or 4'-position does not significantly affect cytotoxicity;
5. Replacing the amine by an OH or H group strongly reduces cytotoxicity.

These points are combined in *N,N*-dimethylidarubicin trisaccharide (**26**), which is 16-fold more cytotoxic than doxorubicin (**1**). It is also 1.5-fold more cytotoxic than clinically used variants idarubicin (**17**) which causes various off-target toxicities[37], and aclarubicin (**2**) which is only used in China and Japan. Additionally, this compound is more efficient in terms of histone eviction, without inducing any DNA double strand breaks. Further *in vivo* studies are required on the cardiotoxic profile of **26,** and to establish whether increased cytotoxicity to cancer cells could enlarge the therapeutic window for cancer patients. Such studies may ultimately yield more effective anthracycline variants with limited adverse toxicity.

Experimental Section

Chemistry

The anthracycline analogues **3**-**5** were synthesized as described.[14,29] Syntheses of compounds **6**-**14**, **16**, **18**-**26** and intermediates are described in the Supporting Information and the compounds are >95% pure by HPLC analysis.

Reagents and antibodies

Doxorubicin was obtained from Accord Healthcare Limited, UK, aclarubicin (sc-200160) was purchased from Santa Cruz Biotechnology (USA), daunorubicin was obtained from Sanofi, idarubicin was obtained from Pfizer, etoposide was obtained from Pharmachemie (the Netherlands). Primary antibodies used for Western blotting: γH2AX (1:1000, 05-036, Millipore), β-actin (1:10000, A5441, Sigma). Secondary antibody used for blotting: IRDye 800CW goat anti-mouse IgG (H+L) (926-32210, Li-COR, 1:10000).

Cell culture

K562 cells (B. Pang, Leiden University Medical Center, the Netherlands) were maintained in RPMI-1640 medium supplemented with 8% FCS. MelJuSo cells were maintained in IMDM supplemented with 8% FCS. MelJuSo cells stably expressing PAGFP-H2A were maintained in IMDM supplemented with 8% FCS and G-418, as described.[12] U2Os cells (ATCC® HTB-96) were maintained in DMEM medium supplemented with 8% FCS. Cell lines were maintained in a humidified atmosphere of 5% CO_2 at 37°C, regularly tested for the absence of mycoplasma and the origin of cell lines was validated using STR analysis.

Short-term cell viability assay

Cells were seeded into 96-well format (2000 cells/well). Twenty-four hours after seeding, cells were treated with indicated compounds for 2 hours at various concentrations. Subsequently, compounds were removed, and cells were left to grow for an additional 72 hours. Cell viability was measured using the CellTiter-Blue viability assay (Promega). Relative survival was normalized to the untreated control and corrected for background signal.

Western blot and constant-field gel electrophoresis (CFGE)

Cells were seeded into 12-well format (250.000 cells/well), treated with indicated drugs at 10μM for 2 hours. Subsequently, drugs were removed by extensive washing and cells were collected and processed immediately for the assays. For Western blot, cells were lysed directly in SDS-sample buffer (2% SDS, 10% glycerol, 5% β-mercaptoethanol, 60mM Tris-HCl pH 6.8 and 0.01% bromophenol blue). Samples were separated by SDS-PAGE and transferred to a PVDF membrane (Immobilon-P, 0.45μm, Millipore). Blocking of the filters and antibody incubations were done in PBS supplemented with 0.1 (v/v)% Tween and 5% (w/v) milk powder (Skim milk powder, LP0031, Oxiod). Blots were imaged by the Odyssey Classic imager (Li-Cor). Intensity of bands was quantified using ImageJ or Image Studio software. For CFGE: DNA double strand breaks were quantified by constant-field gel electrophoresis as described.[28] Images were quantified using ImageJ software.

Microscopy analysis

For PAGFP-H2A photoactivation and time-lapse confocal imaging, cells were seeded in a 35mm glass bottom petri dish (Poly-d-lysine-Coated, MatTek Corporation), and imaged 16 hours later as described[12], for one hour following addition of 10μM of the indicated compounds. Time-lapse confocal imaging was performed on a Leica SP8 confocal microscope system 63x lens, equipped with a climate chamber. Movies were quantified using Image J software.

Quantification and statistical analysis

Each experiment was assayed in triplicate, unless stated otherwise. Error bars denote ±SD. Statistical analyses were performed using Prism 8 software (GraphPad Inc.). ns, not significant, *p = < 0.05, **p = < 0.01, ***p = < 0.001

Associated content

Supporting Information

The Supporting Information is available free of charge at https://pubs.acs.org/doi/10.1021/acs.jmedchem.3c00853.

Supplementary figures S1 and S2, gH2AX evaluation for compounds **1**-**26** tested at 1mM and 5 mM concentrations respectively, and S3 the correlation between chromatin- or DNA damage and cytotoxicity for compounds **1**-**26**. Detailed synthetic procedures and analytical spectra (1D/2D NMR, HRMS) of compounds **6**-**14**, **16**, **18**-**26** and their intermediates.

Molecular formula strings and tabulated biological assays data (CSV).

Author information

Author Contributions

M.A.v.G., S.Y.v.d.Z., D.P.A.W., J.D.C.C., H.S.O. and JN conceived the experiments. D.P.A.W. and M.B.L.V. under supervision of G.A.v.d.M., J.D.C.C. and H.S.O. performed the synthesis. M.A.v.G., S.Y.v.d.Z., and R.A.W. under supervision of J.N. performed all biochemical and cellular experiments. M.A.v.G. and S.Y.v.d.Z., contributed equally to this work.

Funding Sources

This work was supported by grants from the Dutch Cancer Society KWF to JN, a Spinoza Prize grant to JN and by the Institute for Chemical Immunology an NWO Gravitation project funded by the Ministry of Education, Culture and Science of the Netherlands to HO and JN.

Notes

Jacques Neefjes is a shareholder in NIHM, that aims to produce aclarubicin for clinical use.

Acknowledgements

Thadée Grocholski (University of Turku, Finland) is kindly acknowledged for his gift of ε-rhodomycinone. We would like to thank Ilana Berlin for input and fruitful discussions.

Abbreviations

PAGFP-H2A, photo-activatable-histone H2A.

References

(1) Lown, J. W. Discovery and Development of Anthracycline Antitumour Antibiotics. *Chemical Society Reviews*. **1993**, *22*.

(2) *WHO model list of essential medicines - 22nd list, 2021*. https://www.who.int/publications/i/item/WHO-MHP-HPS-EML-2021.02 (accessed 2023-04-14).

(3) Anthracycline Chemistry and Biology I. **2008**, *282*.

(4) Weiss, R. B. The Anthracyclines: Will We Ever Find a Better Doxorubicin? *Seminars in oncology*. **1992**, *19*, 670–686.

(5) Nielsen, D.; Maare, C.; Skovsgaard, T. Cellular Resistance to Anthracyclines. *General Pharmacology: The Vascular System*. **1996**, *27*, 251–255.

(6) Rayner, D. M.; Cutts, S. M. Anthracyclines. *Side Effects of Drugs Annual*. **2014**, *36*, 683–694.

(7) Sadurska, E. Current Views on Anthracycline Cardiotoxicity in Childhood Cancer Survivors. *Pediatric Cardiology*. **2015**, *36*, 1112–1119.

(8) Lotrionte, M.; Biondi-Zoccai, G.; Abbate, A.; Lanzetta, G.; D'Ascenzo, F.; Malavasi, V.; Peruzzi, M.; Frati, G.; Palazzoni, G. Review and Meta-Analysis of Incidence and Clinical Predictors of Anthracycline Cardiotoxicity. *The American journal of cardiology*. **2013**, *112*, 1980–1984.

(9) Felix, C. A. Secondary Leukemias Induced by Topoisomerase-Targeted Drugs. *Biochimica et Biophysica Acta*. **1998**, *1400*, 233–255.

(10) Mistry, A. R.; Felix, C. A.; Whitmarsh, R. J.; Mason, A.; Reiter, A.; Cassinat, B.; Parry, A.; Walz, C.; Wiemels, J. L.; Segal, M. R.; Adès, L.; Blair, I. A.; Osheroff, N.; Peniket, A. J.; Lafage-Pochitaloff, M.; Cross, N. C. P.; Chomienne, C.; Solomon, E.; Fenaux, P.; Grimwade, D. DNA Topoisomerase II in Therapy-Related Acute Promyelocytic Leukemia. *New England Journal of Medicine*. **2005**, *352*, 1529–1538.

(11) Nitiss, J. L. Targeting DNA Topoisomerase II in Cancer Chemotherapy. *Nature Reviews Cancer 2009 9:5*. **2009**, *9*, 338–350.

(12) Pang, B.; Qiao, X.; Janssen, L.; Velds, A.; Groothuis, T.; Kerkhoven, R.; Nieuwland, M.; Ovaa, H.; Rottenberg, S.; Van Tellingen, O.; Janssen, J.; Huijgens, P.; Zwart, W.; Neefjes, J. Drug-Induced Histone Eviction from Open Chromatin Contributes to the Chemotherapeutic Effects of Doxorubicin. *Nature Communications 2013 4:1*. **2013**, *4*, 1–13.

(13) Qiao, X.; Van Der Zanden, S. Y.; Wander, D. P. A.; Borràs, D. M.; Song, J. Y.; Li, X.; Duikeren, S. Van; Gils, N. Van; Rutten, A.; Herwaarden, T. Van; Tellingen, O. Van; Giacomelli, E.; Bellin, M.; Orlova, V.; Tertoolen, L. G. J.; Gerhardt, S.; Akkermans, J. J.; Bakker, J. M.; Zuur, C. L.; Pang, B.; Smits, A. M.; Mummery, C. L.; Smit, L.; Arens, R.; Li, J.; Overkleeft, H. S.; Neefj, J. Uncoupling DNA Damage from Chromatin Damage to Detoxify Doxorubicin. *Proceedings of the National Academy of Sciences of the United States of America*. **2020**, *117*, 15182–15192.

(14) Wander, D. P. A.; van der Zanden, S. Y.; Vriends, M. B. L.; van Veen, B. C.; Vlaming, J. G. C.; Bruyning, T.; Hansen, T.; van der Marel, G. A.; Overkleeft, H. S.; Neefjes, J. J. C.; Codée, J. D. C. Synthetic (N , N -Dimethyl)Doxorubicin Glycosyl Diastereomers to Dissect Modes of Action of Anthracycline Anticancer Drugs. *The Journal of Organic Chemistry*. **2021**, *86*, 5757–5770.

(15) Wander, D. P. A.; Van Der Zanden, S. Y.; Van Der Marel, G. A.; Overkleeft, H. S.; Neefjes, J.; Codée, J. D. C. Doxorubicin and Aclarubicin: Shuffling Anthracycline Glycans for Improved Anticancer Agents. *Journal of Medicinal Chemistry*. **2020**, *63*, 12814–12829.

(16) Tong, G. L.; Wu, H. Y.; Smith, T. H.; Henry, D. W. Adriamycin Analogs. 3. Synthesis of N-Alkylated Anthracyclines with Enhanced Efficacy and Reduced Cardiotoxicity. *Journal of Medicinal Chemistry*. **1979**, *22*, 912–918.

(17) Kuratsu, J.; Arita, N.; Kurisu, K.; Uozumi, T.; Hayakawa, T.; Ushio, Y. A Phase II Study of KRN8602(MX2), a Novel Morpholino Anthracycline Derivative, in Patients with Recurrent Malignant Glioma. *Journal of neuro-oncology*. **1999**, *42*, 177–181.

(18) Yu, S.; Zhang, G.; Zhang, W.; Luo, H.; Qiu, L.; Liu, Q.; Sun, D.; Wang, P. G.; Wang, F. Synthesis and Biological Activities of a 3'-Azido Analogue of Doxorubicin Against Drug-Resistant Cancer Cells. *International Journal of Molecular Sciences*. **2012**, *13*, 3671.

(19) HORTON, D.; PRIEBE, W.; VARELA, O. Synthesis and Antitumor Activity of 3′-Deamino-3′-Hydroxydoxorubicin. A Facile Procedure for the Preparation of Doxorubicin Analogs. *The Journal of Antibiotics*. **1984**, *37*, 853–858.

(20) Florent, J. C.; Gaudel, G.; Monneret, C.; Hoffmann, D.; Kraemer, H. P. Synthesis and Antitumor Activity of Isodoxorubicin Analogues. *Journal of medicinal chemistry*. **1993**, *36*, 1364–1368.

(21) Zhang, X. US Patent: Processes for Preparing 13-Deoxy Anthracycline Derivatives. https://patents.google.com/patent/US5948896A/en.

(22) Kolar, C.; Kneissl, G.; Knödler, U.; Dehmel, K. Semisynthetic ε-(Iso)Rhodomycins: A New Glycosylation Variant and Modification Reactions. *Carbohydrate Research*. **1991**, *209*, 89–100.

(23) Kolar, C.; Kneijl, G. Semisynthetische Rhodomycine: Neue Glycosylierungsverfahren Zur Synthese von Anthracyclin-Oligosacchariden. *Angewandte Chemie*. **1990**, *102*, 827–828.

(24) Johdo, O.; Watanabe, Y.; Ishikura, T.; Akihiro, Y.; Naganawa, H.; Sawa, T.; Takeuchi, T. Anthracycline Metabolites from Streptomyces Violaceus A262. II. New Anthracycline Epelmycins Produced by a Blocked Mutant Strain SU2-730. *The Journal of antibiotics*. **1991**, *44*, 1121–1129.

(25) van der Zanden, S. Y.; Qiao, X.; Neefjes, J. New Insights into the Activities and Toxicities of the Old Anticancer Drug Doxorubicin. *The FEBS Journal*. **2021**, *288*, 6095–6111.

(26) Kuo, L. J.; Yang, L. X. γ-H2AX- A Novel Biomaker for DNA Double-Strand Breaks. *In Vivo*. April 2008, pp 305–310.

(27) Speth, P. A. J.; van Hoesel, Q. G. C. M.; Haanen, C. Clinical Pharmacokinetics of Doxorubicin. *Clinical Pharmacokinetics*. **1988**, *15*, 15–31.

(28) Wlodek, D.; Banáth, J.; Olive, P. L. Comparison between Pulsed-Field and Constant-Field Gel Electrophoresis for Measurement of DNA Double-Strand Breaks in Irradiated Chinese Hamster Ovary Cells. *International journal of radiation biology*. **1991**, *60*, 779–790.

(29) Wander, D. P. A.; van der Zanden, S. Y.; van der Marel, G. A.; Overkleeft, H. S.; Neefjes, J.; Codée, J. D. C. Doxorubicin and Aclarubicin: Shuffling Anthracycline Glycans for Improved Anticancer Agents. *Journal of Medicinal Chemistry*. **2020**, *63*, 12814–12829.

(30) *GPX-100 in Treating Patients With Solid Tumors - Full Text View - ClinicalTrials.gov*. https://clinicaltrials.gov/ct2/show/NCT00003403 (accessed 2023-05-11).

(31) *Study of GPX-100 in the Treatment of Metastatic Breast Cancer - Full Text View - ClinicalTrials.gov*. https://clinicaltrials.gov/ct2/show/NCT00123877 (accessed 2023-05-11).

(32) Wetzler, M.; Thomas, D. A.; Wang, E. S.; Shepard, R.; Ford, L. A.; Heffner, T. L.; Parekh, S.; Andreeff, M.; O'Brien, S.; Kantarjian, H. M. Phase I/II Trial of Nanomolecular Liposomal Annamycin in Adult Patients with Relapsed/Refractory Acute Lymphoblastic Leukemia. *Clinical lymphoma, myeloma & leukemia*. **2013**, *13*, 430–434.

(33) *US5977327A - Synthesis of annamycin - Google Patents*. https://patents.google.com/patent/US5977327A/en (accessed 2023-05-11).

(34) Marczak, A.; Denel-Bobrowska, M.; Rogalska, A.; Łukawska, M.; Oszczapowicz, I. Cytotoxicity and Induction of Apoptosis by Formamidinodoxorubicins in Comparison to Doxorubicin in Human Ovarian Adenocarcinoma Cells. *Environmental Toxicology and Pharmacology*. **2015**, *39*, 369–383.

(35) WASOWSKA, M.; OSZCZAPOWICZ, I.; WIETRZYK, J.; OPOLSKI, A.; MADEJ, J.; DZIMIRA, S.; OSZCZAPOWICZ, J. Influence of the Structure of New Anthracycline Antibiotics on Their Biological Properties. *Anticancer Research*. **2005**, *25*, 2043.

(36) Fang, L.; Zhang, G.; Li, C.; Zheng, X.; Zhu, L.; Xiao, J. J.; Szakacs, G.; Nadas, J.; Chan, K. K.; Wang, P. G.; Sun, D. Discovery of a Daunorubicin Analogue That Exhibits Potent Antitumor Activity and Overcomes P-Gp-Mediated Drug Resistance. *Journal of Medicinal Chemistry*. **2006**, *49*, 932–941.

(37) Seiter, K. Toxicity of the Topoisomerase II Inhibitors. *Expert Opinion on Drug Safety*. **2005**, *4*, 219–234.

Supporting information chapter 2

A: Supplemental Figures

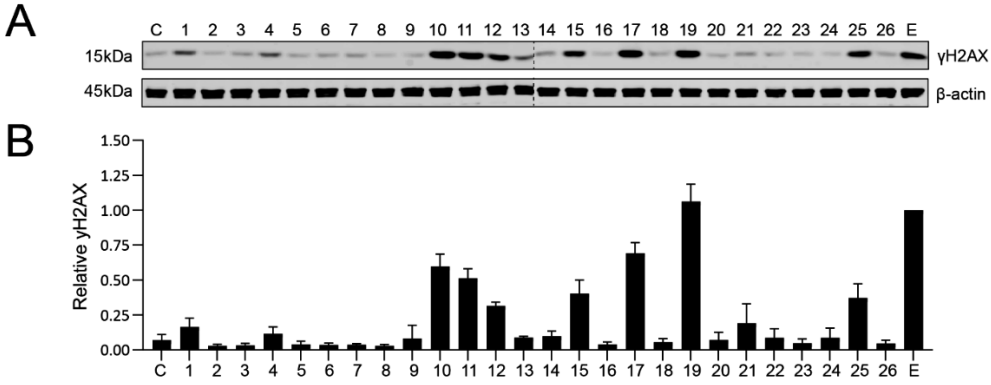

Figure S1 – DNA damage capacity of the full set of anthracycline derivatives 1-26. Numbers correspond to the structures in Figure 1, C; unmanipulated control. (A) K562 cells were treated for 2 h with *1 μM* of the indicated compounds, etoposide [E] was used as positive control. γH2AX levels were examined by Western blot. Actin was used as a loading control, and position of molecular weight markers is indicated. (B) Quantification of γH2AX signal normalized to the loading control. Results are presented as mean ± SD of three independent experiments.

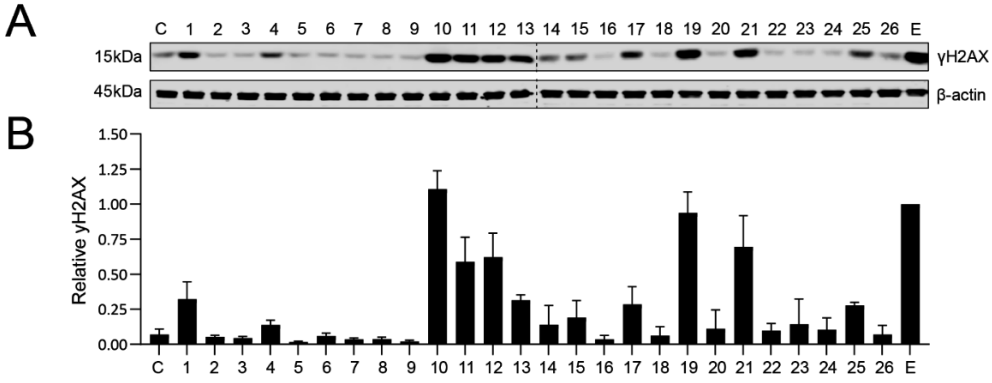

Figure S2 – DNA damage capacity of the full set of anthracycline derivatives 1-26. Numbers correspond to the structures in Figure 1, C; unmanipulated control. (A) K562 cells were treated for 2 h with *5 μM* of the indicated compounds, etoposide [E] was used as positive control. γH2AX levels were examined by Western blot. Actin was used as a loading control, and position of molecular weight markers is indicated. (B) Quantification of γH2AX signal normalized to the loading control. Results are presented as mean ± SD of three independent experiments.

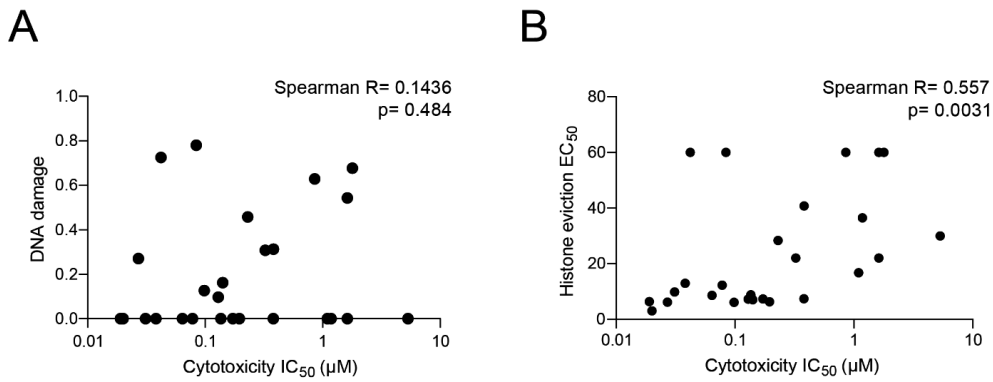

Figure S3 – (A) Correlation values between cytotoxicity (IC_{50}) and DNA damaging capacity (expressed as fraction of broken DNA). Graphical representation of the relationship between cytotoxicity and DNA damage capacity. (B) Correlation values between cytotoxicity (IC_{50}) and rate of histone eviction (EC_{50}). Graphical representation of the relationship between cytotoxicity and histone eviction rate.

B: Synthesis of compounds 6-26 and accompanying analytical data.
Available free of charge at https://pubs.acs.org/doi/10.1021/acs.jmedchem.3c00853.

CHAPTER 3

Genome-Wide CRISPR-Screening Identifies p53 as Regulator of Cancer Cell Sensitivity to the Histone Evicting Anthracycline Aclarubicin

Sabina Y. van der Zanden[1], Merle A. van Gelder[1], Amina Teunissen[1], Aart G. Jochemsen[1], Ruud H.M. Wijdeven[1,2] & Jacques Neefjes[1]

[1] Department of Cell and Chemical Biology, ONCODE institute, Leiden University Medical Center, 2333 ZC Leiden, The Netherlands.

[2] Alzheimer Center Amsterdam, department of Neurology, Amsterdam Neuroscience Amsterdam, University Medical Center Amsterdam, The Netherlands.

Submitted to Cell Death and Disease

Abstract

The anthracycline family, with its prime member doxorubicin, is one of the cornerstones in cancer chemotherapy and acts by poisoning topoisomerase II, resulting in DNA double stranded breaks. One of its members, aclarubicin, is considered a distinct member of the family due to its inability to inflict DNA double strand breaks. Despite this, aclarubicin is an effective anti-cancer drug by evicting histones resulting in chromatin damage. How aclarubicin-induced chromatin damage induces cell death remains largely unknown. Here, we performed a genome-wide CRISPR screen to identify factors regulating sensitivity of cells to aclarubicin and identified p53 as a critical factor for cellular sensitivity. Even though aclarubicin does not induce DNA breaks, treatment resulted in a swift initiation of the p53 DNA damage pathway by stabilization and activation of p53, and subsequent induction of apoptosis. Furthermore, response to aclarubicin treatment could fairly well be predicted in cell lines solely based on p53-status. These data suggest that p53 can be activated for apoptosis induction by at least two different pathways, DNA- and chromatin damage. Together, these data suggest p53 could be an important factor to stratify patients for the treatment with Aclarubicin.

Introduction

Aclarubicin belongs to the family of anthracycline drugs, which are among the most widely used anti-cancer drugs. Including other members like doxorubicin, epirubicin, daunorubicin and idarubicin, these drugs are used to treat a wide spectrum of tumors.[1,2] The classical mechanism of action of anthracyclines is poisoning of topoisomerase II, via intercalation of the compound into the DNA and formation of topoisomerase II-DNA complexes.[3,4] These formed adducts result in enzyme-mediated DNA double strand breaks, inducing activation of p53 and DNA damage response pathways for cell cycle arrest and/or cell death.[5] Aclarubicin, on the other hand, inhibits topoisomerase at a different step in the catalytic cycle, preventing enzyme binding to the DNA.[3,4] As a consequence, treatment with aclarubicin does not lead to induction of DNA breaks.[6–8] The anthracyclines differ from other topoisomerase II poisons, such as the podophyllotoxin etoposide, as that they have a second mechanism of action. When the anthraquinone moiety of anthracyclines intercalates into the DNA double helix, the sugar moiety emanates into the DNA minor groove and competes with histones for space, causing destabilization of nucleosomes and eviction of histones.[4,6,9] This activity has multiple consequences, including attenuated DNA damage responses, altered transcriptomics and deregulation of the epigenome at defined regions of the genome, collectively referred to as chromatin damage.[6,8] Evaluation of this activity amongst various anthracycline variants has shown that chromatin damage is essential to the effectivity of this class of anti-cancer drugs.[7,10,11] This is illustrated by the anthracycline amrubicin and the topoisomerase inhibitor etoposide, which are abstained from chromatin damage activity and considerably less effective.[7] Furthermore, the combination of DNA- and chromatin damage (as is the case for doxorubicin, epirubicin, daunorubicin and idarubicin) has been shown to conspire to cause a number of severe side effects [8], including dose-dependent cardiotoxicity, therapy-related malignancies and gonadotoxicity.[12,13] On the contrary, variants deficient for DNA damage activity, such as aclarubicin, lack the severe side effects displayed by the other family members.[7]

Although aclarubicin is an effective anti-cancer drug used for the treatment of AML patients[14], the mechanism by which chromatin damage leads to cell death is not fully understood. Therefore, we performed a genome-wide CRISPR knockout screen to identify regulators of aclarubicin sensitivity, yielding p53 as the most prominent hit. Indeed, p53 depletion decreased sensitivity to aclarubicin, and mutational status of p53 could be used as a proxy for sensitivity of cells to aclarubicin. Mechanistically, aclarubicin treatment leads to DNA-binding, phosphorylation and stabilization of p53, resulting in induction of apoptosis even in the absence of DNA breaks. Thus, chromatin damage induced by aclarubicin can be sensed by p53 and translated into a cellular response also observed in a DNA damage response leading to the induction of cell death. Together, this uncovers a second mechanism of induction of p53-mediated apoptosis by anthracycline cancer drugs.

Results

CRISPR-screening identifies p53 as regulator of aclarubicin sensitivity

Doxorubicin is a widely used chemotherapeutic that by intercalation into the DNA traps the enzyme topoisomerase II, forming a drug-DNA-enzyme adduct resulting in the formation of DNA double strand breaks.[3] Furthermore, intercalation into the DNA leads to the induces chromatin damage via eviction of histones (Fig. 1A).[6,15] Unlike doxorubicin, this dual action mechanism is not observed for all clinical relevant anthracyclines drugs, where amrubicin only induces DNA double strand breaks (Fig. 1A and S1A) and aclarubicin has only histone eviction activity (Fig. 1A and S1B). However, how chromatin damage activity induces cell death remains unclear. To identify proteins contributing to aclarubicin induced cell death following chromatin damage, we performed a genome-wide CRISPR knockout screen. MelJuSo melanoma cells were used as model cell line, since these are fairly sensitive to aclarubicin (IC_{50} of about 100nM) and take up the drug efficiently.[6,7] Cells were transduced with the Brunello genome-wide CRISPR library (4 gRNAs per gene) and treated five days later with aclarubicin for nine days at a concentration of 100nM (Fig. 1B). After this, surviving cells were harvested, genomic DNA was isolated, sequenced and compared to the untreated control. Hit calling was based on statistical significance in both biological replicates using RSA analysis, as well as an absolute fold enrichment of > 2.5 for at least 2 gRNAs per gene. This yielded two prominent hits: apoptotic TRAIL receptor DR4 (encoded by TNFRSF10A) and tumor suppressor p53 (TP53) (Fig. 1C and S1C). Lower hits included Caspase-8 and FADD, the two signaling adaptors for DR4, as well as the transcriptional regulators DR1 and CBFB. However, the fold enrichments for these hits were low, suggesting only a minor contribution of these genes to aclarubicin sensitivity. Overall, these results suggest a role for p53 and apoptotic signaling in aclarubicin sensitivity.

To validate the involvement of p53 in aclarubicin sensitivity, we transduced MelJuSo cells with the top two gRNAs from the screen, creating two different pools of p53-deficient cells. One of these yielded a robust depletion of p53, whereas gRNA #2 (which targets the domain of TP53 involved in DNA binding) lead to mutated p53 protein (Fig. 1D and S1D). Importantly, both cell lines were completely insensitive to treatment with the MDM2-inhibitor RG7112 that stabilizes p53, validating the generation of two functional TP53-knockout cell lines (Fig. 1E). These p53-knockout MelJuSo cells were more resistant to aclarubicin following continuous 72hrs exposure and short pulse treatment (Fig. 1F and S1E), as well as in long-term colony forming assays (Fig. 1G and H). Thus, our CRISPR-screen identified a role for p53 in sensitivity of cells to aclarubicin.

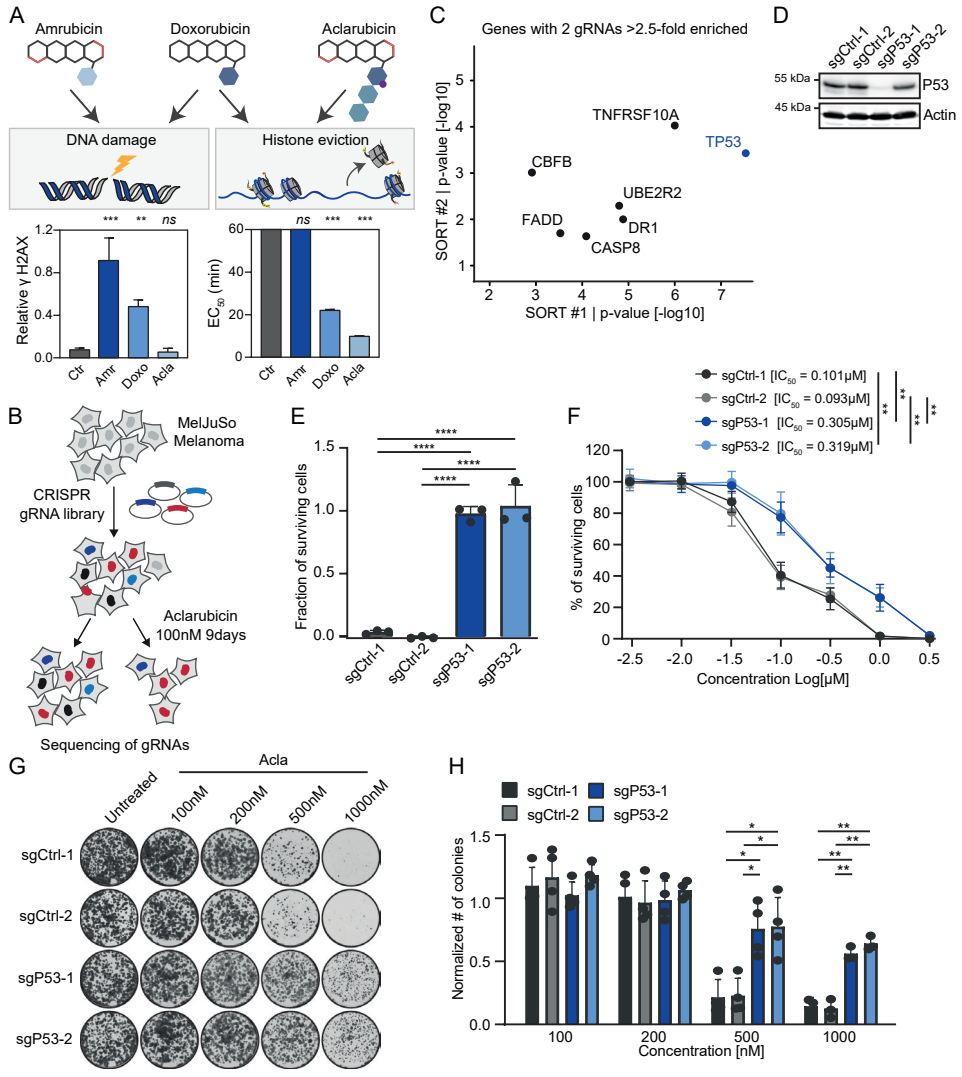

Fig. 1 genome-wide CRISPR screening identifies p53 as a regulator of sensitivity to Aclarubicin. **A** Top panel: Schematic overview of the DNA damage (via targeting topoisomerase II) and chromatin damage (via eviction of histones) activity of amrubicin, doxorubicin and aclarubicin. Bottom panel: DNA double strand breaks induced by these three anthracyclines upon treatment of 10μM for 2h in MelJuSo cells and histone eviction capacity of these drugs indicated by EC_{50} (time in which 50% of the histonen are evicted). Ordinary one-way ANOVA with multiple comparisons, ** p< 0.01, *** p< 0.001, **** p< 0.0001. **B** Schematic representation of the screening outline. MelJuSo melanoma cells were transduced with the Brunello genome-wide CRISPR knockout library, and cells were either or not treated with aclarubicin (100nM) for 9 days followed by gRNA sequencing. **C** Genes for which at least two different gRNAs were enriched (> 2.5-fold) in both aclarubicin-treated samples and which were significantly enriched based on RSA analysis. **D** MelJuSo cells transduced with the indicated CRISPR constructs were analyzed for p53-expression using Western blot.

Fig. 1 continued – **E** MelJuSo cells as in **C** were treated with HMD201 for 3 days and viability was assessed and normalized to untreated cells. N=3 independent experiments. Ordinary one-way ANOVA with multiple comparisons, **** p< 0.0001. **F** Indicated MelJuSo cells were treated for 2h with various concentrations of aclarubicin after which the drug was washed out and cells were left to grow for another 3 days before assessing cell viability. N=3 independent experiments. IC_{50} for each cell line is indicated. Two-tailed t-test, ** p< 0.01. **G** Colony formation assay for indicated MelJuSo cells. Cells were treated for 2h with aclarubicin, after which the drug was washed out and cells were left to grow out for 6-9 days before fixation and staining with Crystal Violet. **H** Quantification of four independent colony formation experiments, signal was normalized to the respective untreated cells. Ordinary two-way ANOVA with multiple comparisons, * p< 0.05, ** p< 0.01.

P53 is a major determinant in cellular sensitivity to aclarubicin

To test whether the function of p53 is conserved in multiple cell lines, we used the same approach to deplete p53 from 93.05 melanoma cells. In both long-term and short-term growth assays, p53-deficient cells were more resistant to aclarubicin (Fig. 2A and B and Fig. S2A). Similarly, p53-deficient MEL202 uveal melanoma and HCT116 colon lines were less sensitive to aclarubicin (Fig. 2C). To identify whether p53-status is a critical determinant for the sensitivity of cells to aclarubicin, we tested a panel of 16 different p53-wt and p53-mutant cell lines. Interestingly, based on the IC_{50}-values, the two groups almost completely segregated, arguing that the sensitivity of cells to aclarubicin can quite accurately be predicted based on p53-mutational status (Fig. 2D). This dependence on p53 activity suggests that aclarubicin might synergize with p53-stabilizing drugs. To test this, MelJuSo cells were incubated with low-dose of HDM201 (p53-MDM2 inhibitor) in the presence of different doses of aclarubicin. While aclarubicin single treatment already decreased cell viability, the combination treatment was even more effective, indicating that p53 stabilization by HDM201 acts synergistically with aclarubicin-induced chromatin damage activity (Fig. 2E). A similar observation was made for MEL202 cells, where co-treatment of the MDM2 antagonist RG7112 synergized with various concentrations of aclarubicin (Fig. 2F). These data indicate that p53 status is a major determinant for sensitivity towards the anthracycline drug aclarubicin.

Aclarubicin stabilizes and activates p53

The fact that aclarubicin induces histone eviction together with the involvement of p53 in cellular sensitivity suggests that p53 can sense the inflicted chromatin damage and subsequently translates this into a downstream signal. P53-activating signals, such as DNA damage, lead to p53 phosphorylation and stabilization, after which p53 induces the expression of target genes involved in cell cycle arrest and cell death.[16] To study the function of p53 upon induction of chromatin damage, we tested whether p53 levels were affected by aclarubicin exposure. Already after 2h of treatment, p53 stabilization and enhanced p53-S15 phosphorylation was observed by Western blot

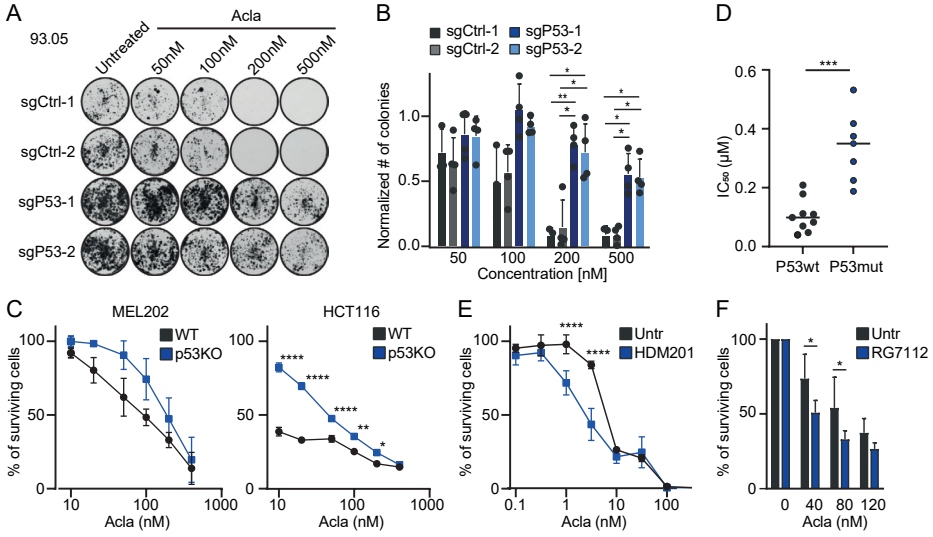

Fig. 2 p53 is a major determinant in the sensitivity of cells to aclarubicin. A Colony forming assay for 93.05 melanoma cells transduced with the indicated CRISPR constructs. Cells were treated with aclarubicin for 2h, washed and 7-9 days later fixed and stained with Crystal Violet. **B** Quantification of three independent experiments, signal was normalized to the respective untreated cells. Ordinary two-way ANOVA with multiple comparisons, * p< 0.05, ** p< 0.01. **C** Mel202 and HCT116 control cells or p53KO were treated with aclarubicin for 2h, washed, and 3 days later viability was assessed. Mel202 data represent a biological replicate, HCT116 data represent a technical triplicate. Ordinary two-way ANOVA with multiple comparisons, * p< 0.05, ** p< 0.01, **** p< 0.0001. **D** From 16 cell lines from different tissues (9 p53 WT and 7 p53 mutant) the IC_{50} was determined by exposing cells to aclarubicin for 2h and measuring viability three days later. IC_{50} represent the average of three independent experiments, and cell lines were clustered based on p53 status. Two-tailed t-test, *** p< 0.001. **E** MelJuSo cells were treated with the indicated concentrations of aclarubicin for 2h, drug was washed out, and 500nM HDM201 was added when indicated. Three days later, viability was measured and normalized to the untreated control either or not treated with HDM201. Data represent four independent experiments, Ordinary two-way ANOVA with multiple comparisons **** p< 0.0001. **F** MEL202 cells were treated for 2h with the indicated concentrations of aclarubicin, drug was washed away and cells were left to grow out in the presence or absence of 250nM RG7112. Three days later, cell viability was measured and normalized to the non-aclarubicin treated controls. Data represent three (120nM) or four (40 and 80nM) independent experiments. Statistical significance was determined by a Student's t-test * p< 0.05.

(Fig. 3A). In addition, aclarubicin treatment resulted in a p53-dependent increased expression of p53-target genes such as p21 (Fig. 3A, 3B), MDM2 and PUMA (Fig. 3B). For other genotoxic triggers, ATM kinase is activated by phosphorylation, subsequently inducing p53 phosphorylation.[17] ATM was also phosphorylated following aclarubicin

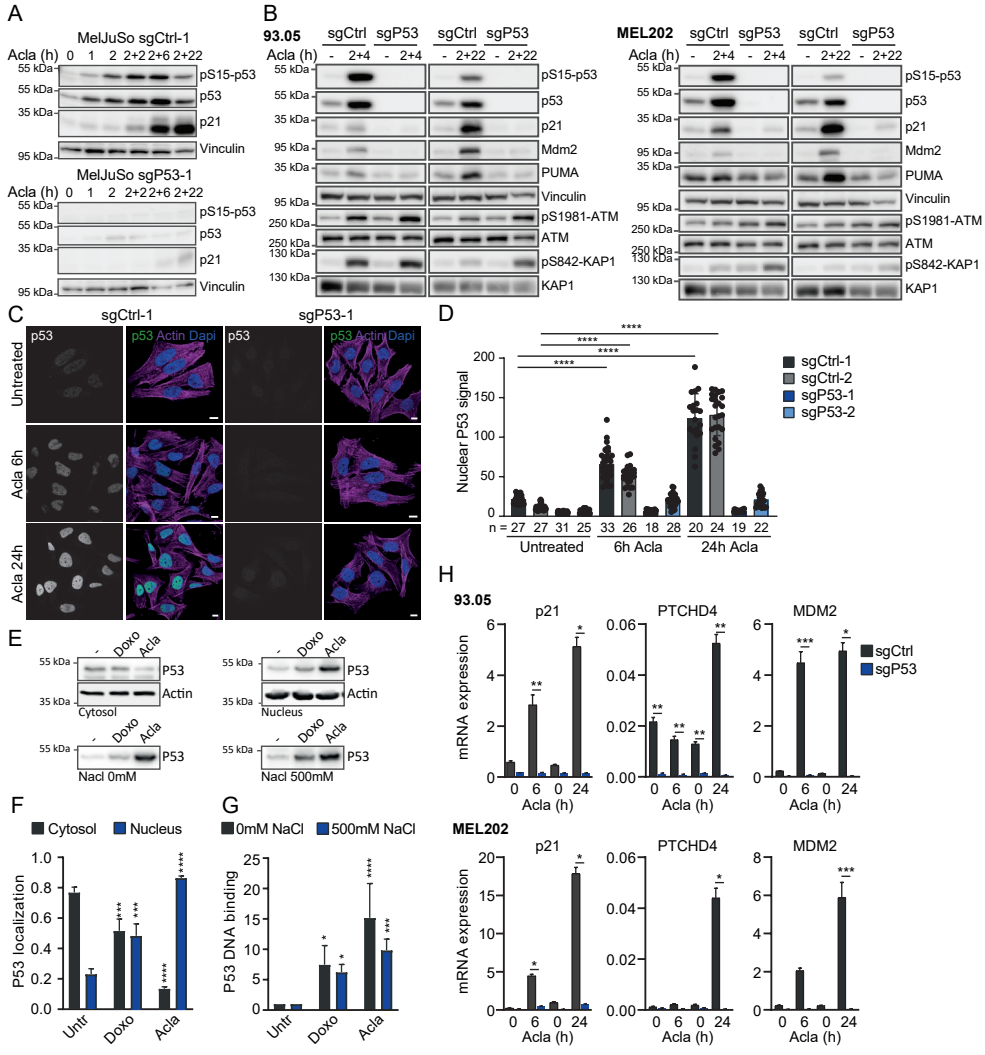

Fig. 3 Aclarubicin induces phosphorylation and activation of p53. A MelJuSo cells were exposed to 200nM aclarubicin for the indicated time points and washed away after maximum 2h, after which cells were left to recover for the indicated time points before lysis and analysis by Western blot. **B** 93.05 and MEL202 melanoma cells were exposed to aclarubicin for 2h, washed and lysed 4h or 22h later, before analysis of the indicated proteins by Western blot. **C** Representative confocal image of fixed MelJuSo cells stained for endogenous p53. Cells were treated with 200nM aclarubicin for 2h, washed and fixed at the indicated time points post treatment. DAPI and actin are stained as nuclear and cytosolic marker, respectively. Scale bar; 10µm. **D** Quantification of endogenous p53 levels. N = number of cells analyzed per condition. Ordinary two-way ANOVA with multiple comparison, **** $p < 0.0001$. **E** Chromatin binding assay for endogenous p53 in MelJuSo cells. Cells were treated with 10µM doxo- or aclarubicin for 45 minutes followed by fractionation. P53 localization and DNA binding was analyzed by Western Blot. **F** Quantification of cytosolic and nuclear p53 localization.

Fig. 3 continued – Ordinary two-way ANOVA with multiple comparisons *** p< 0.001, **** p< 0.0001. **G** Quantification of DNA binding. Ordinary two-way ANOVA with multiple comparisons * p< 0.05, *** p< 0.001, **** p < 0.0001. **H** 93.05 and MEL202 cells were exposed for 2h to 200nM aclarubicin and RNA was isolated 4h (6h) or 22h (24h) post treatment. Expression of indicated mRNA was detected using qRT-PCR and normalized to housekeeping gene expression.

N=2 independent experiments, data represent technical triplicates. Statistical significance was determined by a Student's t-test, * p<0.05, ** p< 0.01, *** p< 0.001.

treatment, as well as KAP1, another ATM substrate, suggesting that the histone evicting anthracycline aclarubicin likewise activates ATM and the subsequent stress response (Fig. 3B). Furthermore, nuclear stabilization for endogenous p53 by aclarubicin treatment was observed by microscopy (Fig. 3C and D and Fig. S3A).

To confirm that enhanced nuclear p53 also associated with DNA to drive transcription, we analyzed DNA-binding of p53 using a chromatin-association assay. Indeed, p53 was found to accumulate in the nucleus upon treatment with aclarubicin (doxorubicin was used as a positive control[18], while at the same time cytosolic p53 levels were diminished (Fig. 3E and F). Furthermore, aclarubicin treatment resulted in more p53 binding to DNA (Fig. 3E and G). To verify that aclarubicin treatment activates p53, subsequently leading to DNA binding and transcription of its target genes, we performed qRT-PCR experiments for different p53-target genes. Expression of several p53-target genes were drastically increased by aclarubicin, whereas expression of these genes was unaltered in p53-null cells upon aclarubicin treatment (Fig. 3H, S3B and S3C). Taken together, these data indicates that anthracycline variants that only have histone eviction activity, such as aclarubicin also activate p53 for increased expression of its target genes.

Aclarubicin activates p53 to induce apoptosis

p53 induces the expression of several pro-apoptotic genes[16], suggesting aclarubicin-induced p53 activation inflicts cell death via apoptosis. In line with this, several pro-apoptotic factors such as PUMA, DR4 and DR5 were upregulated by aclarubicin-treatment (Fig. 3B, 4A), whereas the anti-apoptotic factor survivin was downregulated (Fig. S4). Most of this effect was governed by p53, since it was absent in the p53-null cells. However, for some factors, such as the pro-apoptotic factors BIM and BMF, increased expression was also observed in the p53-deficient cells (Fig. 4A). Furthermore, direct apoptosis induction by aclarubicin was measured using a Caspase-GLO assays. In all three melanoma cell lines tested, a robust increase in caspase activation after aclarubicin was observed, which was largely absent in cells deficient for p53 (Fig. 4B). Similar results were obtained when detecting the cleavage of caspase substrate PARP by Western blot (Fig. 4C and D).

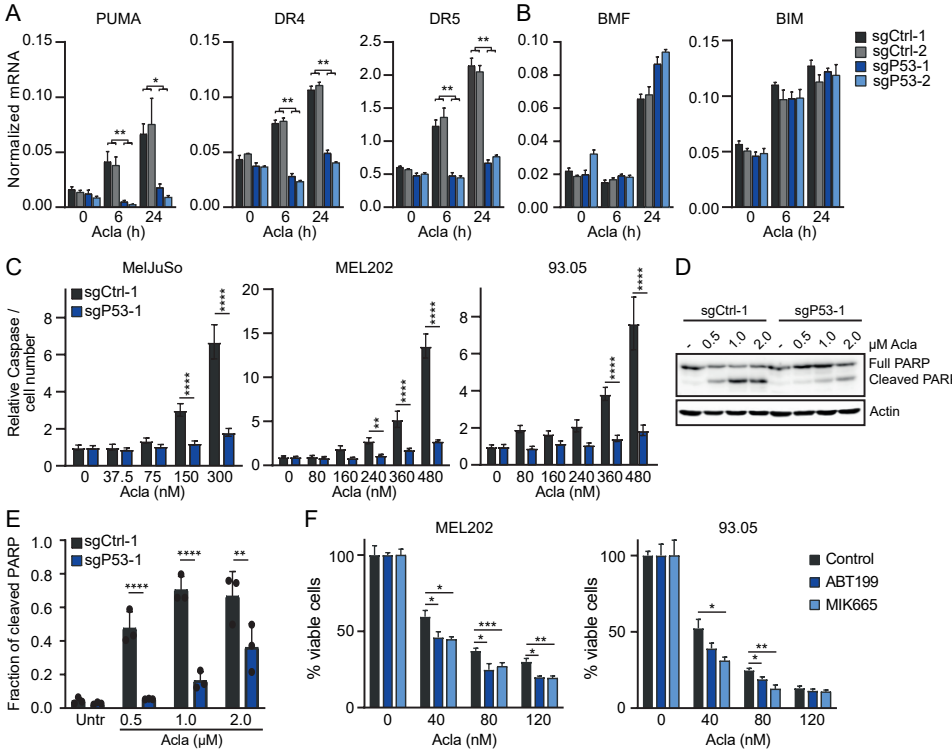

Fig. 4 Aclarubicin induces p53-dependent apoptosis. A-B Indicated MelJuSo cells were treated with 200nM aclarubicin for 2h and RNA was isolated 4h (6h) or 22h (24h) post treatment. Expression of indicated mRNA was detected using qRT-PCR and normalized to housekeeping gene expression. N=2 independent experiments, data represent technical triplicates. Statistical significance was determined by a Student's t-test, * p<0.05, ** p< 0.01. **C** Indicated cells were exposed to different concentrations of aclarubicin for 2h. Three days later cell viability and Caspase-Glo signal was detected. Caspase-Glo signal was normalized to the cell count. N=2 independent experiments, data represent technical triplicates. Two-way ANOVA with multiple comparisons, ** p< 0.01, **** p< 0.0001. **D** Indicated MelJuSo cells were exposed to different concentrations of aclarubicin for 2h, 24h post treatment cells were collected. PARP cleavage was analyzed by Western blot. Position of PARP and its cleaved form is indicated. Actin was used as a loading control. **E** Quantification of the fraction of cleaved PARP. Two-way ANOVA with multiple comparisons, ** p< 0.01, **** p< 0.0001. **F** Indicated cell lines were treated for 2h with different concentrations of aclarubicin, drug was washed away and cells were left to grow out in the presence or absence of 200nM MIK665 or 4uM ABT-199. Three days later, cell viability was measured and normalized to the non-aclarubicin treated controls. Data represent three independent experiments. Student's t-test * p< 0.05, ** p< 0.01, *** p< 0.001.

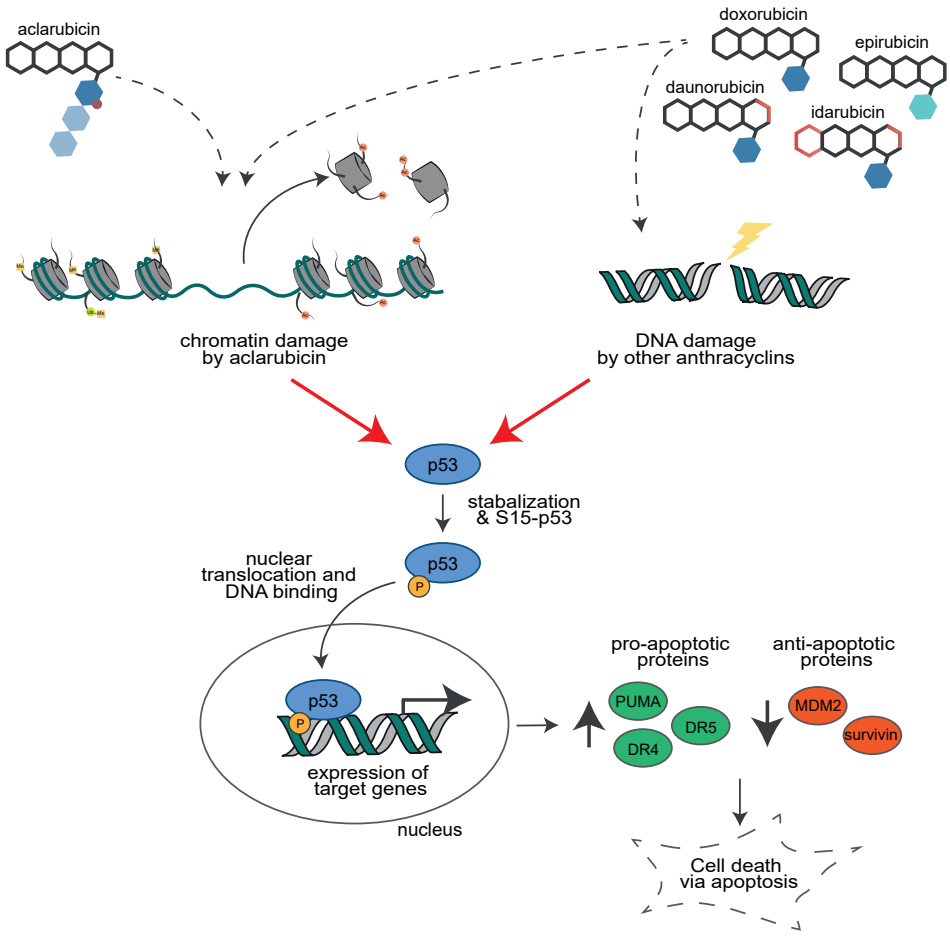

Fig. 5 Model of p53 mediated apoptosis upon anthracycline treatment. Topoisomerase II poisons like doxo-, dauno-, epi- and idarubicin introduce DNA damage via the formation of topoisomerase-DNA complexes. These drug-mediated DNA breaks subsequently leads to p53 activation. The histone evicting anthracycline aclarubicin can also inflicts p53 relocalization and activation of downstream signaling. Clinical anthracycline drugs (with both DNA- and chromatin damage) thus activate p53 dependent apoptosis by two different mechanism.

Several activators of apoptosis have been developed, such as inhibitors of the anti-apoptotic factors BCL-2 (ABT-199, also known as venetoclax) and MCL-1 (MIK665).[19] We tested whether these inhibitors synergize with aclarubicin treatment to increase cell toxicity. When using sublethal concentrations of either ABT-199 or MIK665, aclarubicin synergized with these inhibitors to tip the balance and induce cell death in all three melanoma cell lines (Fig. 4D, 4E). Thus, aclarubicin treatment leads to activation of p53, which then induces cell death via activation of the apoptosis pathway (Fig. 5).

Discussion

Aclarubicin has been considered a distinct member of the anthracycline family due to its inability to poison Topoisomerase II and inflict DNA double strand breaks. We and others have recently shown that its ability to evict histones is critical to its anti-cancer activity. But, how this activity translates to cell death has remained unclear. Using CRISPR-screening, we identified and established a key role for p53 in this process, where cellular sensitivity can be predicted fairly well solely based on p53-status. Furthermore, we showed that aclarubicin activates a p53-dependent transcriptional program inducing cell cycle arrest and apoptosis similar to DNA damaging compounds. Thus, even in the absence of DNA breaks, chromatin damage as caused by aclarubicin treatment can activate p53 and induce cell death. Thus, regular topoisomerase II-poisoning anthracyclines have two pathways initiating p53 activation for apoptosis; one initiated by the DNA damage response (as is the case for DNA damage inducing variant such as doxorubicin and daunorubicin) and the other one initiated by the chromatin damage response as visualized through the response to aclarubicin. Whether p53 itself can sense aclarubicin-induced chromatin damage or how p53 gets mobilized upon aclarubicin treatment remains to be elucidated. Possibly ATM plays a role in this, since we observe ATM activation shortly after aclarubicin treatment. In addition, in the absence of p53, apoptosis is still observed, but at greatly reduced efficiency. This implies that multiple chromatin damage sensing mechanisms might be in play.

Our data that chromatin damage activates p53 and induces apoptosis are in line with reports about other chromatin damaging agents such as the curaxins.[20,21] Curaxins can trap the FACT-complex on DNA, leading to activation of casein kinase 2(CK2) and thereby phosphorylation of p53 at Ser392. Aclarubicin treatment also induces FACT binding to DNA[21], suggesting that the aclarubicin- induced phosphorylation at p53 residue Ser392 we observe is likely mediated by FACT and CK2. However, this is likely not the sole mechanism of p53 activation. Where only p53 phosphorylation at Ser392 is observed for chromatin damage induced by curaxins[20,22], we identified additional swift induction of the DNA damage marker p53-Ser15 upon treatment with aclarubicin. This specific modification on p53 is likely induced by ATM, since we observe ATM activation determined by phosphorylation on residue Ser1981. The existence of multiple chromatin damage sensing mechanisms would also explain why we failed to identify any proteins of this pathway in the CRISPR screen. Upon p53 activation, several downstream signaling cascades are activated, leading to apoptosis. Whilst we observe p53-dependent apoptosis, and cell death is increased upon addition of apoptosis-activators, other forms of cell death are induced by aclarubicin as well, because blocking apoptosis using apoptosis inhibitor Z-VAD-FMK did not render cells significantly more resistant to aclarubicin (Fig. S5). Thus,

while p53-dependent apoptosis might be the dominant mechanism, in its absence cells will succumb via alternative pathways.

Aclarubicin is used for the treatment of acute myeloid leukemia (AML), as part of the CAG regimen (cytarabine, aclarubicin and G-CSF), both as first line treatment and for relapsed cases.[14,23,24] Our data suggest that p53-mutations would be a good stratification method for aclarubicin-treatment to identify which patients would benefit and simultaneously prevent that patients receive ineffective treatment. While p53 is mutated in only about 5-10% of the de novo AML cases, it is more frequently observed in therapy-related AML (25-33%).[25–28] In both cases, loss of p53 is strongly correlated with poor outcome and prognosis. Unfortunately, these patients will probably benefit less from an aclarubicin-based treatment, and other treatments have to be developed surpassing the prerequisite for p53. Alternatively, aclarubicin could still be effective in inducing cell death of p53-deficient cells, but then requires higher concentrations. This could be a basis for 'high-dose chemotherapy'. As aclarubicin lacks many treatment limiting side effects[7,14], using it at a higher dose can be considered. The stratification of the p53 status of AML and other tumors may be a reason to aim for normal or high-dose chemotherapies in the treatment of cancer patients. Recently, the BCL-2 inhibitor venetoclax (ABT-199) was approved as frontline treatment for AML, which is particularly useful for patients that are unable to tolerate classical intense chemotherapy, including older patients (>75 years old). Our data shows that aclarubicin synergizes with ABT-199 to increase cell toxicity, indicating that p53 wild-type AML patients would benefit from the combination therapy, with limited toxicity due to low adverse effects of both drugs.

In conclusion, we identified p53 as a major determinant in cellular sensitivity towards the anthracycline drug aclarubicin. While aclarubicin does not induce DNA double strand breaks, like other anthracycline family members, the chromatin damage induced by this drugs inflicts p53 relocalization and activation, resulting in p53 dependent apoptosis.

Materials and methods

Reagents

Aclarubicin (sc-200160) was purchased from Santa Cruz Biotechnology (USA) and dissolved in dimethylsulfoxide at 5mg/ml concentration, aliquoted and stored at -20°C for further use. Doxorubicin was obtained from Pharmachemie (the Netherlands). HDM201 and RG7112 were obtained from (Selleckchem), Venetoclax/ABT-199 (Tocris), MIK665 (MedChemExpress).

Cell culture

MelJuSo cells were cultured in IMDM supplemented with 8% fetal calf serum and cell line authentication was performed by Eurofins Genomics (19-ZE-000487). HEK293T cells (obtained from ATCC (CRL-3216)) and the cutaneous melanoma cell line 93.05 , a gift from Sjoerd van den Burg en Els Verdegaal (LUMC, Leiden, The Netherlands), were cultured in DMEM supplemented with 8% fetal calf serum. MEL202 cells were grown in mixture RPMI/DMEM-F12 + 10% FCS. The MEL202 cell line was provided by Dr. Bruce Ksander, Dept. Ophthalmology, Harvard University, Boston, USA. The generation of monoclonal p53-KO derivatives of 93.05 and MEL202 cells has been described.[29] HCT116-Ctrl and p53KO cells were a gift from Bert Vogelstein and grown in DMEM/10% FCS.[30] p53-wildtype (A549, FM3, HeLa, MelJuSo, U2OS, U87) and p53-mutant (BT474, BXPC3, DU145, K562, PC3, SKBR3 and U118) cells were cultured and tested as described before.[10] All cell lines were maintained in a humidified atmosphere of 5% CO_2 at 37°C and regularly tested for the absence of mycoplasma.

CRISPR-activation and knockout screen

For knockout screening, the human CRISPR Brunello genome-wide knockout library was a gift from David Root and John Doench (Addgene #73178). Two batches of $1x10^8$ MelJuSo melanoma cells were infected at an MOI of 0.3. Transduced cells were selected using puromycin (1µg/ml) for five days. After the selection procedure, cells were treated continuously with aclarubicin at a concentration of 100nM for 9 days. After this, cells were grown out for an additional 3 days and genomic DNA was isolated from the aclarubicin-treated cells, as well as from the control population that was grown in parallel. gDNAs were amplified using the established protocol.[31] gRNAs were sequenced using the Illumina NovaSeq6000 and inserts were mapped to the reference. Statistical analysis was done using RSA analysis, enrichment >2.5 was considered a candidate hit.[32]

Transductions

For the generation of viral particles, HEK293T cells were transfected using polyethyleneimine (Polyscience Inc.) with packaging plasmids pRSVrev, pHCMV-G VSV-G and pMDLg/pRRE in combination with the lentiviral construct. Virus was harvested, filtered and target cells were transduced in the presence of 8µg/ml polybrene (Millipore).

Hit validation and subcloning

For validation of the knockout screen, two individual guides per gene were cloned into the LentiCRISPR v2 vector (a gift from Feng Zhang, Addgene plasmid #52961) and the indicated cells were transduced and selected using puromycin. Guide sequences were as follows: p53-1: 5'-CCATTGTTCAATATCGTCCG-3', p53-2: 5'- GGTGCCCTATGAGCCGCCTG-3'. For genomic validation, genomic DNA was isolated and a PCR fragment of ±300bp was cloned into an emptied GFP-C1 vector (clonetech) using NEBBuilder HiFi fidelity assembly mix using the

following primers: p53-1-fw: ATATCTGGAGTTCCGCATATGGGTAAGGACAAGGGTTGGGC, p53-1-rv: CGCTCTAGATCCGGTGGATCCGGAAGGGACAGAAGATGACAGGG, p53-2-fw: ATATCTGGAGTTCCGCATATGGTCCCCAGGCCTCTGATTC, p53-2-rv: CGCTCTAGATCCGGTGGATCCGAGGCCCTTAGCCTCTGTAAGC. Sequences were verified using Ori Fw: GGAGCCTATGGAAAAACGCC and Ori rv: TTAACGCTTACAATTTACGCG.

Long-term proliferation assays

Cells were seeded into 12-well plates (5000 cells/well). The next day, drugs were added at concentrations indicated and incubated for 2 hours. Subsequently, cells were washed extensively and left to grow for 7 to 9 days. For fixing and staining, cells were washed with PBS and incubated for 20 min at RT with Crystal violet staining solution (0.05% w/v Crystal Violet, 1% formaldehyde, 1% methanol in 1X PBS). Quantification of colonies was done by extraction of the crystal violet. To do so, colonies were incubated for 20 min. at RT with 15% acetic acid (500µL). Read out was done by measuring the absorbance using a CLARIOstar plate reader (BMG Labtech).

Short-term growth assays

Cells were seeded into 96-well plates and exposed the next day with indicated drugs and concentrations. When indicated, drugs were removed two hours later and cells were cultured for an additional 72 hours. Cell viability was measured using the CellTiter-Blue viability assay (Promega). Relative survival was normalized to the untreated control and corrected for background signal.

Apoptosis assay

Cells were seeded in triplicate in white-walled 96-well plates with clear bottoms and in clear 96-well plates. The next day, the cells were exposed to indicated compound(s). Three days later, caspase 3 /7 activity was assessed with the use of the Caspase-Glo 3/7 Assay (Promega), and cell viability was assessed with the CellTiter-Blue Cell Viability Assay. Relative caspase activity was normalized to cell number.

Chromatin association assay

Cells were seeded into 6cm dishes (1x10^6 cells/well). The next day, indicated drugs were added for 30 min. at 10µM final concentration. Cells were lysed in lysis buffer (25mM HEPES pH 7.6, 5mM $MgCl_2$, 25mM KCl, 0.05mM EDTA, 10% glycerol, 0.1% NP-40) for 30 minutes at 4°C and nuclei were spun down and resuspended in 75µL buffer (20mM Tris-HCl pH 7.6, 3mM EDTA). Of this, 25µL samples were adjusted to the indicated NaCl concentrations to a total volume of 50µL and incubated for 20 min. on ice. Subsequently, chromatin was spun down and resuspended in SDS-sample buffer (2% SDS, 10% glycerol, 5% β-mercaptoethanol, 60 mM Tris-HCl pH 6.8 and 0.01% bromophenol blue) after which samples were analyzed by SDS-PAGE and Western blotting.

Western blot

Upon treatment as indicated, cells were washed extensively to remove drugs. Cells were collected and lysed directly in SDS-sample buffer (2% SDS, 10% glycerol, 5% β-mercaptoethanol, 60 mM Tris-HCl pH 6.8 and 0.01% bromophenol blue). Lysates were resolved by SDS/PAGE followed by Western blotting. Primary antibodies used for blotting: P53 (DO-1, sc-126 Santa Cruz), γH2AX (1:1000, 05-036, Millipore), β-actin (A5441, Sigma), pS15p-53 (#9284, Cell Signaling Technology), pS1981-ATM (Clone 10H11.E12; Rockland Immunochemicals), ATM (Clone Y170; Merck Millipore), pS842-KAP1 (A300-767A; Bethyl Laboratories), KAP1 (A300-274A; Bethyl Laboratoris), Mdm2 (Clone 3G9; Merck Millipore), PUMA (Clone G3; Santa Cruz Biotechnology), p21 (clone CP74; Merck Millipore), PARP (#9542, Cell Signaling Technology), Vinculin (clone hVIN-1; Sigma-Aldrich). Images were quantified with ImageJ.

Microscopy

For endogenous p53 staining cells were seeded on coverslips, and the next day exposed for the indicated time with 200nM aclarubicin. Upon treatment, cells were fixed in 4% formaldehyde, permeabilized with 0.1% Triton, blocked in 0.5% BSA and stained with mouse monoclonal anti-P53 (DO1, sc-126, Santa Cruz), goat-anti-mouse-Alexa-Fluor-488 (Thermo fisher Scientific), Alexa-Fluor-647-phalloidin (A22287, Thermo fisher Scientific) and DAPI. Cells were analyzed by a Leica SP8 confocal microscope system with 63x lens. Cells stably expressing PAGFP-H2A were used for histone eviction experiments. Photoactivation and time-lapse confocal imaging were performed as described [6] and loss of fluorescence from the photoactivated region after different treatments was quantified. Quantification was done using ImageJ software.

RT-PCR

RNA was isolated using the SV total RNA isolation kit (Promega), after which cDNA was synthesized using the reverse transcriptase reaction mixture as indicated by Promega. qPCR was performed using SYBR green mix (Roche Diagnostics, Indianapolis, IN, USA) in a C1000 touch Thermal Cycler (Bio-Rad laboratories, Hercules, CA, USA). In independent experiments the expression of target genes was determined and normalized to at least two housekeeping genes *CAPNS1* and *SRPR*. Primers for detection:

Primer name	Sequence Forward	Sequence Reverse
BIM/BCL2L11	5′-CATCGCGGTATTCGGTTC	5′-GCTTTGCCATTTGGTCTTTTT
BMF	5′-TTTATGGCAATGCTGGCTATCG	5′-GCAATCTGTACCTCTGCTTGATG
CAPNS1	5′-ATGGTTTTGGCATTGACACATG	5′-GCTTGCCTGTGGTGTCGC
CDKN1A/p21	5′-AGCAGAGGAAGACCATGTGGA	5′-AATCTGTCATGCTGGTCTGCC
DR4/TNFRSF10A	5′-CTACCTCCATGGGACAGCAC	5′-TGCAGCTGAGCTAGGTACGA
DR5/TNFRSF10B	5′-AAGACCCTTGTGCTCGTTGT	5′-AGGTGGACACAATCCCTCTG
MDM2	5′-ACGCACGCCACTTTTTCTCT	5′-TCCGAAGCTGGAATCTGTGAG
NOXA	5′ ACTGTTCGTGTTCAGCTC	5′- AGCACACTCGACTTCC
PTCHD4	5′- TATTTTGCTCCAGGCTGAGG	5′-ATGGCTCTGGCTGACTTGAC
PUMA/BBC3	5′-GACCTCAACGCACAGTA	5′- TAATTGGGCTCCATCT
SRPR	5′-CATTGCTTTTGCACGTAACCAA	5′-ATTGTCTTGCATGCGGCC
Survivin	5′-AAAGCATTCGTCCGGTTG	5′-TCCGCAGTTTCCTCAAATTC

Data and statistical analysis

For in vitro experiment, each sample was assayed in biological triplicate, unless stated otherwise. No statistical methods were used to predetermine sample size. All error bars denote mean + SD. Statistical analysis were performed using Prism 8 software (Graphpad Inc.) or Microsoft excel. Western blot and confocal data were quantified using ImageJ software. Significance is represented on the graphs as follow: ns, not significant, *$p < 0.05$, **$p < 0.01$, ***$p < 0.001$, ****$p < 0.0001$.

Acknowledgements

This work was supported by the Institute for Chemical Immunology, an NWO Gravitation project funded by the Ministry of Education, Culture and Science of the Netherlands and a Spinoza award both to J.N. We thank J.J Akkermans for help with the genomic validation of the MelJuSo P53 KO lines.

References

(1) Hortobágyi, G. N. Anthracyclines in the Treatment of Cancer. An Overview. *Drugs*. **1997**, *54 Suppl 4*, 1–7.

(2) Martins-Teixeira, M. B.; Carvalho, I. Antitumour Anthracyclines: Progress and Perspectives. *ChemMedChem*. **2020**, *15*, 933–948.

(3) Nitiss, J. L. Targeting DNA Topoisomerase II in Cancer Chemotherapy. *Nature Reviews Cancer 2009 9:5*. **2009**, *9*, 338–350.

(4) van der Zanden, S. Y.; Qiao, X.; Neefjes, J. New Insights into the Activities and Toxicities of the Old Anticancer Drug Doxorubicin. *The FEBS Journal*. **2021**, *288*, 6095–6111.

(5) Perego, P.; Corna, E.; De Cesare, M.; Gatti, L.; Polizzi, D.; Pratesi, G.; Supino, R.; Zunino, F. Role of Apoptosis and Apoptosis-Related Genes in Cellular Response and Antitumor Efficacy of Anthracyclines. *Current medicinal chemistry*. **2001**, *8*, 31–37.

(6) Pang, B.; Qiao, X.; Janssen, L.; Velds, A.; Groothuis, T.; Kerkhoven, R.; Nieuwland, M.; Ovaa, H.; Rottenberg, S.; Van Tellingen, O.; Janssen, J.; Huijgens, P.; Zwart, W.; Neefjes, J. Drug-Induced Histone Eviction from Open Chromatin Contributes to the Chemotherapeutic Effects of Doxorubicin. *Nature Communications 2013 4:1*. **2013**, *4*, 1–13.

(7) Qiao, X.; Van Der Zanden, S. Y.; Wander, D. P. A.; Borràs, D. M.; Song, J. Y.; Li, X.; Duikeren, S. Van; Gils, N. Van; Rutten, A.; Herwaarden, T. Van; Tellingen, O. Van; Giacomelli, E.; Bellin, M.; Orlova, V.; Tertoolen, L. G. J.; Gerhardt, S.; Akkermans, J. J.; Bakker, J. M.; Zuur, C. L.; Pang, B.; Smits, A. M.; Mummery, C. L.; Smit, L.; Arens, R.; Li, J.; Overkleeft, H. S.; Neefj, J. Uncoupling DNA Damage from Chromatin Damage to Detoxify Doxorubicin. *Proceedings of the National Academy of Sciences of the United States of America*. **2020**, *117*, 15182–15192.

(8) Pang, B.; de Jong, J.; Qiao, X.; Wessels, L. F. A.; Neefjes, J. Chemical Profiling of the Genome with Anti-Cancer Drugs Defines Target Specificities. *Nature chemical biology*. **2015**, *11*, 472–480.

(9) Yang, F.; Kemp, C. J.; Henikoff, S. Anthracyclines Induce Double-Strand DNA Breaks at Active Gene Promoters. *Mutation Research/Fundamental and Molecular Mechanisms of Mutagenesis*. **2015**, *773*, 9–15.

(10) Wander, D. P. A.; Van Der Zanden, S. Y.; Van Der Marel, G. A.; Overkleeft, H. S.; Neefjes, J.; Codée, J. D. C. Doxorubicin and Aclarubicin: Shuffling Anthracycline Glycans for Improved Anticancer Agents. *Journal of Medicinal Chemistry*. **2020**, *63*, 12814–12829.

(11) Wander, D. P. A.; van der Zanden, S. Y.; Vriends, M. B. L.; van Veen, B. C.; Vlaming, J. G. C.; Bruyning, T.; Hansen, T.; van der Marel, G. A.; Overkleeft, H. S.; Neefjes, J. J. C.; Codée, J. D. C. Synthetic (N , N -Dimethyl)Doxorubicin Glycosyl Diastereomers to Dissect Modes of Action of Anthracycline Anticancer Drugs. *The Journal of Organic Chemistry*. **2021**, *86*, 5757–5770.

(12) Lotrionte, M.; Biondi-Zoccai, G.; Abbate, A.; Lanzetta, G.; D'Ascenzo, F.; Malavasi, V.; Peruzzi, M.; Frati, G.; Palazzoni, G. Review and Meta-Analysis of Incidence and Clinical Predictors of Anthracycline Cardiotoxicity. *The American journal of cardiology*. **2013**, *112*, 1980–1984.

(13) Mistry, A. R.; Felix, C. A.; Whitmarsh, R. J.; Mason, A.; Reiter, A.; Cassinat, B.; Parry, A.; Walz, C.; Wiemels, J. L.; Segal, M. R.; Adès, L.; Blair, I. A.; Osheroff, N.; Peniket, A. J.; Lafage-Pochitaloff, M.; Cross, N. C. P.; Chomienne, C.; Solomon, E.; Fenaux, P.; Grimwade, D. DNA Topoisomerase II in Therapy-Related Acute Promyelocytic Leukemia. *New England Journal of Medicine*. **2005**, *352*, 1529–1538.

(14) Qiao, X.; van der Zanden, S. Y.; Li, X.; Tan, M.; Zhang, Y.; Song, J. Y.; van Gelder, M. A.; Hamoen, F. L.; Janssen, L.; Zuur, C. L.; Pang, B.; van Tellingen, O.; Li, J.; Neefjes, J. Diversifying the

Anthracycline Class of Anti-Cancer Drugs Identifies Aclarubicin for Superior Survival of Acute Myeloid Leukemia Patients. *Molecular Cancer*. **2024**, *23*, 1–16.

(15) Yang, F.; Kemp, C. J.; Henikoff, S. Doxorubicin Enhances Nucleosome Turnover around Promoters. *Current biology : CB*. **2013**, *23*, 782–787.

(16) Lavin, M. F.; Gueven, N. The Complexity of P53 Stabilization and Activation. *Cell Death & Differentiation 2006 13:6*. **2006**, *13*, 941–950.

(17) Canman, C. E.; Lim, D. S.; Cimprich, K. A.; Taya, Y.; Tamai, K.; Sakaguchi, K.; Appella, E.; Kastan, M. B.; Siliciano, J. D. Activation of the ATM Kinase by Ionizing Radiation and Phosphorylation of P53. *Science (New York, N.Y.)*. **1998**, *281*, 1677–1679.

(18) Scala, F.; Brighenti, E.; Govoni, M.; Imbrogno, E.; Fornari, F.; Treré, D.; Montanaro, L.; Derenzini, M. Direct Relationship between the Level of P53 Stabilization Induced by RRNA Synthesis-Inhibiting Drugs and the Cell Ribosome Biogenesis Rate. *Oncogene*. **2016**, *35*, 977–989.

(19) Mukherjee, N.; Skees, J.; Todd, K. J.; West, D. A.; Lambert, K. A.; Robinson, W. A.; Amato, C. M.; Couts, K. L.; Van Gullick, R.; MacBeth, M.; Nassar, K.; Tan, A. C.; Zhai, Z.; Fujita, M.; Bagby, S. M.; Dart, C. R.; Lambert, J. R.; Norris, D. A.; Shellman, Y. G. MCL1 Inhibitors S63845/MIK665 plus Navitoclax Synergistically Kill Difficult-to-Treat Melanoma Cells. *Cell death & disease*. **2020**, *11*.

(20) Gasparian, A. V.; Burkhart, C. A.; Purmal, A. A.; Brodsky, L.; Pal, M.; Saranadasa, M.; Bosykh, D. A.; Commane, M.; Guryanova, O. A.; Pal, S.; Safina, A.; Sviridov, S.; Koman, I. E.; Veith, J.; Komar, A. A.; Gudkov, A. V.; Gurova, K. V. Curaxins: Anticancer Compounds That Simultaneously Suppress NF-KB and Activate P53 by Targeting FACT. *Science Translational Medicine*. **2011**, *3*.

(21) Nesher, E.; Safina, A.; Aljahdali, I.; Portwood, S.; Wang, E. S.; Koman, I.; Wang, J.; Gurova, K. V. Role of Chromatin Damage and Chromatin Trapping of FACT in Mediating the Anticancer Cytotoxicity of DNA-Binding Small Molecule Drugs. *Cancer research*. **2018**, *78*, 1431.

(22) Luzhin, A.; Rajan, P.; Safina, A.; Leonova, K.; Stablewski, A.; Wang, J.; Robinson, D.; Isaeva, N.; Kantidze, O.; Gurova, K. Comparison of Cell Response to Chromatin and DNA Damage. *Nucleic acids research*. **2023**, *51*, 11836–11855.

(23) Wei, G.; Ni, W.; Chiao, J. W.; Cai, Z.; Huang, H.; Liu, D. A Meta-Analysis of CAG (Cytarabine, Aclarubicin, G-CSF) Regimen for the Treatment of 1029 Patients with Acute Myeloid Leukemia and Myelodysplastic Syndrome. *Journal of hematology & oncology*. **2011**, *4*.

(24) Jin, J.; Wang, J. X.; Chen, F. F.; Wu, D. P.; Hu, J.; Zhou, J. F.; Hu, J. Da; Wang, J. M.; Li, J. Y.; Huang, X. J.; Ma, J.; Ji, C. Y.; Xu, X. P.; Yu, K.; Ren, H. Y.; Zhou, Y. H.; Tong, Y.; Lou, Y. J.; Ni, W. M.; Tong, H. Y.; Wang, H. F.; Mi, Y. C.; Du, X.; Chen, B. A.; Shen, Y.; Chen, Z.; Chen, S. J. Homoharringtonine-Based Induction Regimens for Patients with de-Novo Acute Myeloid Leukaemia: A Multicentre, Open-Label, Randomised, Controlled Phase 3 Trial. *The Lancet. Oncology*. **2013**, *14*, 599–608.

(25) Daver, N. G.; Iqbal, S.; Huang, J.; Renard, C.; Lin, J.; Pan, Y.; Williamson, M.; Ramsingh, G. Clinical Characteristics and Overall Survival among Acute Myeloid Leukemia Patients with TP53 Gene Mutation or Chromosome 17p Deletion. *American journal of hematology*. **2023**, *98*, 1176–1184.

(26) Papaemmanuil, E.; Gerstung, M.; Bullinger, L.; Gaidzik, V. I.; Paschka, P.; Roberts, N. D.; Potter, N. E.; Heuser, M.; Thol, F.; Bolli, N.; Gundem, G.; Van Loo, P.; Martincorena, I.; Ganly, P.; Mudie, L.; McLaren, S.; O'Meara, S.; Raine, K.; Jones, D. R.; Teague, J. W.; Butler, A. P.; Greaves, M. F.; Ganser, A.; Döhner, K.; Schlenk, R. F.; Döhner, H.; Campbell, P. J. Genomic Classification and Prognosis in Acute Myeloid Leukemia. *The New England journal of medicine*. **2016**, *374*, 2209–2221.

(27) George, B.; Kantarjian, H.; Baran, N.; Krocker, J. D.; Rios, A. TP53 in Acute Myeloid Leukemia: Molecular Aspects and Patterns of Mutation. *International journal of molecular sciences*. **2021**, *22*.

(28) Wong, T. N.; Ramsingh, G.; Young, A. L.; Miller, C. A.; Touma, W.; Welch, J. S.; Lamprecht, T. L.; Shen, D.; Hundal, J.; Fulton, R. S.; Heath, S.; Baty, J. D.; Klco, J. M.; Ding, L.; Mardis, E. R.; Westervelt, P.; Dipersio, J. F.; Walter, M. J.; Graubert, T. A.; Ley, T. J.; Druley, T. E.; Link, D. C.; Wilson, R. K. Role of TP53 Mutations in the Origin and Evolution of Therapy-Related Acute Myeloid Leukaemia. *Nature*. **2015**, *518*, 552–555.

(29) Heijkants, R. C.; Teunisse, A. F. A. S.; de Jong, D.; Glinkina, K.; Mei, H.; Kielbasa, S. M.; Szuhai, K.; Jochemsen, A. G. MDMX Regulates Transcriptional Activity of P53 and FOXO Proteins to Stimulate Proliferation of Melanoma Cells. *Cancers*. **2022**, *14*, 4482.

(30) Bunz, F.; Dutriaux, A.; Lengauer, C.; Waldman, T.; Zhou, S.; Brown, J. P.; Sedivy, J. M.; Kinzler, K. W.; Vogelstein, B. Requirement for P53 and P21 to Sustain G2 Arrest after DNA Damage. *Science (New York, N.Y.)*. **1998**, *282*, 1497–1501.

(31) Joung, J.; Konermann, S.; Gootenberg, J. S.; Abudayyeh, O. O.; Platt, R. J.; Brigham, M. D.; Sanjana, N. E.; Zhang, F. Genome-Scale CRISPR-Cas9 Knockout and Transcriptional Activation Screening. *Nature Protocols 2017 12:4*. **2017**, *12*, 828–863.

(32) König, R.; Chiang, C. Y.; Tu, B. P.; Yan, S. F.; DeJesus, P. D.; Romero, A.; Bergauer, T.; Orth, A.; Krueger, U.; Zhou, Y.; Chanda, S. K. A Probability-Based Approach for the Analysis of Large-Scale RNAi Screens. *Nature methods*. **2007**, *4*, 847–849.

Supporting information chapter 3

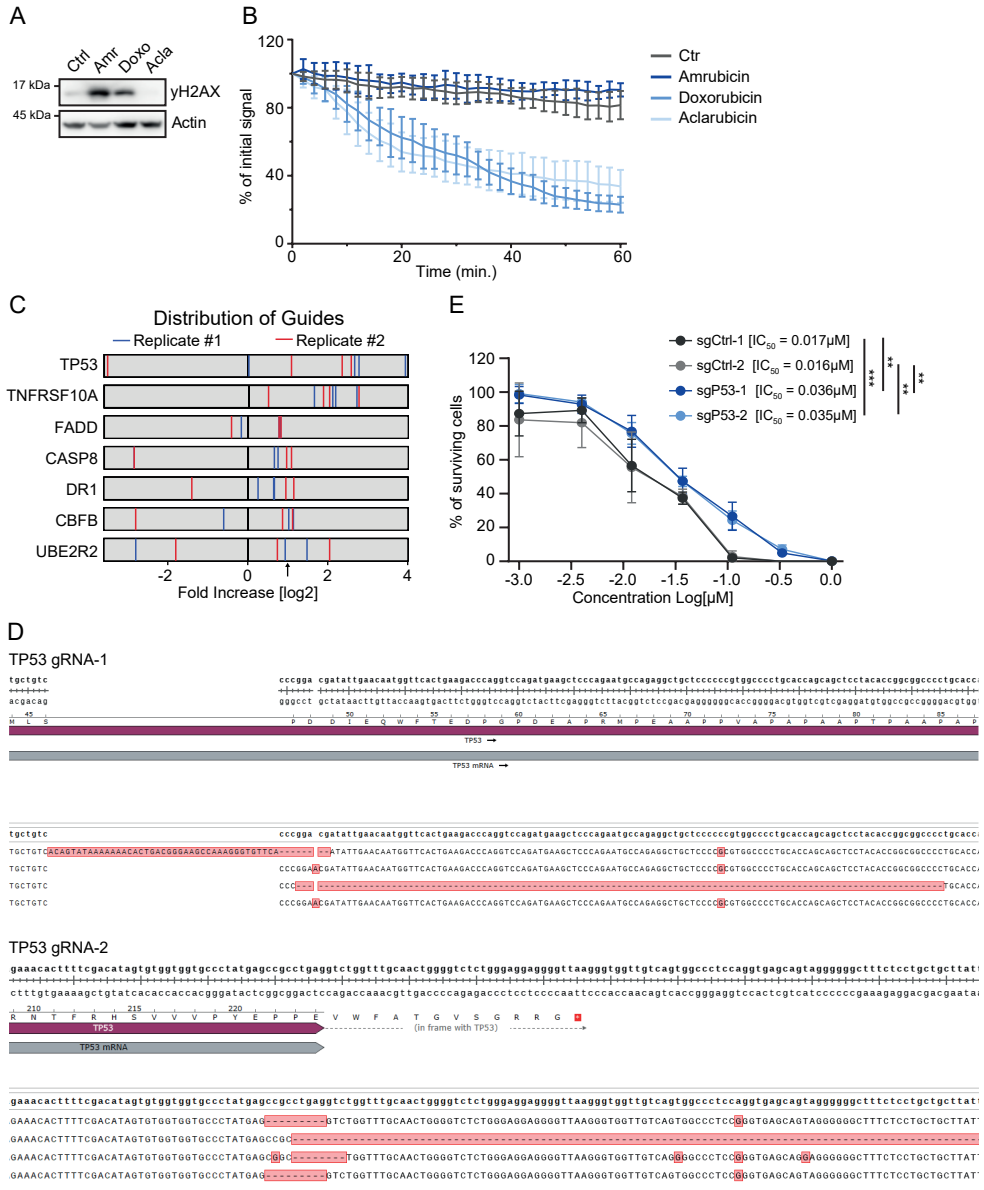

Fig. S1 p53 as a regulator of sensitivity to aclarubicin. A Western blot showing DNA double strand breaks induced by three different anthracycline drugs in MelJuSo cells treated for 2hr with 10uM. Actin was used as a loading control. Corresponding to quantification in Fig. 1A, bottom panel. **B** Fluorescent signal of photo activated GFP-H2A histones was followed in living cells over time upon treatment with the different drugs. Quantification of loss of initial signal upon histone eviction is plotted. Corresponding to quantification of EC_{50} in Fig. 1A, bottom panel.

Fig S1. Continued – **C** gRNA enrichment for hits with at least two guides per sort enriched >2.5-fold. Arrow depicts 2.5-fold threshold and red and blue stripes represent enrichment of individual gRNAs compared to the non-sorted population. **D** Snapshot of Snapgene, showing genomic validation of pooled MelJuSo P53-knock out cell lines. **E** Indicated MelJuSo cells were treated for 72h with various concentrations of aclarubicin followed by assessing the cell viability. N=3 independent experiments. IC_{50} for each cell line is indicated. Two-tailed t-test, ** p< 0.01, *** p< 0.001.

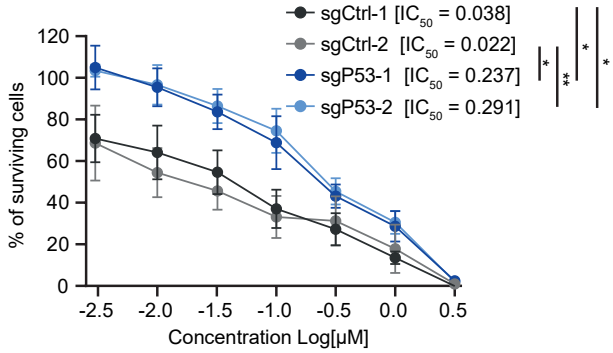

Fig. S2 p53 as a major determinant in sensitivity to Aclarubicin. Indicated 93.05 cells were treated for 2h with various concentrations of aclarubicin after which the drug was washed out and cells were left to grow for another 3 days before assessing cell viability. N=3 independent experiments. IC_{50} for each cell line is indicated. Two-tailed t-test, * p< 0.05, ** p< 0.01.

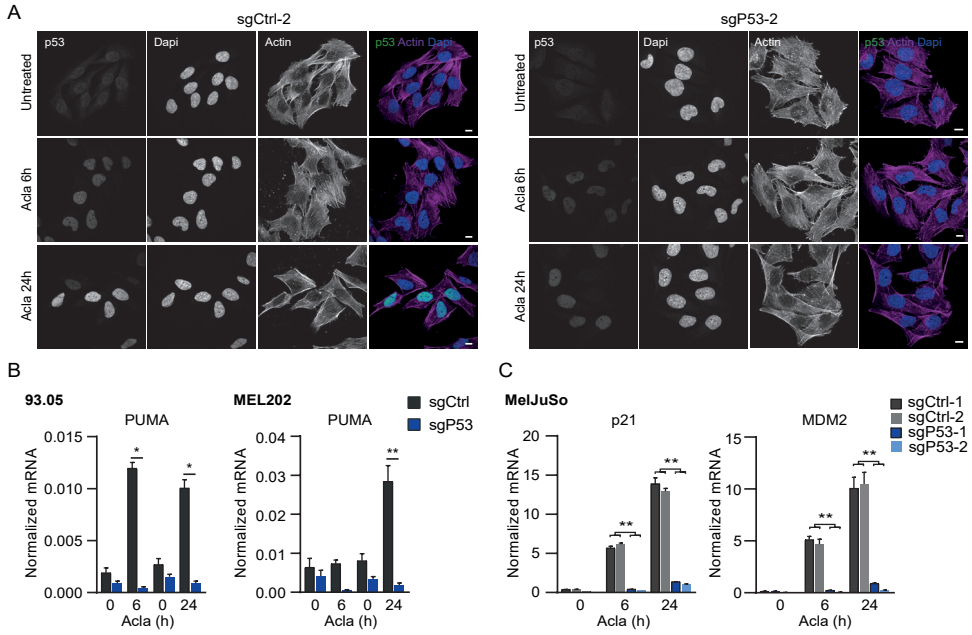

Fig. S3 Aclarubicin induces nuclear accumulation and activation of p53. A Representative confocal images of fixed MelJuSo cells stained for endogenous p53. Cells were treated with 200nM aclarubicin for 2h, washed and fixed at the indicated time points post treatment. DAPI and actin are stained as nuclear and cytosolic marker, respectively. Scale bar; 10µm. **B** 93.05 and MEL202 cells were exposed for 2h to 200nM aclarubicin and RNA was isolated 4h (6h) or 22h (24h) post treatment. Expression of indicated mRNA was detected using qRT-PCR and normalized to housekeeping gene expression. N=2 independent experiments, data represent technical triplicates. Statistical significance was measured using a Student's t-test, * $p<0.05$, ** $p< 0.01$. **C** Indicated MelJuSo cells were exposed for 2h to 200nM aclarubicin and RNA was isolated 4h (6h) or 22h (24h) post treatment. Expression of indicated mRNA was detected using qRT-PCR and normalized to housekeeping gene expression. N=2 independent experiments, data represent technical triplicates. Statistical significance was determined by a Student's t-test, ** $p< 0.01$.

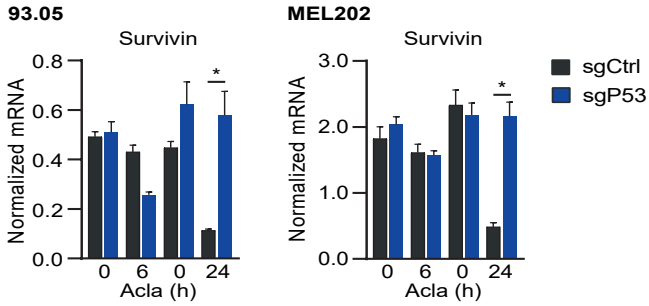

Fig. S4 Aclarubicin induces p53-dependent decrease of survivin expression. Indicated cells were treated with 200nM aclarubicin for 2h and RNA was isolated 4h (6h) or 22h (24h) post treatment. Expression of indicated mRNA was detected using qRT-PCR and normalized to housekeeping gene expression. N=2 independent experiments, data represent technical triplicates. Statistical significance was determined by a Student's t-test, * p<0.05.

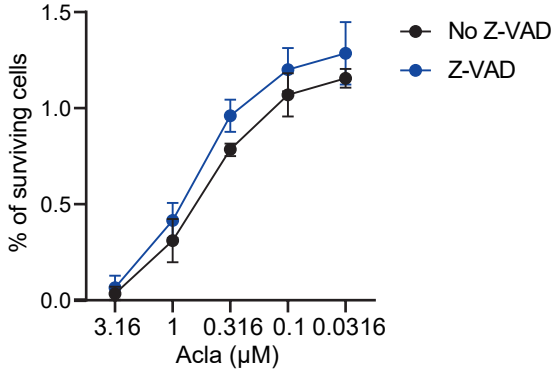

Fig. S5 Z-VAD did not render cells significantly more resistant to aclarubicin. MelJuSo cells were treated for 2h with different concentrations of aclarubicin, drug was washed away and cells were left to grow out in the presence or absence of Z-VAD-FMK. Three days later, cell viability was measured and normalized to the non-aclarubicin treated controls. Data represent two independent experiments. Statistical significance was determined by a wo-way ANOVA with multiple comparisons, data is ns.

CHAPTER 4

Novel *N*,*N*-Dimethyl-Idarubicin Analogues are Effective Cytotoxic Agents for ABCB1-Overexpressing, Doxorubicin-Resistant Cells

Merle A. van Gelder[1], Yufeng Li[1], Dennis P.A. Wander[1,2], Ilana Berlin[1], Herman S. Overkleeft[2], Sabina Y. van der Zanden[1,*], Jacques J. C. Neefjes[1,*]

[1] Department of Cell and Chemical Biology, ONCODE Institute, Leiden University Medical Center, Einthovenweg 20, 2333 CZ Leiden, The Netherlands

[2] Leiden Institute of Chemistry, Leiden University, Einsteinweg 55, 2333 CC Leiden, The Netherlands

Journal of Medicinal Chemistry, **2024**

Abstract

Anthracyclines comprise one of the most effective anticancer drug classes. Doxorubicin, daunorubicin, epirubicin, and idarubicin have been in clinical use for decades, but their application remains complicated by treatment-related toxicities and drug resistance. We previously demonstrated that the combination of DNA damage and histone eviction exerted by doxorubicin drives its associated adverse effects. However, whether the same properties dictate drug resistance is unclear. In the present study, we evaluate a library of 40 anthracyclines on their cytotoxicity, intracellular uptake, and subcellular localization in K562 wildtype versus ABCB1-transporter overexpressing, doxorubicin-resistant cells. We identify several highly potent cytotoxic anthracyclines. Among these, *N,N*-dimethyl-idarubicin **11** and anthracycline **26** (composed of the idarubicin aglycon and the aclarubicin trisaccharide) stand out, due to their histone eviction-mediated cytotoxicity towards doxorubicin-resistant cells. Our findings thus uncover understudied anthracycline variants warranting further investigation in the quest for safer and more effective anticancer agents that circumvent cellular export by ABCB1.

Introduction

Anthracyclines are among the most valuable anticancer drugs in current clinical use. They boast remarkably broad anti-cancer activity and have therefore become integral to the treatment of numerous tumor types.[1] Despite their high effectivity, clinical application of anthracyclines is hindered by severe side effects as well as drug resistance.[2,3] Recent years have witnessed key breakthroughs in our understanding of anthracycline efficacy and treatment-induced side-effects.[4,5] However, the relationship between anthracycline activity and drug resistance remains incompletely understood.

Doxorubicin and its close structural analogues epirubicin, daunorubicin and idarubicin induce cell death through two main mechanisms of action: generation of DNA double-strand breaks (DNA damage) and eviction of histones from chromatin (chromatin damage).[6] For decades, therapeutic effects of these anthracyclines have been ascribed primarily to their DNA damaging activity. However, recent evidence revealed that the natural product anthracycline, aclarubicin, as well as the synthetic doxorubicin analogue *N,N*-dimethyldoxorubicin exclusively induce histone eviction.[7] These anthracyclines are at least equally as effective against tumor cells as doxorubicin in murine *in vivo* models, but much less toxic to healthy cells and tissues. For instance, *N,N*-dimethyldoxorubicin does not cause cardiotoxicity, secondary tumor formation or gonadal dysfunction *in vivo*, unlike its parent compound doxorubicin.[5] Along the same lines, clinical observations reveal that aclarubicin treatment is less cardiotoxic for cancer patients than doxorubicin treatment, while both compounds appear to be equally effective as anticancer agents.[8,9] Importantly, clinical use of anthracyclines is not only limited by off-target toxicities, but also hindered by the emergence of drug resistance. Drug resistance poses a critical barrier to treatment and remains one of the leading causes of chemotherapy failure in cancer patients.[10] A key event in drug resistance is the upregulation of ATP-binding cassette (ABC) transporters. Notable among these are ABCB1, also known as p-glycoprotein (p-gp)[11], and ABCG2, also referred to as breast cancer resistance protein (BCRP).[12] The ABC transporters are responsible for the efflux of a wide range of chemotherapeutics across the plasma membrane, leading to lower intracellular drug levels and treatment resistance. Doxorubicin and its clinically used analogues (epirubicin, daunorubicin and idarubicin) all are known substrates for ABCB1[13], and several studies have noted increased ABCB1 expression in tumor cells in response to anthracycline chemotherapy.[14]

Ideally, new anthracycline leads for clinical development would address both of the limitations discussed above by eliciting less adverse events *and* circumventing molecular mechanisms that underly drug resistance. Despite promising novel approaches in anthracycline synthesis, such as doxorubicin-conjugate structures and drug carriers, the development of more tolerable anthracyclines has proven difficult.[15,16] In recent

years, we have conducted structure-activity-relationship (SAR) studies on doxorubicin/aclarubicin analogues, where we systematically varied the nature of the tetracycline aglycon, the sugar (unsubstituted or glycosylated 3-amino-2,3-dideoxy-L-fucose including configurational isomers) and the aminosugar N-alkylation pattern. This yielded a comprehensive anthracycline library of 40 entries that serves as the basis of the studies presented here. Biochemical evaluation of the above structural variants revealed a general trend indicating that aminosugar *N*-dimethylation enhances cytotoxicity *in vitro*. In addition, histone eviction capacity has proven to be more predictive of anthracycline cytotoxicity than their DNA damaging activity.[17] In the present study, we considered whether our current anthracycline collection contains novel anticancer agents that combine potent cancer cell killing with low susceptibility to export by ABC transporters. Previous research has suggested that alkylation of the sugar 3'-amino group in doxorubicin/aclarubicin type anthracyclines yields compounds that operate exclusively through histone eviction.[7,17,18] In addition, *N*-methylation of oxaunomycin variants increased their cytotoxicity towards drug resistant cells.[19] The importance of structural variations in the saccharide chains has also been emphasized in the context of drug resistance, since arimetamycin A hybrid structures with doxorubicin and daunorubicin maintained nanomolar activity against drug resistant cells *in vitro*.[20]

Therefore, we now profiled our library of structural variants for their cytotoxicity in wildtype K562 leukemia cells versus those overexpressing ABCB1 or ABCG2. In general, we find that *N,N*-dimethylation renders an anthracycline a poor substrate for ABC transporters. We also compared intracellular anthracycline levels and their subcellular localization to evaluate whether a correlation exists between these factors and cytotoxicity. Our results indicate that intracellular anthracycline levels are not directly linked to the cytotoxicity of anthracyclines, but that subcellular localization, and in particular nuclear concentration, correlates with cytotoxicity, both in the absence and presence of ABCB1 overexpression. Collectively, we identify derivatives of doxorubicin, epirubicin and idarubicin with high effectivity against cancer cells, which have been rendered doxorubicin resistant through overexpression of ABC transporters. Relevant structural changes did not reduce either the DNA intercalation affinity of compounds or their targeting of Topoisomerase IIα (TopoIIα). Given that these derivatives specifically induce histone eviction without causing DNA double strand breaks, they may also feature more favorable side-effect profiles as compared to their parent compounds.

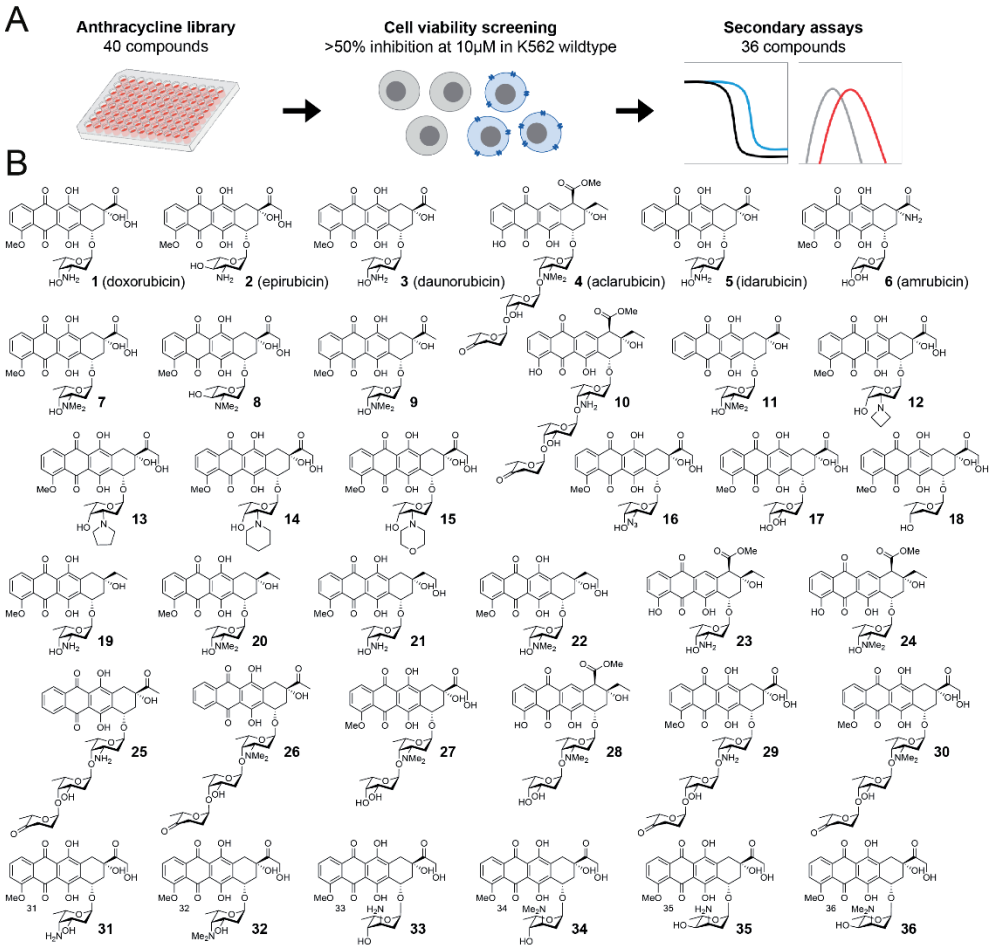

Figure 1. Workflow and chemical structures of compounds evaluated in this study. (A) Schematic overview of the threshold for inclusion of the 36 anthracycline variants used for cellular assays. (B) Chemical structures of compounds evaluated in all cellular assays. These contain the clinically used anthracyclines doxorubicin (**1**), epirubicin (**2**), daunorubicin (**3**), aclarubicin (**4**), idarubicin (**5**), and the synthetic anthracyclines (**6**-**36**).

Results and Discussion

Anthracyclines are commonly used in the treatment of hematological malignancies. To evaluate the effects of different anthracycline variants, we performed cytotoxicity profiling of 40 compounds (Figure S1) in the human myelogenous leukemia cell line K562. Of these, compounds 1-6 are in clinical use and commercially available, whereas synthesis of compounds 7-36 and S1-S4 was reported previously.[7,17,18] In total, 36 out

of 40 compounds passed the threshold of at least 50% growth inhibition at 10 μM concentration (Figure 1A) and were selected for further evaluation.

Cytotoxicity profiling of anthracycline variants in ABCB1- and ABCG2-mediated drug resistance

Firstly, cytotoxicity profiles of anthracycline variants (**1**-**36**, Figure 1B) in wildtype K562 cells were compared to those in cells overexpressing drug transporters ABCB1 or ABCG2 using a cell growth inhibition assay. In short, cells were treated for 2 hours with different anthracycline variants, washed, and left to grow for 72 hours. Subsequently, cell viability was measured relative to untreated control cells. IC_{50} values for all compounds were plotted for K562 wildtype cells versus ABCB1 (Figure 2A) or ABCG2 (Figure 2B) overexpressing cells. Direct comparisons between 36 compounds per cell line (Figure 2A, B) are complemented by relative (fold-change) analysis of cytotoxic effects of a single compound against wildtype versus ABCB1 or ABCG2 overexpressing cells (Figure 2C). Both parameters are relevant drug performance measures. Cytotoxicity expressed as IC_{50} value should ideally be low in all cell lines for a compound to be, or become, an effective anticancer agent.

Additionally, fold change in IC_{50} value IC_{50}(ABCB1)/IC_{50}(wildtype) or IC_{50}(ABCG2)/IC_{50}(wildtype) is indicative of transporter substrate status, providing critical SAR information on anthracycline variants as anticancer agents. In agreement with earlier findings on their susceptibility to ABCB1-mediated tumor resistance, anthracycline variants presently in clinical use (**1**-**4**) display poor cytotoxicity profiles against cancer cells overexpressing ABCB1, with 2,5- to 9-fold reduction in potency as compared to their respective cytotoxicity in wildtype cells. Idarubicin (**5**), on the other hand, was nearly equally toxic towards ABCB1 overexpressing as wildtype cells. The same trend of reduced cytotoxicity was observed when testing clinically used anthracyclines (**1**-**4)** against ABCG2 overexpressing cells, although in much smaller magnitude. Idarubicin (**5**) however, was considerably less cytotoxic towards ABCG2 overexpressing cells compared to wildtype cells. Amrubicin (**6**) was poorly cytotoxic in all three cell lines, regardless of drug transporter overexpression. *N,N*-dimethyldoxorubicin (**7**), *N,N*-dimethylepirubicin (**8**) and *N,N*-dimethyldaunorubicin (**9**) all proved to be much more cytotoxic against both ABCB1 and ABCG2 overexpressing cells when compared to their non-methylated counterparts (**1**-**3**). This relationship between the pattern of *N*-methylation and cytotoxicity was also apparent when comparing aclarubicin (**4**) to its primary amine counterpart (**10**). Interestingly, cytotoxicity of idarubicin (**5**) in wildtype cells was superior to that of *N,N*-dimethylidarubicin (**11**), but the fold change in IC_{50} (ABCB1/wildtype) and (ABCG2/wildtype) of compound **11** was negligible. Within the set of cyclic, tertiary amines, compounds **13**-**15** outperformed their parental drug doxorubicin in both wildtype and ABCB1 overexpressing cells, unlike azetidine (**12**). Compounds **12**-**15** were all equally

cytotoxic against wildtype cells and ABCG2 overexpressing cells. Of the three doxorubicin derivates lacking a basic amine, variants **17** and **18** were considerably less cytotoxic than doxorubicin (**1**) in wildtype cells, but the fold change in IC_{50} (ABCB1/wildtype) was close to one. Morpholino-doxorubicin (**15**) and azido-doxorubicin (**16**) proved to be the most effective derivatives of doxorubicin (**1**) in this set of compounds against wildtype and ABCB1 overexpressing cells. This is in line with previous studies reporting on cytotoxicity of 3'-azido and 3'-morpholinyl analogues of doxorubicin and daunorubicin in a treatment-induced drug resistant K562 cell line.[21,22] Yet, azido-doxorubicin (**16**) was markedly less cytotoxic against ABCG2 overexpressing cells. Removal of the aglycone carbonyl function, as in **19**-**22**, generally did not result in compounds with enhanced

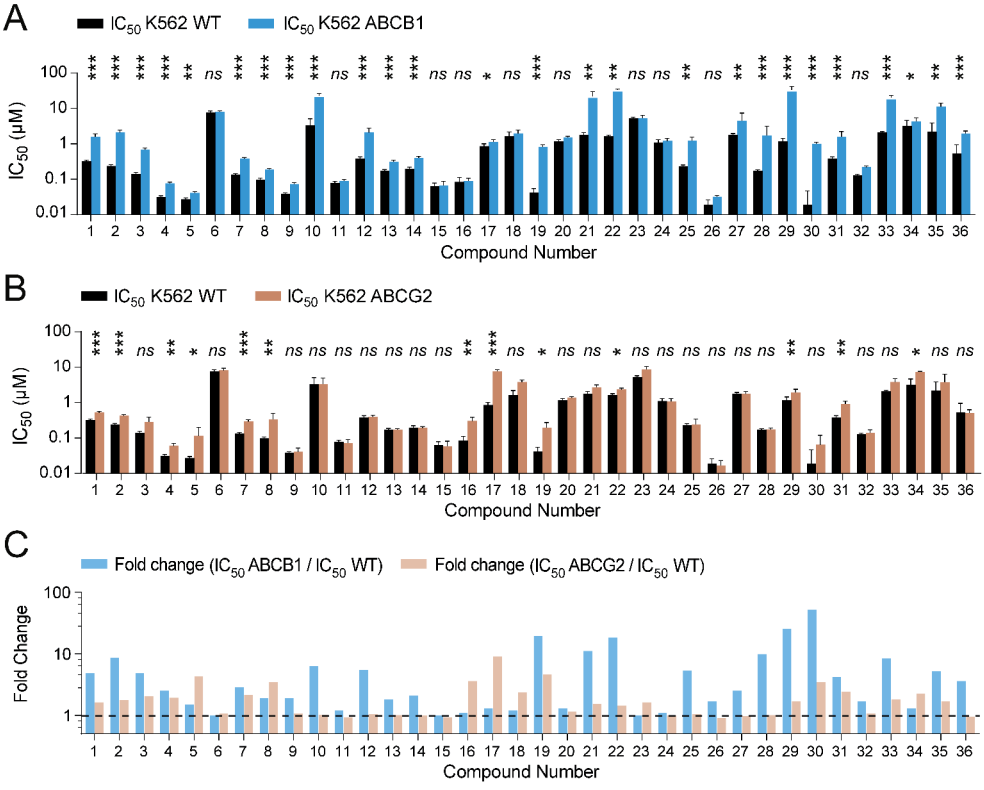

Figure 2. Cytotoxicity profiles of anthracyclines tested in vitro. (A) IC_{50} values are plotted for all compounds tested in wildtype K562 cells and ABCB1 overexpressing cells. (B) IC_{50} values are plotted for all compounds tested in wildtype K562 cells and ABCG2 overexpressing cells. Data is shown as mean ±SD. The X-axis shows the numbers of the compounds corresponding to Figure 1B. Two-way ANOVA; * $p<0.05$; ** $p<0.01$; *** $p<0.001$; ns, not significant. (C) The fold change difference between IC_{50} value in ABCB1 overexpressing versus wildtype cells (IC_{50}(ABCB1)/IC_{50}(wildtype)) and fold change difference between IC_{50} value in ABCG2 overexpressing versus wildtype cells (IC_{50}(ABCG2)/IC_{50}(wildtype)) is plotted for every compound. The dotted line indicates a fold change of 1, e.g. no difference in IC_{50}.

cytotoxicity to either wildtype or ABCB1 overexpressing cells when compared to their respective parent compounds (**1**, **3**).

Compounds **23** and **24**, comprising hybrids between aclarubicin (aglycon part), doxorubicin and *N,N*-dimethyldoxorubicin, also turned out to be weaker cytotoxic agents when compared to their parent compounds (**1**, **7**). However, they displayed no difference in cytotoxicity towards wildtype versus ABCB1 overexpressing cells. Cytotoxicity profiles in ABCG2 overexpressing cells followed the same trend for compounds **19**-**24**, though the fold change IC_{50} observed (ABCG2/wildtype) were smaller in comparison. Of the idarubicin-aglycon containing trisaccharides (**25** and **26**), the dimethylated variant (**26**) showed the best cytotoxicity aamong all **36** compounds, with an IC_{50} of 19 nM in

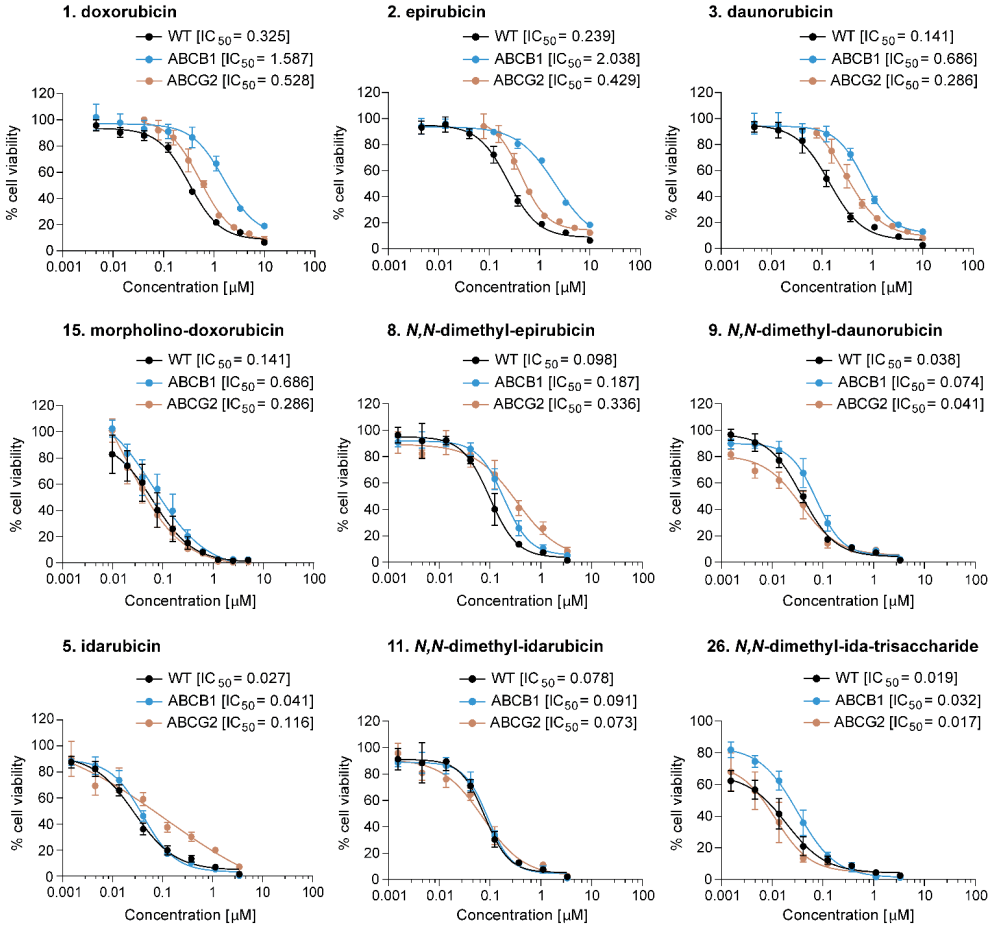

Figure 3. Individual IC_{50} curves are plotted for the clinically used anthracyclines doxorubicin (**1**), epirubicin (**2**), daunorubicin (**3**) and idarubicin (**5**) and the most potent analogues of these anthracyclines in terms of IC_{50} and fold change IC_{50} between wildtype K562 cells and ABCB1 or ABCG2 overexpressing cells.

wildtype cells and ABCG2 overexpression cells, and 32 nM in ABCB1 overexpressing cells. Doxorubicin/aclarubicin hybrid structures (**27**-**30**) proved to be only modestly cytotoxic against ABCB1 and ABCG2 overexpressing cells, and of these compounds, only *N*-dimethyl variants (**28**, **30**) were potent killers of wildtype cells.

Finally, among doxorubicin isomers (**31**-**36**), only regio-isomer (**32**) outperformed doxorubicin (**1**) in killing wildtype, ABCB1 or ABCG2 overexpressing cells.

Examination of the fold change in IC_{50} (ABCB1/wildtype) (threshold set at two) revealed sixteen compounds in our library to be poor ABCB1 substrates, if at all (**5**, **6**, **8**, **9**, **11**, **13**, **15**-**18**, **20**, **23**, **24**, **26**, **32**, **34**). However, most anthracycline variants tested remained effective in ABCG2 overexpressing cells, where cytotoxicity of twenty-three compounds (**3**, **6**, **9**-**15**, **18**, **20**, **21**, **23**-**28**, **30**, **32**, **33**, **35**, **36**) was not significantly altered compared to wildtype cells. The fold change differences between IC_{50} (ABCB1/wildtype) and (ABCG2/wildtype) show a similar trend, but the amplitude is much smaller in the latter case (Figure 2C). Since the clinical relevance of ABCG2 is less well established than that of ABCB1 in the context of anthracyclines[23], we continued with the ABCB1 transporter-mediated drug resistant cells for further evaluation. From our complete library of anthracyclines, morpholino-doxorubicin (**15**), *N,N*-dimethyl-epirubicin (**8**), *N,N*-dimethyl-daunorubicin (**9**), and in particular *N,N*-dimethyl-idarubicin (**11**) and *N,N*-dimethyl-idarubicin-trisaccharide (**26**) stood out because of their low IC_{50} values in wildtype cells and ABCB1 overexpressing cells (Figure 3), and low (**8**, **9**, **15**) to negligible (**11**, **26**) relative fold change in IC_{50} (ABCB1/wildtype). The cytotoxic effects of these compounds (**8**, **9**, **11**, **15**, **26**) were also confirmed in a live/dead assay (Figure S2). Altogether, the aglycon of either daunorubicin (**3**) or idarubicin (**5**), combined with aminosugar *N*-methylation provide the most favorable structural elements for improved cytotoxicity profiles against wildtype as well as ABCB1 overexpressing cells.

Intracellular drug accumulation is not a proxy for cytotoxicity

All anthracycline variants **1**-**36** used in our study are fluorescent, allowing comparison of their accumulation in cells using flow-cytometry (Figure 3A). Both wildtype and ABCB1 overexpressing cells were exposed to each of the compounds, at a concentration of 10 μM, and intracellular fluorescence was measured after 1 or 4 hours of incubation (Figure 3B). Following 1 hour treatment, intracellular fluorescence of most compounds tested was similar between the cell lines, except for the clinically used variants epirubicin (**2**), daunorubicin (**3**) and idarubicin (**5**), as well as the doxorubicin stereoisomer (**35**). After 4 hours of treatment, this trend of reduced intracellular fluorescence comparing wildtype versus ABCB1 overexpressing cells increased for compounds **1**-**3**, but not for idarubicin (**5**). In addition, a significant reduction in fluorescence was observed in ABCB1 overexpressing cells compared to wildtype cells for doxorubicin analogues **21**, **22** and

35, and for idarubicin analogue **25**. Previously highlighted cytotoxic compounds in the ABCB1 background – morpholino-doxorubicin (**15**), dimethyl-epirubicin (**8**), dimethyl-daunorubicin (**9**), dimethyl-idarubicin (**11**) and idarubicin-trisaccharide (**26**) – all appear to accumulate equally well in wildtype and ABCB1 overexpressing cells, as concluded from their comparable intracellular fluorescence. Remarkably, analysis of the complete set of compounds revealed no significant relationship between intracellular accumulation of compounds and their corresponding fold change in IC_{50} (ABCB1/wildtype) (Figure 3C). For instance, intracellular fluorescence of trisaccharide (**30**) was similar in wildtype and ABCB1 overexpressing cells, whereas its fold change in IC_{50} (ABCB1/wildtype) was

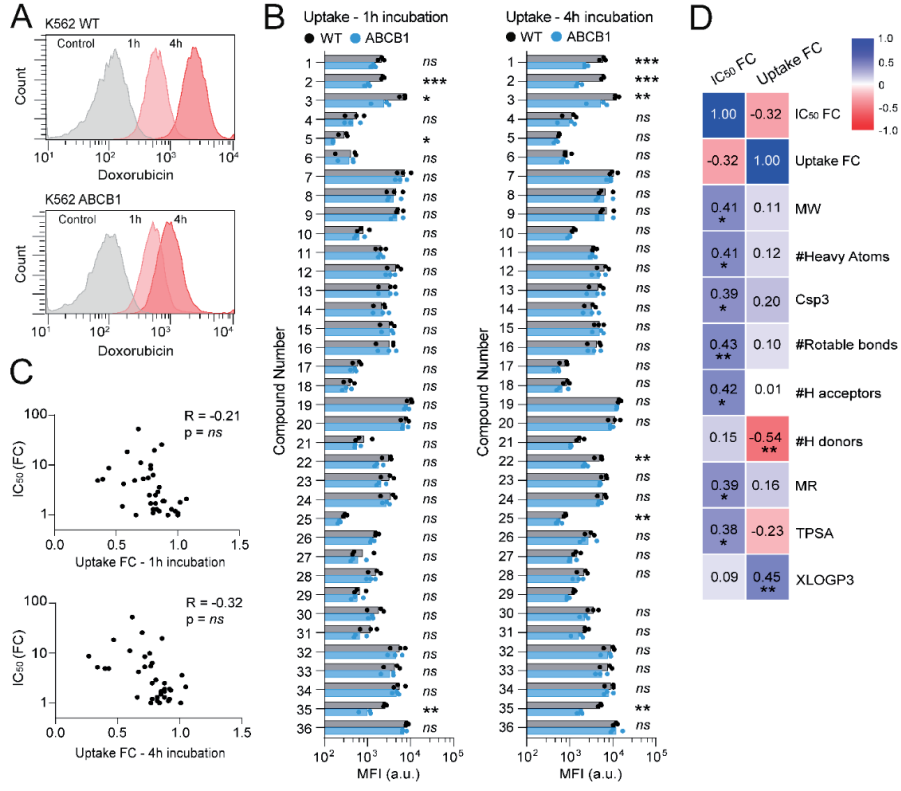

Figure 4. Intracellular fluorescence of all compounds 1 hour and 4 hours post treatment. Mean fluorescent intensity was measured with flow-cytometry (A) and fluorescent intensity was compared 1 hour and 4 hours post treatment (B) between K562 wildtype and ABCB1 overexpressing cells. (C) The fold change in intracellular fluorescence does not significantly correlate to the fold change IC_{50} between wildtype and ABCB1 overexpressing cells. (D) Pearson's r correlation matrix displaying the correlation between computationally predicted biochemical parameters and fold change IC_{50} and fold change intracellular fluorescence. Positive correlations are displayed in blue and negative correlations in red. Color intensity is proportional to correlation coefficients. MW = molecular weight; Csp3 = fraction of carbon atoms with sp 3 hybridization; MR = Molar refractivity; TPSA = topological polar surface area; XLOGP3 = $LogP_{o/w}$.

nearly 50, indicating poor cytotoxicity in ABCB1 overexpressing cells, despite efficient intracellular accumulation. These results show that the extent of uptake does not solely define drug potency in the context of ABCB1-mediated drug resistance.

The ability of a drug to penetrate membranes is dependent on its various properties, which may in turn influence intracellular drug concentrations. To define these, we performed computational predictions of relevant biochemical and biophysical parameters for all 36 compounds (Table S1), including molecular weight (MW), number of heavy atoms, saturation (fraction of sp_3-hybridized carbons), flexibility (rotatable bonds), number of H-bond acceptors and donors, molar refractivity, polarity (topological polar surface area), and lipophilicity (LogP). Association between these properties and the observed fold change in IC_{50} (ABCB1/wildtype) as well as intracellular fluorescence (ABCB1/wildtype) is displayed in a correlation matrix (Figure 3D). This analysis revealed that fold change in IC_{50} correlates to parameters describing the size and polarity of the compounds, whereas the fold change in cellular uptake most strongly correlates with predicted compound lipophilicity. Although the latter is in agreement with previous research on hydrophobic compounds as better substrates for ABCB1[24], we find that intracellular drug accumulation does not directly explain the observed differences in drug cytotoxicity profiles

Nuclear uptake of anthracyclines is a strong predictor of cytotoxicity

Since intracellular anthracycline accumulation did not directly reflect drug potency in killing ABCB1 overexpressing cells, we hypothesized that nuclear tarting may provide a better measure in this regard. To address this, we set out to determine the subcellular localization of clinical anthracyclines (**1**-**5**) and their most potent analogues (**8**, **9**, **11**, **15**, **26**) identified in our cytotoxicity assays (Figure 2). To this end, K562 wildtype and ABCB1 overexpressing cells were treated for a series of timepoints with each anthracycline, lysed, and subjected to fractionation (Figure 5A and 5B). Fluorescence in cytoplasmic and nuclear fractions was then measured with a plate reader. Nuclear accumulation of doxorubicin (**1**), epirubicin (**2**) and daunorubicin (**3**) was significantly decreased after 1 hour and 2 hours treatment in ABCB1 overexpressing cells compared to wildtype cells. On the other hand, aclarubicin (**4**) and idarubicin (**5**) showed comparable nuclear fluorescence in both cell types (Figure 5D). Compounds **8**, **9**, and **15** exhibited superior nuclear accumulation over time compared to their respective clinically used counterparts (**1**, **2** and **3**). For these compounds, as well as compounds **11** and **26**, no significant difference was observed in nuclear fluorescence between wildtype and ABCB1 overexpressing cells. Taken together, nuclear compound fluorescence correlated significantly with the fold change in IC_{50} (ABCB1/wildtype) (Figure 5C). The difference in cytoplasmic accumulation between wildtype cells and ABCB1 overexpressing cells was less substantial (Figure S3A), and the observed cytoplasmic fluorescence was less indicative of the change in cytotoxicity (Figure S3B). To test whether subcellular localization was influenced by ABCB1 activity, we

pre-treated ABCB1 overexpressing cells with the ABCB1 inhibitor Tariquidar (TRQ) prior to anthracycline treatment and subsequent fractionation analysis. Both cytoplasmic and nuclear fluorescence could be restored to levels similar to those observed in wildtype cells, as demonstrated in Supplementary Figure S4 for doxorubicin (**1**) and daunorubicin (**3**). No effect of ABCB1 inhibition was observed for idarubicin (**5**) or compounds **9**, **11** and **15**. This suggests that superior nuclear accumulation of compounds **5**, **9**, **11** and **15** is independent of ABCB1 expression, and that nuclear accumulation is a strong predictor of anthracycline effectivity. Targeting of TopoIIα in the nucleus was also assessed upon treatment with all compounds (**1**-**36**) using confocal time-lapse microscopy (Table S1 and Figure S5). As expected, treatment with the clinically relevant anthracyclines (**1**-**5**) and their most potent analogues (**8**, **9**, **11**, **15**, **26**) was found to cause marked redistribution of nuclear TopoIIα.

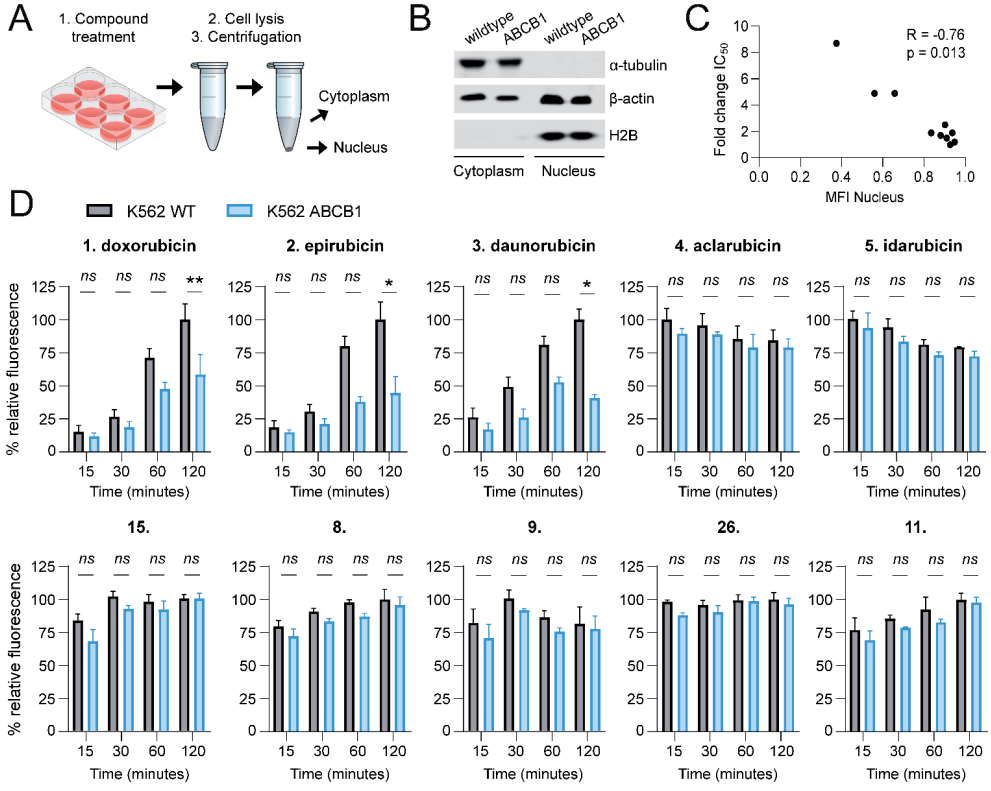

Figure 5. Nuclear accumulation of selected compounds **1**-**5**, **8**, **9**, **11**, **15**, **26**. Numbers correspond to the structures in Figure 1. (A) K562 wildtype and ABCB1 overexpressing cells were treated with 10 µM of the indicated compounds and subjected to fractionation. (B) Separation of the fractions was confirmed with Western Blot. (C) Correlation between fold change IC_{50} and mean fluorescence intensity in nuclear fraction. (D) Mean fluorescence intensity in the nuclear fraction was measured at a series of timepoints (15, 30, 60 and 120 minutes). Fluorescence was normalized to the largest signal. Two-way ANOVA; * $p<0.05$; ** $p<0.01$; *** $p<0.001$; ns, not significant.

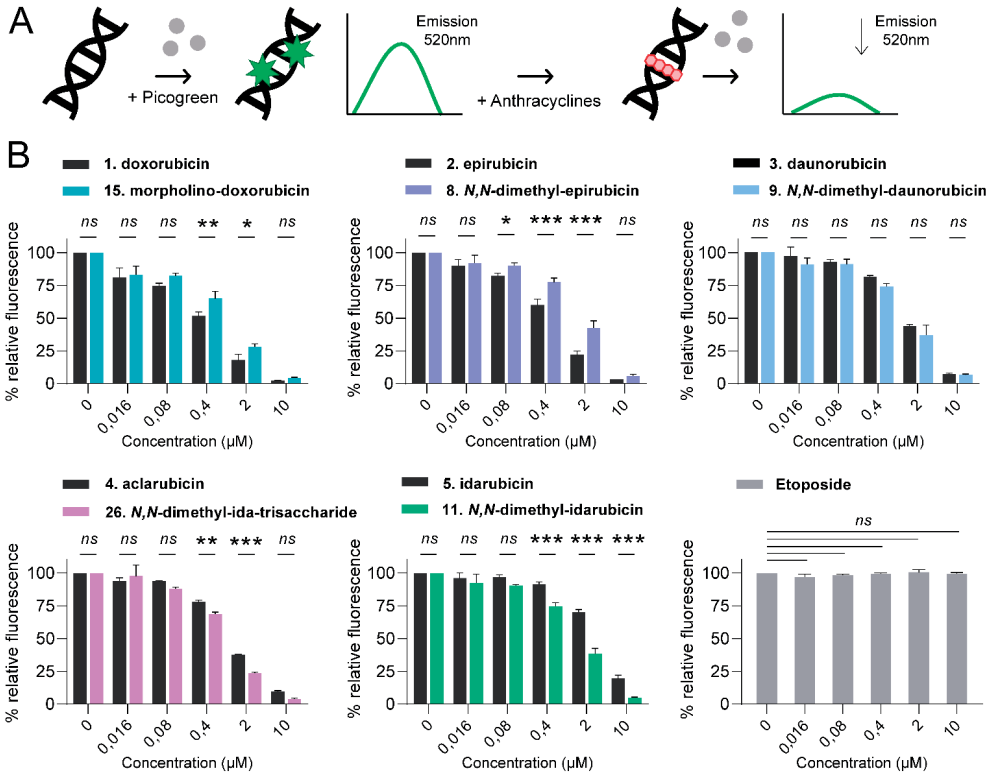

Figure 6. DNA intercalation affinity of selected compounds **1**-**5**, **8**, **9**, **11**, **15**, **26**. Numbers correspond to the structures in Figure 1. (A) The intercalation of anthracyclines into double stranded DNA was tested with a competition dye displacement assay. (B) The percentage of initial fluorescence is plotted against the concentrations of the indicated compounds. Two-way ANOVA; * $p<0.05$; ** $p<0.01$; *** $p<0.001$; ns, not significant.

Further, intercalation of anthracyclines into double stranded DNA was tested with a competition dye displacement assay. DNA intercalation affinity of clinical anthracyclines (**1**-**5)** was compared to that of their most potent analogues (**8**, **9**, **11**, **15**, **26**). Intercalation was determined using PicoGreen, which becomes fluorescent upon binding to double stranded DNA, and addition of compounds displacing intercalated PicoGreen thus results in loss of fluorescence signal (Figure 6A). Plotting remaining fluorescence against compound concentration (Figure 6B) showed that doxorubicin (**1**) and epirubicin (**2**) share higher DNA binding affinity at lower concentrations compared to morpholino-doxorubicin (**15**) and *N,N*-dimethyl-epirubicin (**9**), respectively. Daunorubicin (**3**) and *N,N*-dimethyl-daunorubicin (**10**) were equally effective, and *N,N*-dimethyl-idarubicin (**11**) and *N,N*-dimethyl-idarubicin-trisaccharide (**26**) proved to be particularly efficient intercalating agents. The non-intercalating Topo II poison, etoposide, was used as a

negative control. Ultimately, structural variations of our lead compounds did not alter their canonical anthracycline functions of DNA intercalation and TopoIIα targeting.

Conclusion

Anthracyclines doxorubicin (**1**), daunorubicin (**2**) and epirubicin (**3**) have been in clinical use for decades. However, their effectivity is severely limited, both by treatment-related toxicities and drug resistance. Preferably, anthracyclines of the future should address both of these issues to cause less adverse events while retaining potency against drug resistant cells. In previous studies, we have shown that the archetypal anthracycline, doxorubicin (**1**), as well as its close structural analogues **2** and **3**, exert their anti-cancer activity through two independent mechanisms: induction of DNA double strand breaks and chromatin damage through histone eviction. Uncoupling these activities identified *N,N*-dimethyldoxorubicin (**7**) as an efficient histone-evicting compound that lacks the capacity for DNA double strand break formation and also lacks most of the therapy-related side effects associated with the clinically used anthracyclines. In subsequent studies, we observed that anthracyclines containing an *N,N*-dimethyl aminosugar often harbor this desirable set of properties: they exert their activity exclusively through histone eviction and are generally more cytotoxic to tumor cells than their parent compound. At the same time, they display limited toxicity in healthy cells and tissues. We thus have amassed a set of anthracyclines with potential clinical value, alongside of their relevant structural analogues as controls, namely the 40 compounds used in this study. With their cytotoxicity profiles against tumor cells in hand and their mode(s) of action known, we investigated the second important parameter which determines clinical applicability of new anthracyclines. Namely, performance in a doxorubicin-resistant tumor setting, caused by the overexpression of drug exporter ABCB1.

Side-by-side comparison of cytotoxicity profiles of 36 most cytotoxic compounds in K562 wildtype versus ABCB1 overexpressing cells revealed that the most widely used clinical variants (**1**-**3**) are much less effective in ABCB1 overexpressing cells. This is in agreement with these variants being substrates for ABCB1, and that drug resistance after treatment with these drugs can emerge in the clinic.[13] In total, 16 compounds had a fold change in IC_{50} (ABCB1/wildtype) below two, indicating that these variants retain their cytotoxicity in ABCB1-mediated drug resistant cells. The cytotoxicity of all anthracyclines tested was less affected by ABCG2-mediated drug export. The transporters have overlapping substrate specificities to some extent, but most importantly in transporting the anthracyclines currently in clinical use (**1**-**5**). Our study reveals that it is possible to design anthracyclines that defy ABCB1- and ABCG2-mediated efflux. This is important because, despite many efforts, blocking these transporters by small molecule inhibitors has thus far not resulted

in improved tumor responses in clinical studies.[23,25] Therefore, anthracyclines which are both potent killers of tumor cells and insensitive to ABC transporter-mediated export may be attractive alternatives, especially if novel variants are less toxic to healthy tissues. In this respect, we observe that anthracyclines featuring an *N,N*-dimethyl aminosugar in general are poor substrates for the ABCB1 drug transporter as compared to their non-alkylated counterparts. This is of interest, because the same modification also allows to discriminate between the different mechanisms of action: DNA double strand break generation versus histone eviction. In addition, we show that nuclear accumulation is the strongest predictor of anthracycline effectivity in ABCB1 overexpressing, drug resistant cells, and the most potent analogues identified in this study show improved nuclear accumulation compared to their clinically used counterparts.

Combining these new structure-activity insights into ABC transporter-mediated drug resistance with our earlier findings, we see the emergence of a new set of promising anthracyclines for further (pre)clinical development. The most potent structural variants of clinically used anthracyclines identified in this study are morpholino-doxorubicin (**15**), *N,N*-dimethyl-epirubicin (**8**), *N,N*-dimethyl-daunorubicin (**9**), *N,N*-dimethyl-idarubicin (**11**) and trisaccharidic *N,N*-dimethyl-idarubicin (**26**). We previously showed that these compounds are among the most potent histone evictors, and do not induce DNA double strand breaks.[17] We now find that these variants are more cytotoxic towards both wildtype and ABCB1- or ABCG2- overexpressing cells than their parent compounds. By this virtue we expect that these compounds are superior in circumventing ABCB1-mediated resistance – a significant type of resistance to doxorubicin and its structural analogues. Moreover, because none of these compounds cause DNA damage, there is also less risk of acquired resistance through increased DNA-damage repair or decreased Topoisomerase II expression, a second mechanism of drug resistance observed in doxorubicin-resistant cells.[26,27]

In conclusion, this study contributes to the design and identification of new, more effective and more benign anthracycline drugs. We performed several structure-activity analyses which may help in defining design parameters for potentially successful new anthracyclines. Previously, we unearthed structural elements that determine DNA damage and histone eviction and showed that the combination of these activities is at the root of many side effects. Here, we add structure-activity information on anthracyclines in a drug resistance context, by defining structural elements that enable circumventing ABCB1-mediated export and lead to enhanced nuclear accumulation. The most promising compounds presented here, and in particular idarubicin derivatives **11** and **26**, may deserve further exploration in pre-clinical studies, for instance to explore their effectivity in more advanced drug resistance models as well as to evaluate their *in vivo* efficacy.

Experimental section

The anthracycline variants 7-36 were synthesized as described previously and the compounds are >95% pure by HPLC analysis.[7,17,18]

Reagents and antibodies

Doxorubicin and epirubicin were obtained from Accord Healthcare Limited, UK, daunorubicin was obtained from Sanofi, aclarubicin (sc-200160), idarubicin (sc-204774) and amrubicin (sc-207289) were purchased from Santa Cruz Biotechnology (USA). Tariquidar (SML1790) was purchased from Sigma-Aldrich (USA). Primary antibodies used for Western blotting: ABCB1 (1:1000, 13342, Cell Signaling), Histone H2B (1:1000, 12364, Cell Signaling), β-actin (1:10000, A5441, Sigma), PARP (1:1000, 9542, Cell Signaling). Secondary antibodies used for blotting: IRDye 800CW goat anti-mouse IgG (H+L) (926-32210, Li-COR, 1:10000), IRDye 800CW goat anti-rabbit IgG (H+L) (926-32211, Li-COR, 1:5000).

Cell culture

K562 cells (B. Pang, Leiden University Medical Center, the Netherlands) were maintained in RPMI-1640 medium supplemented with 8% FCS. K562 ABCB1 overexpression cells were generated as described[28] and maintained in RPMI-1640 medium supplemented with 8% FCS. K562 ABCG2 overexpression cells were generated with single-guide RNAs targeting the promoter region of ABCG2 (Forward: CAC CGT GCC GCG CTG AGC CGC CAGC; Reverse: AAA CGC TGG CGG CTC AGC GCG GCAC). The guide RNA sequence was cloned into lentiSAMv2-Puro plasmid containing the gRNA scaffold and dCas9 sequence, and lentivirus was made as previously described.[28] K562/SAM stable cells were transduced with virus containing the respective guide RNAs and then selected using puromycin (2 μg ml–1). Single clones of cells were picked and verified using PCR and Sanger sequencing. K562 ABCB2 overexpression cells were maintained in RPMI-1640 medium supplemented with 8% FCS. All cell lines were maintained in a humidified atmosphere of 5% CO_2 at 37°C, regularly tested for the absence of mycoplasma and the origin of cell lines was validated using STR analysis.

Cell viability assay

Cells were seeded into 96-well format (2000 cells/well). Twenty-four hours after seeding, cells were treated with indicated compounds for 2 hours at various concentrations. Subsequently, the compounds were removed by washing and the cells were left to grow for an additional 72 hours. Cell viability was measured using the CellTiter-Blue viability assay (Promega). Relative survival was normalized to untreated control cells and corrected for background signal.

Flow cytometry

Cells were treated with 10 μM of compound for the indicated time points. Samples were washed with PBS, collected, and fixed with paraformaldehyde. Live/dead staining was performed with DAPI (1:1000). Samples were analyzed by flow cytometry using BD FACS Aria II, with 561-nm laser and 610/20-nm detector. The cellular uptake of anthracyclines and the live/dead ratio were quantified using FlowJo software v10.10.

ADME

The computation of physicochemical descriptors and prediction of ADME parameters was performed with the freely accessible webtool SwissADME.[29]

Subcellular fractionation

Cells were treated for a series of timepoints (15, 30, 60 and 120 minutes) with 10 μM of the indicated compounds. Cells were washed and lysed directly in lysis buffer (50 mM Tris·HCl pH 8.0, 150 mM NaCl, 5 mM $MgCl_2$, 0.5% Nonidet P-40, 2.5% glycerol supplemented with protease inhibitors), collected, vortexed, and incubated on ice for 10 minutes. To collect the cytoplasmic fraction, samples were centrifuged for 10 min, 15,000 × g at 4 °C. Both nuclear (pellet) and cytoplasmic (supernatant) fractions were washed and fluorescence was measured with a plate reader (500-15 excitation/580-30 emission).

Western blot

Cellular fractions were lysed directly in SDS-sample buffer (2%SDS, 10% glycerol, 5% β-mercaptoethanol, 60mM Tris-HCl pH 6.8 and 0.01% bromophenol blue). Samples were separated by SDS-PAGE and transferred to a nitrocellulose membrane. Blocking of the filters and antibody incubations were done in PBS supplemented with 0.1 (v/v)% tween and 5% (w/v) milk powder (Skim milk powder, LP0031, Oxiod). Blots were imaged by the Odyssey Classic imager (Li-Cor).

DNA dye competition assay

1μg/ml circular double stranded DNA was incubated with Quant-iT PicoGreen dsDNA reagent (Termo Fisher Scientific P7581) for 5 minutes at RT. Subsequently, indicated drug concentrations were added to the DNA/PicoGreen reaction and incubated for another 5 minutes at RT followed by measurement of the PicoGreen fluorescence using a CLARIOstar plate reader (BMG labtech) excitation 480 emission 520 (480-20/520-10 filter). The fluorescence was quantified relative to untreated controls. Fluorescent signals of all samples were corrected for the corresponding drug concentrations in the absence of DNA.

Quantification and statistical analysis

Each experiment was performed in triplicate, unless stated otherwise. Error bars denote ±SD. Statistical analyses were performed using Prism 8 software (GraphPad Inc.). ns, not significant, *p = < 0.05, **p = < 0.01, ***p = < 0.001

Associated content

Supporting Information

The Supporting Information is available free of charge at https://pubs.acs.org/doi/10.1021/acs.jmedchem.4c00614.

Table S1 – Biological data for all compounds
Table S2 – ADME parameters for all compounds

Figure S1 – Chemical structures of complete compound library Figure S2 – Cell death assays for selected compounds
Figure S3 – Cytoplasmic accumulation of selected compounds
Figure S4 – Subcellular accumulation in context of ABCB1 inhibition
Figure S5 – TopoIIα imaging for all compounds
Molecular formula strings and tabulated biological assays data (CSV).

Author information

Author Contributions

MvG, SvdZ, IB, HO, and JN conceived the experiments. MvG under supervision of SvdZ and JN performed all biochemical and cellular experiments. YL designed and generated ABCG2-overexpressing K562 cells. DW under supervision of HO prepared the compounds. The manuscript was written by MvG and SvdZ with input from all authors.

Funding Sources

This work was supported by grants from the Dutch Cancer Society KWF (JN) and by the Institute for Chemical Immunology, an NWO Gravitation project funded by the Ministry of Education, Culture and Science of The Netherlands.

Notes

The authors declare the following competing financial interest(s): Jacques J. C. Neefjes is a shareholder in NIHM, that aims to produce aclarubicin for clinical use.

Acknowledgments

We would like to thank Bjorn van Doodewaerd and Tom Schoufour for their technical assistance.

Abbreviations

ABCB1, ATP binding cassette subfamily B member 1; ABCG2, ATP-binding cassette superfamily G member 2; TopoIIα, Topoisomerase IIα; TRQ, Tariquidar

References

(1) Martins-Teixeira, M. B.; Carvalho, I. Antitumour Anthracyclines: Progress and Perspectives. *ChemMedChem*. **2020**, *15*, 933–948.

(2) Qiu, Y.; Jiang, P.; Huang, Y. Anthracycline-Induced Cardiotoxicity: Mechanisms, Monitoring, and Prevention. *Frontiers in cardiovascular medicine*. **2023**, *10*.

(3) Mirzaei, S.; Gholami, M. H.; Hashemi, F.; Zabolian, A.; Farahani, M. V.; Hushmandi, K.; Zarrabi, A.; Goldman, A.; Ashrafizadeh, M.; Orive, G. Advances in Understanding the Role of P-Gp in Doxorubicin Resistance: Molecular Pathways, Therapeutic Strategies, and Prospects. *Drug Discovery Today*. **2022**, *27*, 436–455.

(4) Pang, B.; Qiao, X.; Janssen, L.; Velds, A.; Groothuis, T.; Kerkhoven, R.; Nieuwland, M.; Ovaa, H.; Rottenberg, S.; van Tellingen, O.; Janssen, J.; Huijgens, P.; Zwart, W.; Neefjes, J. Drug-Induced Histone Eviction from Open Chromatin Contributes to the Chemotherapeutic Effects of Doxorubicin. *Nature Communications*. **2013**, *4*, 1–13.

(5) Qiao, X.; Van Der Zanden, S. Y.; Wander, D. P. A.; Borràs, D. M.; Song, J. Y.; Li, X.; Duikeren, S. Van; Gils, N. Van; Rutten, A.; Herwaarden, T. Van; Tellingen, O. Van; Giacomelli, E.; Bellin, M.; Orlova, V.; Tertoolen, L. G. J.; Gerhardt, S.; Akkermans, J. J.; Bakker, J. M.; Zuur, C. L.; Pang, B.; Smits, A. M.; Mummery, C. L.; Smit, L.; Arens, R.; Li, J.; Overkleeft, H. S.; Neefj, J. Uncoupling DNA Damage from Chromatin Damage to Detoxify Doxorubicin. *Proceedings of the National Academy of Sciences of the United States of America*. **2020**, *117*, 15182–15192.

(6) van der Zanden, S. Y.; Qiao, X.; Neefjes, J. New Insights into the Activities and Toxicities of the Old Anticancer Drug Doxorubicin. *The FEBS Journal*. **2020**, febs.15583.

(7) Wander, D. P. A.; Van Der Zanden, S. Y.; Van Der Marel, G. A.; Overkleeft, H. S.; Neefjes, J.; Codée, J. D. C. Doxorubicin and Aclarubicin: Shuffling Anthracycline Glycans for Improved Anticancer Agents. *Journal of Medicinal Chemistry*. **2020**, *63*, 12814–12829.

(8) Rothig, H. J.; Kraemer, H. P.; Sedlacek, H. H. Aclarubicin: Experimental and Clinical Experience. *Drugs under experimental and clinical research*. **1985**, *11*, 123–125.

(9) Mortensen, S. A. Aclarubicin: Preclinical and Clinical Data Suggesting Less Chronic Cardiotoxicity Compared with Conventional Anthracyclines. *European Journal of Haematology*. **1987**, *38*, 21–31.

(10) Dong, J.; Yuan, L.; Hu, C.; Cheng, X.; Qin, J. J. Strategies to Overcome Cancer Multidrug Resistance (MDR) through Targeting P-Glycoprotein (ABCB1): An Updated Review. *Pharmacology & therapeutics*. **2023**, *249*.

(11) Pote, M. S.; Gacche, R. N. ATP-Binding Cassette Efflux Transporters and MDR in Cancer. *Drug Discovery Today*. **2023**, *28*, 103537.

(12) Kukal, S.; Guin, D.; Rawat, C.; Bora, S.; Mishra, M. K.; Sharma, P.; Paul, P. R.; Kanojia, N.; Grewal, G. K.; Kukreti, S.; Saso, L.; Kukreti, R. Multidrug Efflux Transporter ABCG2: Expression and Regulation. *Cellular and Molecular Life Sciences: CMLS*. **2021**, *78*, 6887.

(13) Hodges, L. M.; Markova, S. M.; Chinn, L. W.; Gow, J. M.; Kroetz, D. L.; Klein, T. E.; Altman, R. B. Very Important Pharmacogene Summary: ABCB1 (MDR1, P-Glycoprotein). *Pharmacogenetics and Genomics*. **2011**, *21*, 152.

(14) Mattioli, R.; Ilari, A.; Colotti, B.; Mosca, L.; Fazi, F.; Colotti, G. Doxorubicin and Other Anthracyclines in Cancers: Activity, Chemoresistance and Its Overcoming. *Molecular Aspects of Medicine*. **2023**, *93*, 101205.

(15) Hanušová, V.; Boušová, I.; Skálová, L. Possibilities to Increase the Effectiveness of Doxorubicin in Cancer Cells Killing. *Drug metabolism reviews*. **2011**, *43*, 540–557.

(16) Peter, S.; Alven, S.; Maseko, R. B.; Aderibigbe, B. A. Doxorubicin-Based Hybrid Compounds as Potential Anticancer Agents: A Review. *Molecules (Basel, Switzerland)*. **2022**, *27*.

(17) van Gelder, M. A.; van der Zanden, S. Y.; Vriends, M. B. L.; Wagensveld, R. A.; van der Marel, G. A.; Codée, J. D. C.; Overkleeft, H. S.; Wander, D. P. A.; Neefjes, J. J. C. Re-Exploring the Anthracycline Chemical Space for Better Anti-Cancer Compounds. *Journal of Medicinal Chemistry*. **2023**, *66*, 11390–11398.

(18) Wander, D. P. A.; van der Zanden, S. Y.; Vriends, M. B. L.; van Veen, B. C.; Vlaming, J. G. C.; Bruyning, T.; Hansen, T.; van der Marel, G. A.; Overkleeft, H. S.; Neefjes, J. J. C.; Codée, J. D. C. Synthetic (N , N -Dimethyl)Doxorubicin Glycosyl Diastereomers to Dissect Modes of Action of Anthracycline Anticancer Drugs. *The Journal of Organic Chemistry*. **2021**, *86*, 5757–5770.

(19) Gate, L.; Couvreur, P.; Nguyen-Ba, G.; Tapiero, H. N-Methylation of Anthracyclines Modulates Their Cytotoxicity and Pharmacokinetic in Wild Type and Multidrug Resistant Cells. *Biomedicine & Pharmacotherapy*. **2003**, *57*, 301–308.

(20) Huseman, E. D.; Byl, J. A. W.; Chapp, S. M.; Schley, N. D.; Osheroff, N.; Townsend, S. D. Synthesis and Cytotoxic Evaluation of Arimetamycin A and Its Daunorubicin and Doxorubicin Hybrids. *ACS Central Science*. **2021**, acscentsci.1c00040.

(21) Battisti, R. F.; Zhong, Y.; Fang, L.; Gibbs, S.; Shen, J.; Nadas, J.; Zhang, G.; Sun, D. Modifying the Sugar Moieties of Daunorubicin Overcomes P-Gp-Mediated Multidrug Resistance. *Molecular Pharmaceutics*. **2007**, *4*, 140–153.

(22) Yu, S.; Zhang, G.; Zhang, W.; Luo, H.; Qiu, L.; Liu, Q.; Sun, D.; Wang, P. G.; Wang, F. Synthesis and Biological Activities of a 3'-Azido Analogue of Doxorubicin Against Drug-Resistant Cancer Cells. *International Journal of Molecular Sciences*. **2012**, *13*, 3671.

(23) Robey, R. W.; Pluchino, K. M.; Hall, M. D.; Fojo, A. T.; Bates, S. E.; Gottesman, M. M. Revisiting the Role of Efflux Pumps in Multidrug-Resistant Cancer. *Nature reviews. Cancer*. **2018**, *18*, 452.

(24) Kodan, A.; Futamata, R.; Kimura, Y.; Kioka, N.; Nakatsu, T.; Kato, H.; Ueda, K. ABCB1/MDR1/P-Gp Employs an ATP-Dependent Twist-and-Squeeze Mechanism to Export Hydrophobic Drugs. *FEBS letters*. **2021**, *595*, 707–716.

(25) Lai, J. I.; Tseng, Y. J.; Chen, M. H.; Huang, C. Y. F.; Chang, P. M. H. Clinical Perspective of FDA Approved Drugs With P-Glycoprotein Inhibition Activities for Potential Cancer Therapeutics. *Frontiers in Oncology*. **2020**, *10*, 561936.

(26) Burgess, D. J.; Doles, J.; Zender, L.; Xue, W.; Ma, B.; McCombie, W. R.; Hannon, G. J.; Lowe, S. W.; Hemann, M. T. Topoisomerase Levels Determine Chemotherapy Response in Vitro and in Vivo. *Proceedings of the National Academy of Sciences of the United States of America*. **2008**, *105*, 9053–9058.

(27) Cruet-Hennequart, S.; Prendergast, Á. M.; Shaw, G.; Barry, F. P.; Carty, M. P. Doxorubicin Induces the DNA Damage Response in Cultured Human Mesenchymal Stem Cells. *International Journal of Hematology*. **2012**, *96*, 649–656.

(28) Li, Y.; Tan, M.; Sun, S.; Stea, E.; Pang, B. Targeted CRISPR Activation and Knockout Screenings Identify Novel Doxorubicin Transporters. *Cellular oncology (Dordrecht)*. **2023**, *46*, 1807–1820.

(29) Daina, A.; Michielin, O.; Zoete, V. SwissADME: A Free Web Tool to Evaluate Pharmacokinetics, Drug-Likeness and Medicinal Chemistry Friendliness of Small Molecules. *Scientific Reports 2017 7:1*. **2017**, *7*, 1–13.

Supporting information chapter 4

#	IC_{50} WT (μM)	IC_{50} ABCB1 (μM)	IC_{50} ABCG2 (μM)	Topo IIα targeting	DNA damage	Histone eviction
1	0,325	1,587	0,528	Yes	Yes [7]	Yes [7]
2	0,239	2,083	0,428	Yes	Yes [18]	Yes [18]
3	0,141	0,686	0,286	Yes	Yes [17]	Yes [17]
4	0,031	0,077	0,060	Yes	No [7]	Yes [7]
5	0,027	0,041	0,116	Yes	Yes [17]	Yes [17]
6	7,696	8,068	8,199	No	Yes [17]	No [17]
7	0,136	0,390	0,293	Yes	No [7]	Yes [7]
8	0,098	0,187	0,336	Yes	No [18]	Yes [18]
9	0,038	0,074	0,041	Yes	No [17]	Yes [17]
10	3,324	20,905	3,379	Yes	No [7]	No [7]
11	0,078	0,091	0,073	Yes	No [17]	Yes [17]
12	0,379	2,087	0,396	Yes	No [17]	Yes [17]
13	0,172	0,312	0,173	Yes	No [17]	Yes [17]
14	0,195	0,402	0,193	Yes	No [17]	Yes [17]
15	0,064	0,066	0,059	Yes	No [17]	Yes [17]
16	0,084	0,089	0,303	Yes	Yes [17]	No [17]
17	0,856	1,127	7,799	Yes	Yes [17]	No [17]
18	1,621	1,978	3,827	Yes	Yes [17]	No [17]
19	0,042	0,829	0,196	Yes	Yes [17]	No [17]
20	1,18	1,540	1,368	Yes	No [17]	Yes [17]
21	1,788	19,820	2,736	Yes	Yes [17]	No [17]
22	1,623	29,892	2,341	Yes	No [17]	Yes [17]
23	5,32	5,413	8,695	Yes	No [17]	Yes [17]
24	1,098	1,213	1,091	Yes	No [17]	Yes [17]
25	0,23	1,221	0,242	Yes	Yes [17]	Yes [17]
26	0,019	0,032	0,017	Yes	No [17]	Yes [17]
27	1,796	4,511	1,752	Yes	No [7]	Yes [7]
28	0,174	1,715	0,175	Yes	No [7]	Yes [7]
29	1,173	30,123	1,957	Yes	Yes [7]	No [7]
30	0,019	1,000	0,065	Yes	No [7]	Yes [7]
31	0,381	1,588	0,914	Yes	Yes [17]	Yes [17]
32	0,129	0,220	0,139	Yes	No [17]	Yes [17]
33	2,117	17,975	3,861	Yes	Yes [18]	No [18]
34	3,244	4,377	7,325	Yes	Yes [18]	Yes [18]
35	2,206	11,423	3,729	Yes	Yes [18]	Yes [18]
36	0,535	1,928	0,510	Yes	Yes [18]	Yes [18]
S1	>10	-	-		No	No

#	IC_{50} WT (μM)	IC_{50} ABCB1 (μM)	IC_{50} ABCG2 (μM)	Topo IIα targeting	DNA damage	Histone eviction
S2	>10	-	-		No	Yes
S3	>10	-	-		No	No
S4	>10	-	-		No	Yes

Table S1 – The compound numbers shown in column one correspond to the structure of Figure S1. Cytotoxicity (IC_{50} values) towards K562 wildtype, ABCB1 overexpressing and ABCG2 overexpressing cells were calculated for all compounds. Targeting of TopoIIα was examined after treatment with 10 μM of compounds. Individual images are depicted in Figure S4. DNA damage and histone eviction data was reported on before, data indicated with ^[7] was reproduced from reference #7, copyright 2020 American Chemical Society, data indicated with ^[18] was reproduced from reference #18, copyright 2021 American Chemical Society, data indicated with ^[17] was reproduced from reference #17, copyright 2023 American Chemical Society.'

#	MW	Heavy atoms	Fraction Csp3	Rotatable bonds	H-bond acceptors	H-bond donors	MR	TPSA	LOGP	LogS
1	543,5	39	0,44	5	12	6	132,7	206,1	1,27	-3,46
2	543,5	39	0,44	5	12	6	132,7	206,1	1,27	-3,46
3	527,5	38	0,44	4	11	5	131,5	185,8	1,83	-4,04
4	811,9	58	0,62	10	16	4	203,5	217,1	3,8	-5,29
5	497,5	36	0,42	3	10	5	125,0	176,6	1,86	-3,95
6	483,5	35	0,4	3	10	5	120,2	176,6	0,92	-3,81
7	571,6	41	0,48	6	12	5	142,5	183,3	2,25	-3,9
8	571,6	41	0,48	6	12	5	142,5	183,3	2,25	-3,9
9	555,6	40	0,48	5	11	4	141,3	163,1	2,81	-4,47
10	783,8	56	0,6	9	16	5	193,7	239,8	2,82	-4,87
11	525,6	38	0,46	4	10	4	134,8	153,8	2,84	-4,38
12	583,6	42	0,5	6	12	5	149,1	183,3	2,23	-3,94
13	597,6	43	0,52	6	12	5	153,9	183,3	2,59	-4,2
14	611,6	44	0,53	6	12	5	158,7	183,3	2,95	-4,46
15	613,6	44	0,52	6	13	5	155.0	192,5	1,73	-3,92
16	569,5	41	0,44	6	14	5	134,8	229,8	3,08	-3,93
17	544,5	39	0,44	5	12	6	131,1	200,3	1,53	-3,25
18	528,5	38	0,44	5	11	5	130.0	180,1	2,5	-4,07
19	513,5	37	0,48	4	10	5	131,3	168,8	2,57	-4,51
20	541,6	39	0,52	5	10	4	141,1	146.0	3,55	-4,95
21	529,5	38	0,48	5	11	6	132,5	189.0	1,9	-3,94
22	557,6	40	0,52	6	11	5	142,3	166,2	2,88	-4,37
23	557,6	40	0,46	5	12	6	137,7	206,1	2,28	-3,6
24	585,6	42	0,5	6	12	5	147,5	183,3	3,26	-4,04

#	MW	Heavy atoms	Fraction Csp3	Rotatable bonds	H-bond acceptors	H-bond donors	MR	TPSA	LOGP	LogS
25	739,8	53	0,58	7	15	5	183.0	230,6	2,6	-4,64
26	767,8	55	0,6	8	15	4	192,8	207,8	3,07	-5,06
27	701,7	50	0,57	8	15	6	172,5	222.0	2,13	-4,2
28	699,7	50	0,58	8	14	5	175,6	201,8	2,94	-4,63
29	785,8	56	0,59	9	17	6	190,7	260,1	2,01	-3,05
30	813,8	58	0,61	10	17	5	200,5	237,3	2,99	-3,78
31	543,5	39	0,44	5	12	6	132,7	206,1	1,27	-3,48
32	571,6	41	0,48	6	12	5	142,5	183,3	2,25	-4,21
33	543,5	39	0,44	5	12	6	132,7	206,1	1,27	-4,13
34	571,6	41	0,48	6	12	5	142,5	183,3	2,25	-4,56
35	543,5	39	0,44	5	12	6	132,7	206,1	1,27	-3,46
36	571,6	41	0,48	6	12	5	142,5	183,3	2,25	-3,9

Table S2 – The computational predictions of physicochemical parameters. The prediction of ADME parameters was performed with the freely accessible webtool SwissADME.[29]

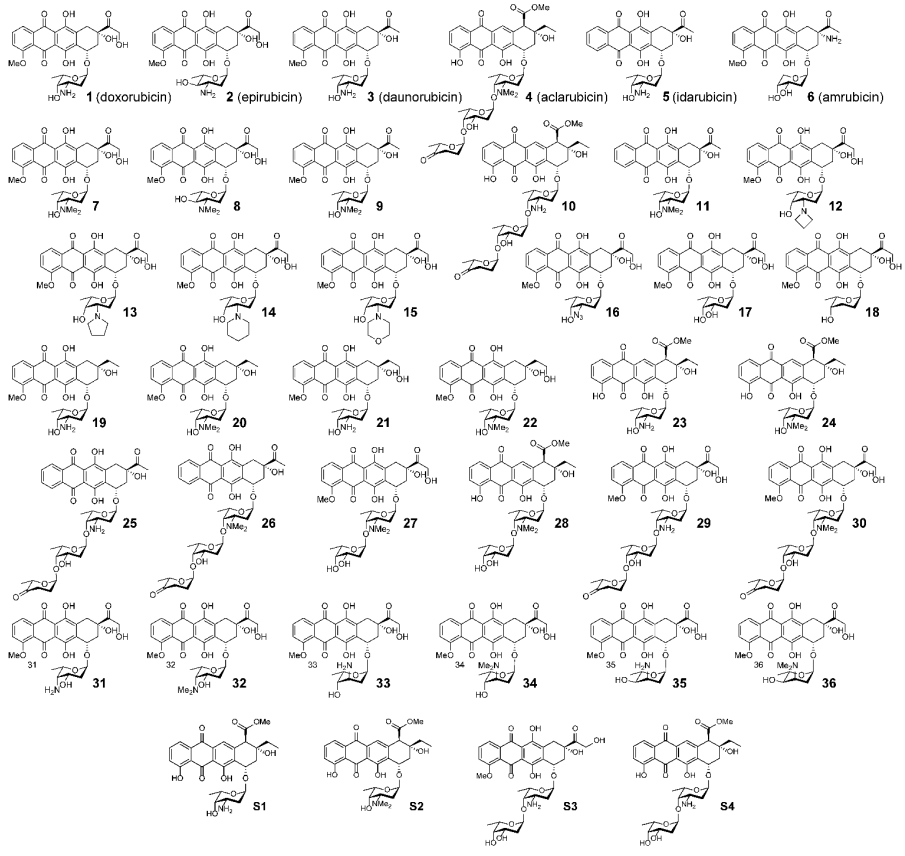

Figure S1 - Chemical structures of all compounds evaluated in this study; **1**-**36** and **S1**-**S4**.

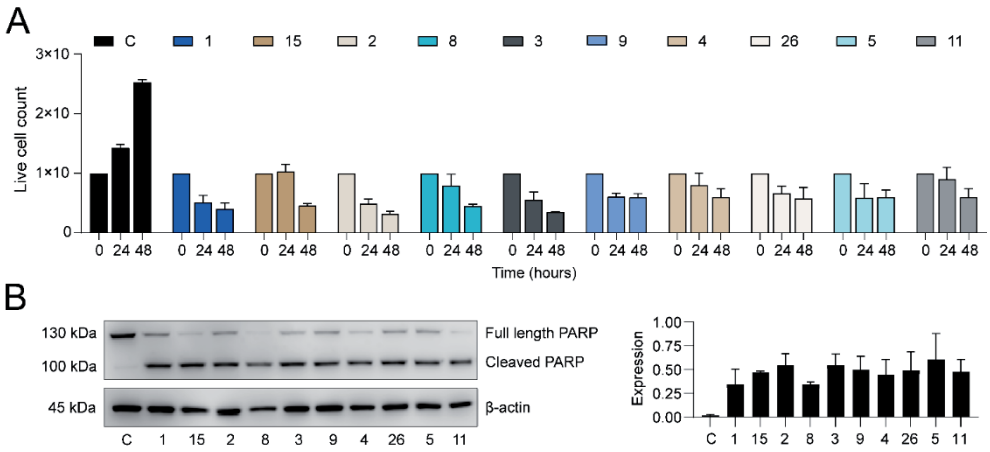

Figure S2 – Cell death in response to selected compounds 1-5, 8, 9, 11, 15, 26. Numbers correspond to the structures in Figure 1, C; unmanipulated control. (A) K562 wildtype cells were treated with 1 μM of the indicated compounds. The live / dead ratio was determined with DAPI staining and measured with flow-cytometry. (B) K562 wildtype cells were treated with 5 μM of the indicated compounds for 24 hours. PARP cleavage was examined by Western blot. Actin was used as a loading control, and molecular weight markers are indicated. Results are presented as mean ± SD of two independent experiments.

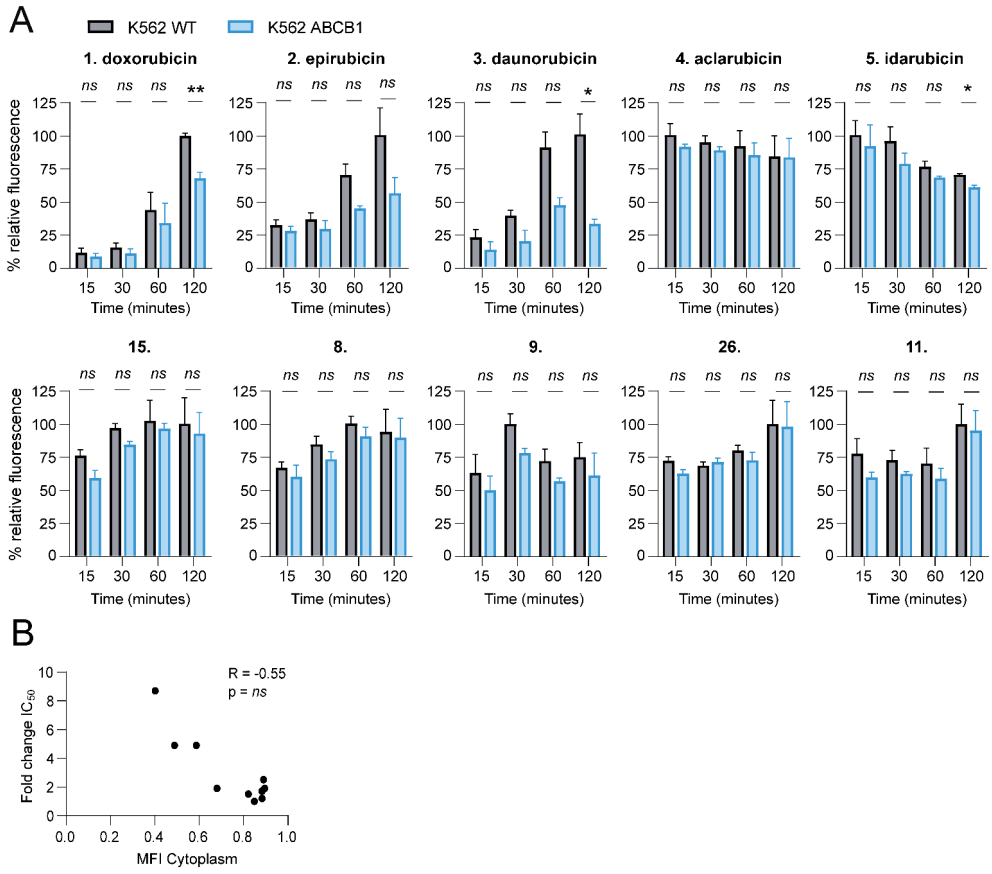

Figure S3 – Cytoplasmic accumulation of selected compounds **1**-**5**, **8**, **9**, **11**, **15**, **26**. Numbers correspond to the structures in Figure 1. (A) K562 wildtype and ABCB1 overexpressing cells were treated with 10 µM of the indicated compounds and subjected to fractionation. Mean fluorescence intensity in the cytoplasmic fraction was measured at a series of timepoints (15, 30, 60 and 120 minutes). Fluorescence was normalized to the largest signal. Two-way ANOVA; * $p<0.05$; ** $p<0.01$; *** $p<0.001$; ns, not significant. (B) Correlation between fold change IC_{50} and mean fluorescence intensity in cytoplasmic fraction.

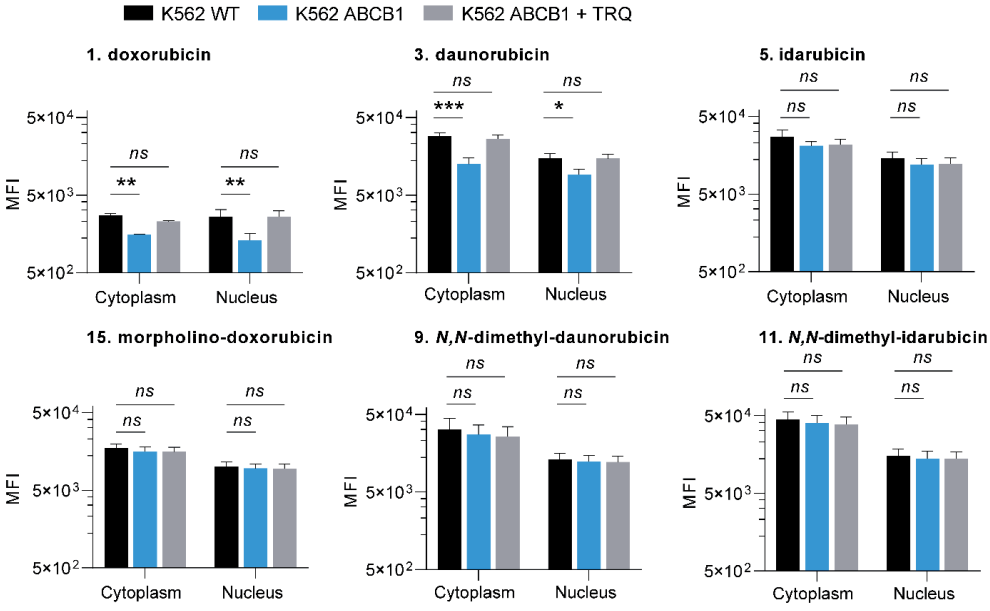

Figure S4 – Nuclear and cytoplasmic accumulation of selected compounds **1**, 3, **5**, **9**, **11**, **15**. Numbers correspond to the structures in Figure 1. K562 wildtype and ABCB1 overexpressing cells were treated with 10 μM of the indicated compounds, in the presence and absence of ABCB1-inhibitor Tariquidar. Mean fluorescent intensity was measured in cytoplasmic and nuclear fractions of K562 wildtype cells, ABCB1 overexpressing cells and ABCB1 overexpressing cells treated with Tariquidar (TRQ). Two-way ANOVA; * $p<0.05$; ** $p<0.01$; *** $p<0.001$; ns, not significant.

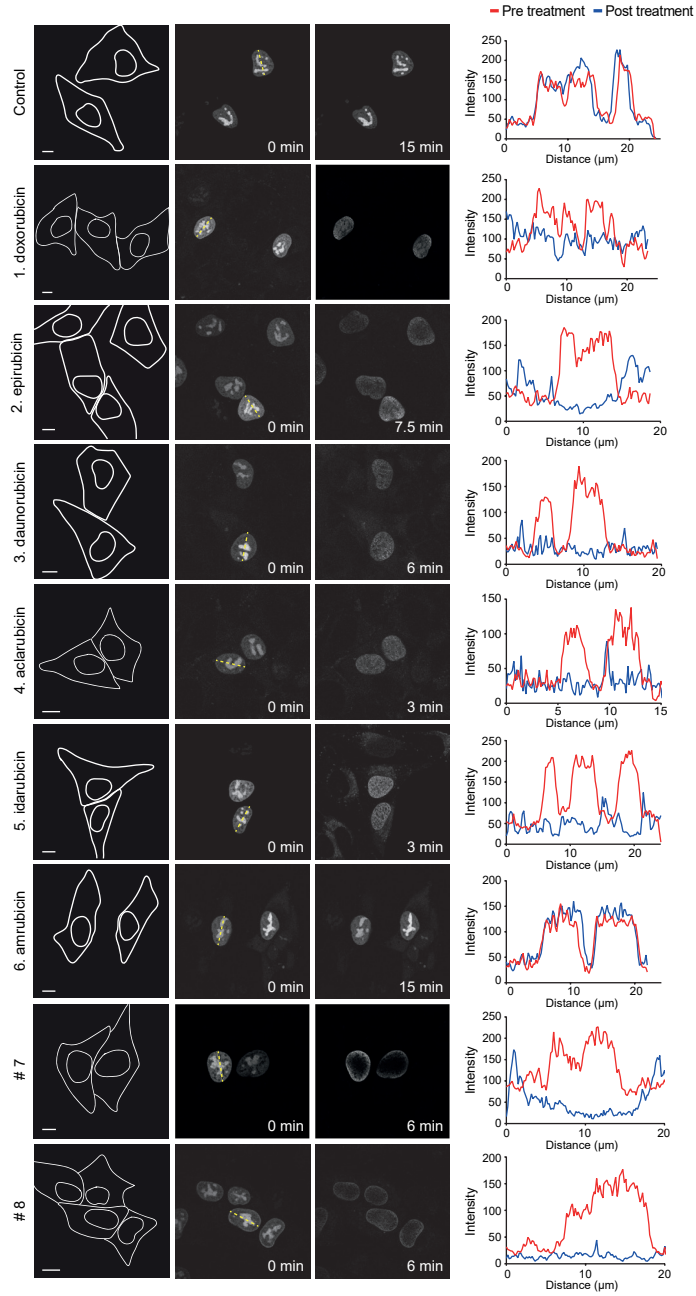

Figure S5 – Topoisomerase IIα relocalization for compounds **1**-**8**. Numbers correspond to the structures in Figure 1. Redistribution of GFP-TopoIIα transiently expressed in wildtype MelJuso. Cells were treated with 10 µM of indicated compounds and GFP-TopoIIα signal was measured over time. Scale bar 10µm. GFP signal was quantified pre- and post-treatment with the compounds and plotted as fluorescence over distance of dotted yellow line.

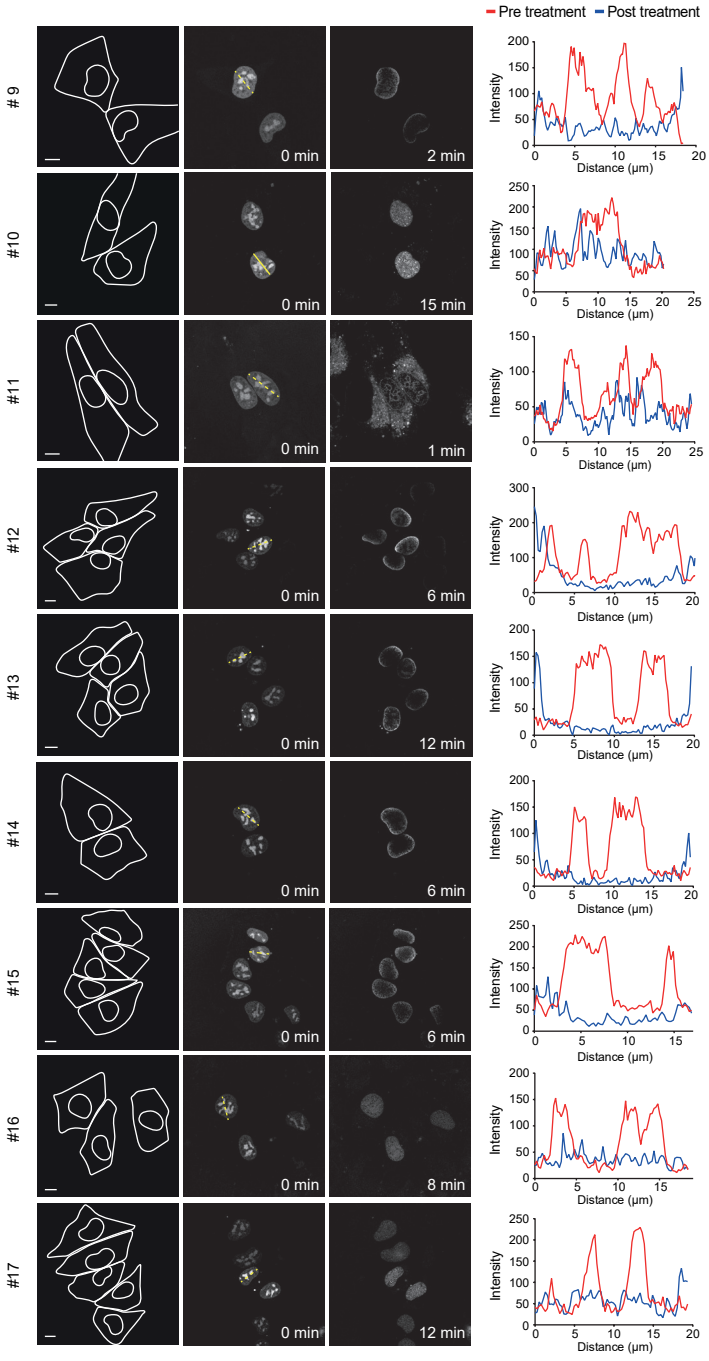

Figure S5 – Continued; Topoisomerase IIα relocalization for compounds **9**-**17**. Numbers correspond to the structures in Figure 1.

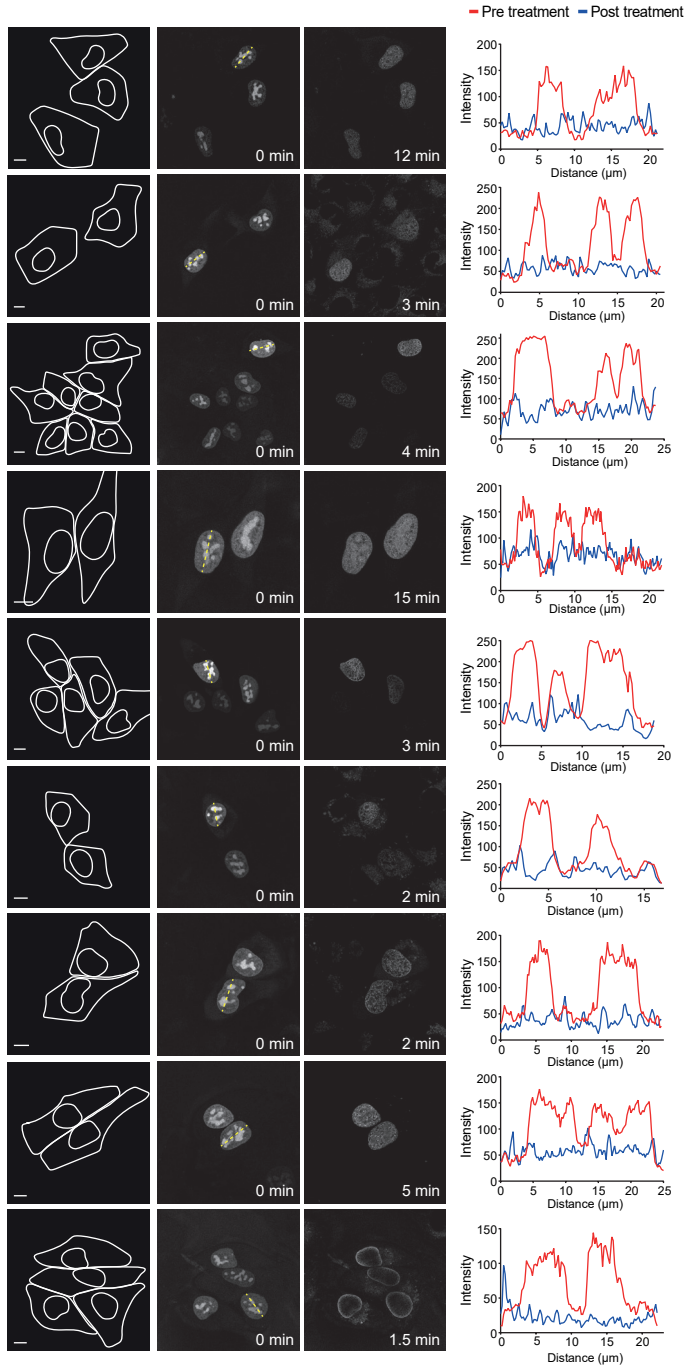

Figure S5 – Continued; Topoisomerase IIα relocalization for compounds **18**-**26**. Numbers correspond to the structures in Figure 1

CHAPTER 5

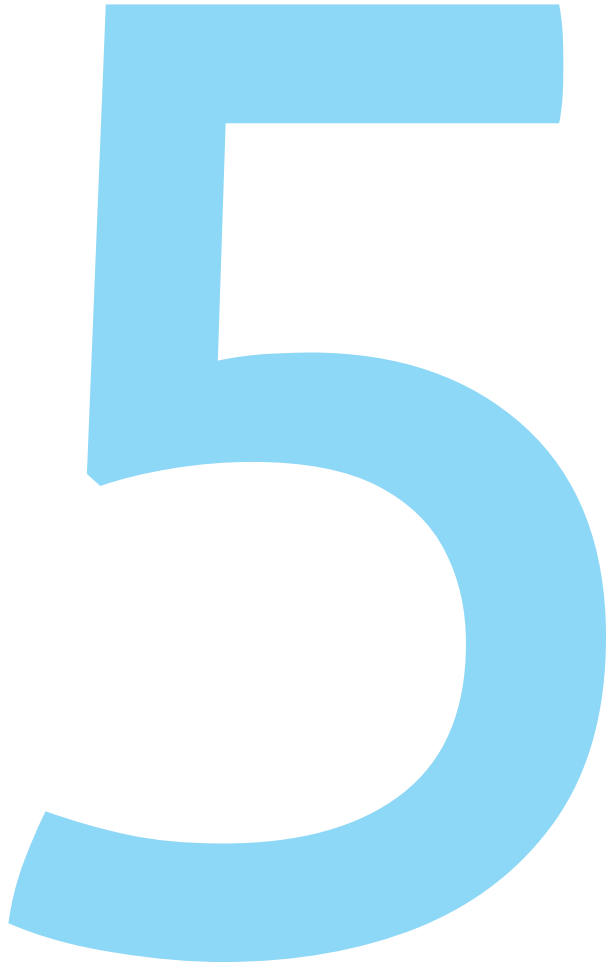

Conclusion and Future Prospects

Anthracyclines are potent chemotherapeutics used to treat various cancers, such as leukemias, lymphomas, and solid tumors. They are characterized by their tetracyclic structure, which facilitates DNA intercalation, connected to an amino sugar that can interact with the DNA backbone phosphodiesters through salt bridges.[1] This intrinsic capacity underlies two main modes of anthracycline action: the generation of DNA double stranded breaks (DNA damage) and eviction of histones from chromatin (chromatin damage).[2] Despite their effectiveness, anthracycline treatment is associated with severe side effects, including long-term issues such as cardiotoxicity, gonadotoxicity and secondary tumorigenesis.[3] These side effects are particularly concerning due to their significant impact on the quality of life of cancer patients. Previous research has suggested that the DNA-damaging function of anthracyclines is primarily linked to these side effects, indicating that anthracyclines that only cause chromatin damage might be preferable over standard therapy.

In **chapter 2**, we evaluated a total of 26 anthracycline variants for their cytotoxicity, DNA damage and chromatin damage activities, making it one of the largest structure-activity relationship study of anthracyclines to date. From this study, we derived several general guidelines regarding the potency and modes of action of anthracyclines. These are: (1) The main cytotoxic activity of the compounds is associated with histone eviction rather than DNA double strand break induction; (2) Generally, *N,N*-dimethylation eliminates DNA double strand break formation without compromising cytotoxicity; (3) Small modifications in the tetracyclic aglycone further contribute to cytotoxicity, as illustrated by the differences in cytotoxicity between doxorubicin and idarubicin; (4) The position of the amine on the sugar moiety has minor effects; and (5) Replacing the amine by an OH or H group significantly reduces cytotoxicity.

The importance of distinguishing between different modes of anthracycline action has been demonstrated by previous studies, which showed that the combination of DNA damage and histone eviction—as exhibited by doxorubicin—results in the major side effects associated with this drug.[4] Anthracyclines that solely induce chromatin damage, such as aclarubicin and *N,N*-dimethyldoxorubicin, are at least as effective against tumor cells as doxorubicin but are less toxic to healthy cells and tissues. For instance, *N,N*-dimethyldoxorubicin does not cause cardiotoxicity, secondary tumor formation, or gonadal dysfunction in murine *in vivo* models.[4] Furthermore, clinical observations indicate that aclarubicin treatment is less cardiotoxic for cancer patients than doxorubicin treatment, while both compounds appear equally effective as anticancer agents.[5,6] These results suggest that separating DNA damage from chromatin damage activities may guide the development of novel variants that lack the major long-term side effects that are associated with currently used anthracycline variants.

Although *N,N*-dimethyldoxorubicin was proven less cardiotoxic in *in vivo* murine models, this has not yet been established in patients. Given the thousands of research papers suggesting that impaired mitochondrial function is associated with cardiotoxicity, we selected six compounds from **chapter 2,** including *N-N*-dimethyldoxorubicin, to investigate their effects on mitochondrial function.

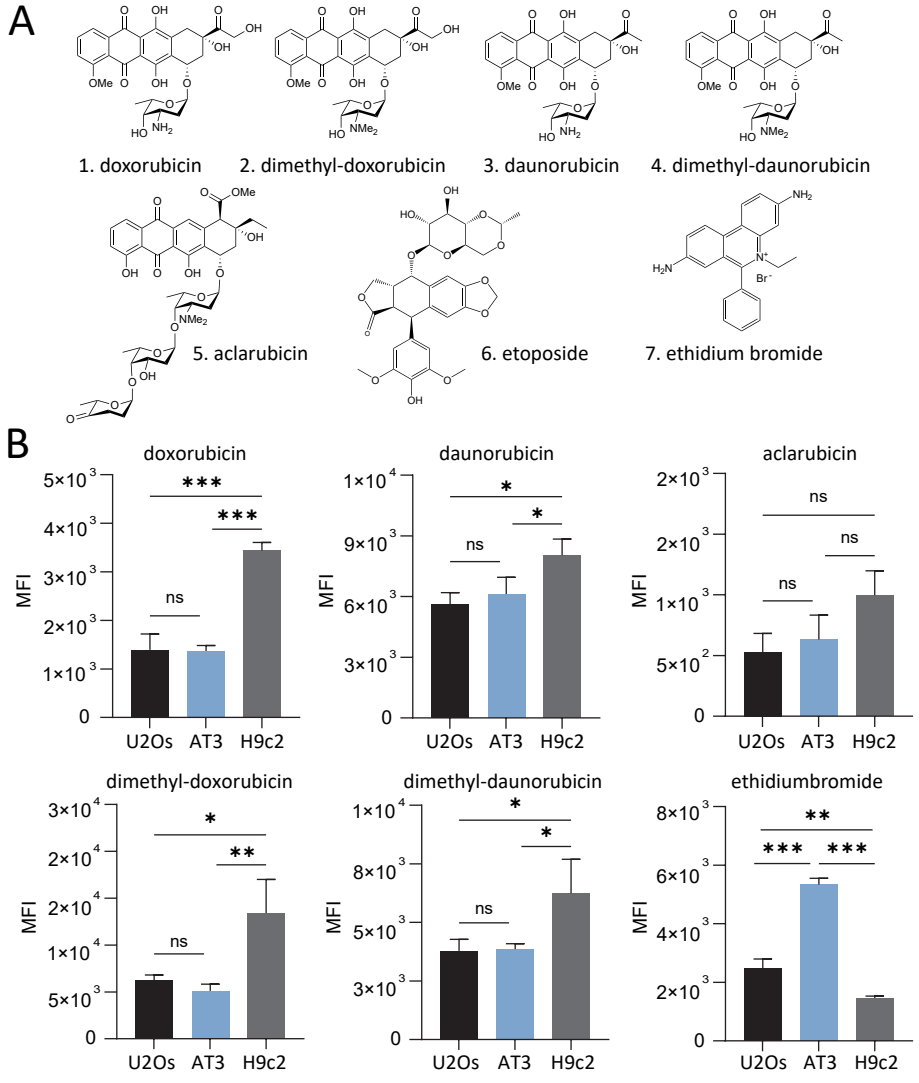

Figure 1 – Chemical structures of anthracycline variants and their cellular uptake. (A) Chemical structures of different anthracycline variants, etoposide, and ethidium bromide. (B) Cellular uptake after 2 hours incubation with different compounds. Intracellular accumulation was measured with flow-cytometry, and mean fluorescent intensity is plotted for all compounds. Ordinary one-way ANOVA, * $p < 0,05$; ** $p < 0,01$; *** $p < 0.001$.

Of these variants, doxorubicin (**1**) and daunorubicin (**3**) induce both DNA and chromatin damage, while *N,N*-dimethyldoxorubicin (**2**), *N,N*-dimethyldaunorubicin (**4**) and aclarubicin (**5**) induce only chromatin damage. Etoposide (**6**) was included as a control that induces only DNA damage, and ethidium bromide (**7**) served as a control for DNA intercalation. (Figure 1A).

We conducted initial experiments as part of a structure-activity relationship study focusing on mitochondrial function. First, we compared the cellular uptake of these anthracyclines and ethidium bromide in two cancer cell lines (U2Os and HeLa) and a myoblast derived cardiac cell line (H9c2). Interestingly, the uptake of all anthracyclines was increased in H9c2 cells compared to both cancer cell lines, although this was not the case for ethidium bromide (Figure 1B). This finding aligns with previous research suggesting that heart tissue is a preferential site for anthracycline accumulation. The most significant effect was observed for doxorubicin, which showed a two-fold higher cellular uptake in cardiac cells compared to the cancer cell lines used. The cell type specific uptake of anthracyclines may be related to the expression of import transporters. Several members of the solute carrier (SLC) superfamily of membrane transporters have been linked to cell-type specific toxicity profiles in response to anthracyclines.[7] However, comparing the cytotoxicity of these compounds in cardiac H9c2 cells to that in U2Os and AT3 cancer cells revealed that all selected compounds, including doxorubicin, were significantly less cytotoxic in H9c2 cells despite the increased uptake (data not shown). This may be due to the higher proliferation rates of both cancer cell lines compared to the cardiac cells. Our data indicate that cellular uptake of anthracyclines is not directly linked to cytotoxicity in the cell lines used in this study, but future research could address whether the expression of SLC importers are regulating cell-type specific accumulation and toxicities of anthracyclines.

In terms of molecular mechanism, we explored whether there is overlap between the effects observed in the nucleus and those in the mitochondria. We confirmed the DNA damaging activity of the selected compounds in the nucleus and aimed to assess the damage to mitochondrial DNA too. Doxorubicin and daunorubicin caused DNA double stranded breaks in genomic DNA (Figure 2A), but we could not detect any mitochondrial DNA damage (Figure 2B). High concentrations of hydrogen peroxide did induce damage of mitochondrial DNA, as expected based on previous reports.[8] In contrast to previous reported literature[9], we could not detect any lesions caused by doxorubicin using the long-range PCR method. Earlier research has indicated a depletion of mtDNA in response to anthracyclines[10], which may contribute to this discrepancy, as our protocol controls for total mtDNA levels. Although the long-range PCR method is frequently used, it has some major limitations. First, DNA lesions that do not significantly stall progression of DNA polymerases will not be detected. Compounds that cause oxidative stress, such as

H_2O_2, are thought to produce more than one type of lesion[11] and anthracyclines may act similarly. The nature of specific lesions cannot be detected with PCR-based methods, but this limitation is shared by other methods available.[12] In addition, the method is based on the expectancy that for most DNA damaging agents, lesions will be introduced randomly in both genomic DNA and mitochondrial DNA. In the case of anthracyclines, this assumption may be incorrect, based on observations of preferential sites of DNA double stranded breaks induction in genomic DNA.[13]

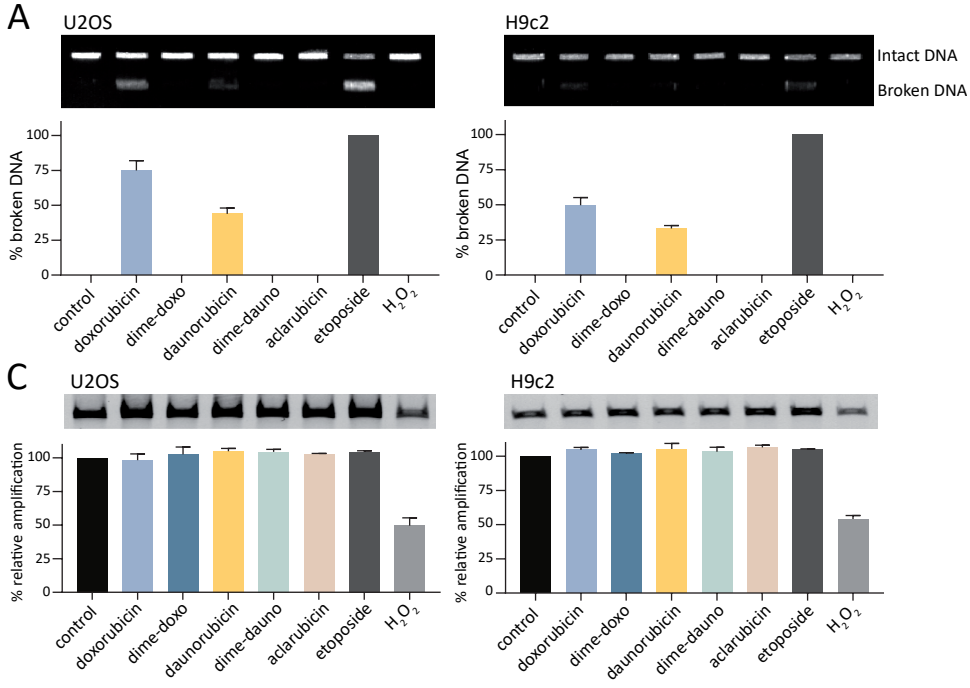

Figure 2 – Nuclear and mitochondrial DNA damage induced by anthracyclines. (A) Nuclear DNA double strand breaks were directly visualized by CFGE in U2OS cells and H9c2 cells. The position of intact and broken DNA is indicated, broken DNA was quantified relative to total DNA. (B) Mitochondrial DNA damage was assessed using long-range PCR in U2OS cells and H9c2 cells. DNA amplification was quantified relative to untreated control cells.

Due to the circular nature of mtDNA (16.6 kb)[14] we validated whether these anthracyclines intercalate into circular plasmid DNA of similar size and examined any differences between anthracycline variants in terms of intercalation. The intercalation of anthracyclines was tested using a competition dye displacement assay with ethidium bromide (Figure 3A) and PicoGreen (Figure 3B). These dyes were chosen because of their

fluorescence upon binding to double-stranded DNA and the addition of compounds that displace the dye results in a loss of fluorescence signal. Plotting the remaining fluorescence against compound concentrations (Figure 3B) revealed that doxorubicin has the highest DNA binding affinity, followed by *N,N*-dimethyldoxorubicin, which was only slightly less efficient. Daunorubicin and *N,N*-dimethyldaunorubicin demonstrated equal DNA intercalation efficiency. The non-intercalating Topo II inhibitor etoposide was used as a negative control. From these results we can deduct that these anthracycline variants could all intercalate into circular, and thus likely also mitochondrial DNA. However, we cannot fully account for the degree in which these anthracycline variants accumulate in the mitochondria to start with. We performed a pilot experiment that confirmed accumulation of doxorubicin, *N,N*-dimethyldoxorubicin, daunorubicin and *N,N*-dimethyldaunorubicin in the mitochondria (data not shown). There are numerous reports about doxorubicin and daunorubicin entering and accumulating in mitochondria[15], but it remains a challenge to compare different anthracycline variants with flow-cytometry or microscopy because of their different fluorescence properties.

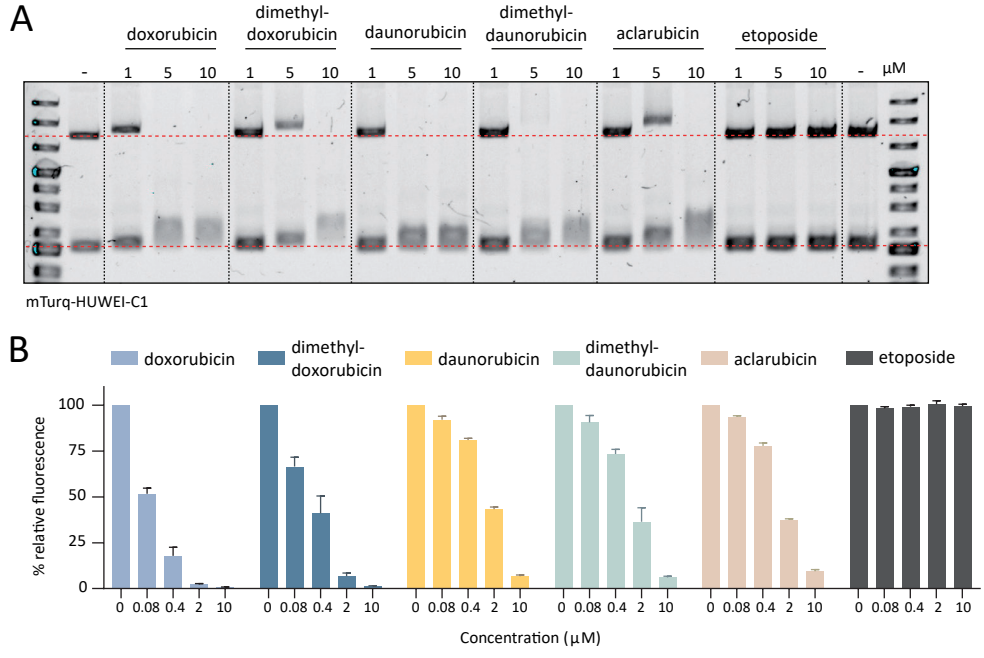

Figure 3 – DNA intercalation affinity of anthracycline variants. (A) The intercalation of anthracyclines into circular double-stranded DNA was tested in a competition dye displacement assay with ethidium bromide. (B) Intercalation affinity was quantified with PicoGreen. The percentage of initial fluorescence is plotted against the concentrations of the indicated compounds.

Previous research has shown that anthracyclines can alter genomic DNA transcription, and that the effects are region-specific for different anthracyclines.[16] We aimed to validate if mitochondrial DNA transcription is similarly altered in response to anthracycline treatment. To this end, we selected genes from three different regions of the circular mitochondrial DNA: mt-ND1, mt-CYB, and mt-CO1. These genes encode proteins that are part of the mitochondrial respiratory chain: NADH dehydrogenase 1, cytochrome b, and cytochrome c oxidase I, respectively.

In both cell lines tested, we observed a trend towards decreased expression of mt-ND1 and mt-CYB in response to anthracycline treatment, while the effects on mt-CO1 expression were less pronounced (Figure 4). Treatment with etoposide or hydrogen peroxide did not alter the expression of mt-ND1, mt-CYB, or mt-CO1, supporting the hypothesis that DNA intercalation is important for the disruption of gene expression. Region-specific DNA intercalation may also contribute to the observed differences between anthracyclines.

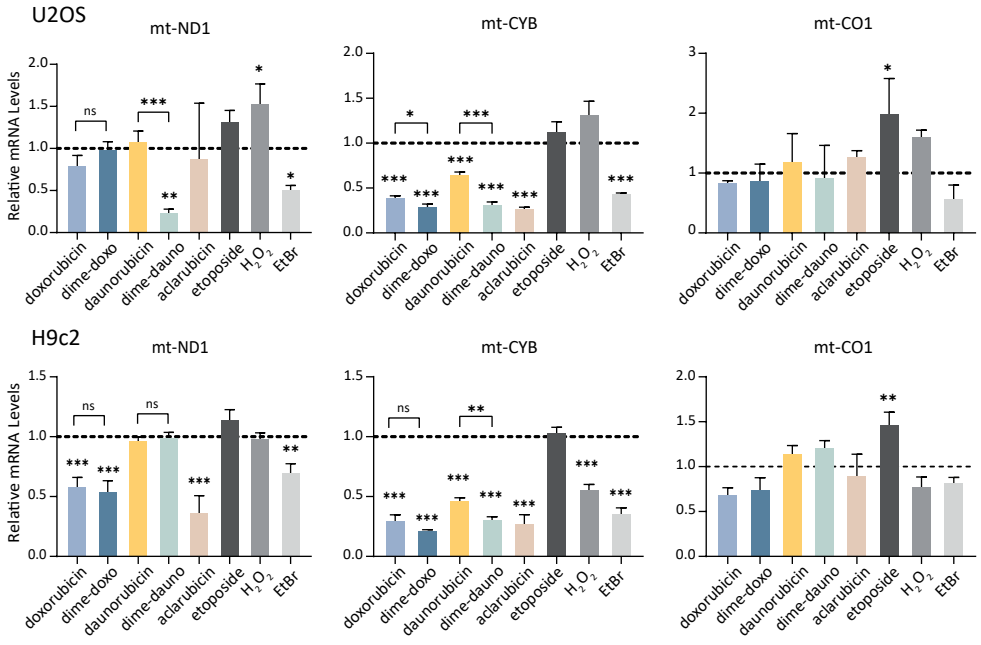

Figure 4 – The effect of anthracycline variants on the expression of mitochondrial genes. The expression of mRNA levels of mt-ND1, mt-CYB and mt-CO1 was measured with RT-QPCR in U2OS cells and H9c2 cells 4 hours post anthracycline treatment. Ordinary one-way ANOVA with Dunnett's multiple comparison test, * $p < 0,05$; ** $p < 0,01$; *** $p < 0.001$.

The location of mt-CYB near the D-loop and origin of replication for the mitochondrial heavy strand – sites serving as central hubs for mtDNA replication and transcription[17] – could explain why the expression of this gene is particularly affected compared to mt-ND1 and mt-CO1. Regiospecificity has been described for different anthracycline variants in the context of genomic DNA. For instance, doxorubicin specifically induces double-stranded breaks near active promoter regions[13], and the intercalation of daunorubicin is partially dependent on GC content.[18] This regiospecificity extends to different chromatin states, with doxorubicin and daunorubicin preferentially binding to open chromatin regions, while aclarubicin also intercalates into condensed chromatin.[16] Future research employing a ChIP-seq-like protocol specifically designed for mitochondrial DNA may provide valuable insights into the relationship between mitochondrial gene expression, and anthracycline intercalation sites.

To examine potential direct effects on mitochondrial DNA integrity and transcription we studied proteins involved in mitochondrial DNA maintenance and transcription. To this end, we made U2OS cell lines in which either mitochondrial transcription factor A (TFAM), factor B2 (TFB2M) or mitochondrial RNA polymerase (mtRNAP) were endogenously tagged with GFP. TFAM coats the mitochondrial genome and, together with TFB2M and mtRNAP, forms the transcription machinery.[17] Microscopic images show that the GFP signal overlaps with the MitoTracker signal, indicating that these proteins localize in the mitochondria (Figure 5).

Protein levels of TFAM were reduced in response to *N,N*-dimethyldoxorubicin, *N,N*-dimethyldaunorubicin and aclarubicin compared to doxorubicin, daunorubicin and the controls etoposide and H_2O_2. Similarly, treatment with the DNA intercalator ethidium bromide, also leads to a significant reduction of TFAM levels. The protein levels of TFB2M and mtRNAP, which act in a complex with TFAM, show a similar trend but to a lesser degree. The rapid degradation of TFAM when not bound to mtDNA, in contrast to stable levels of unbound TFB2M and mtRNAP, may partially explain these results. Through intercalation into mtDNA these anthracyclines may interfere and compete for binding sites of TFAM, hereby instigating TFAM degradation and inhibiting mtDNA transcription. Whether direct protein interactions between anthracyclines and the mitochondrial transcription machinery drive changes in mitochondrial gene expression remains to be elucidated, perhaps through novel immunoprecipitation techniques. Altogether, the preliminary data we obtained regarding the effects of different anthracycline variants on mitochondrial DNA integrity, transcription and translation do not yet provide a conclusive structure-activity relationship study. While all anthracyclines influenced mitochondrial function, the differences between variants were minimal. These results strengthen our hypothesis that cardiotoxicity may primarily arise from DNA damage activity in combination with chromatin damage, as observed with doxorubicin but not with *N,N*-dimethyldoxorubicin.

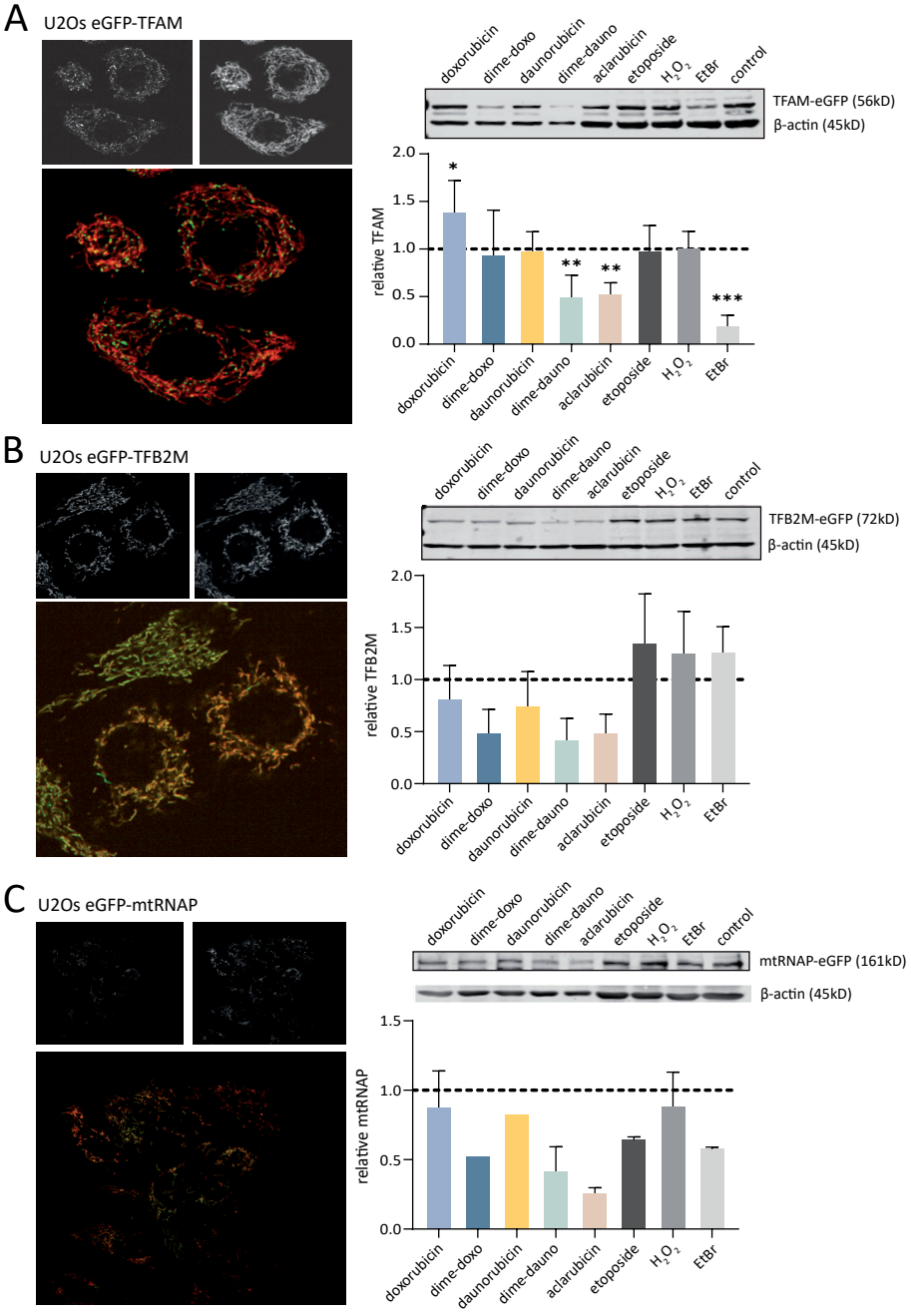

Figure 5 – Protein levels of TFAM, TFB2M and mtRNAP after anthracycline treatment. (A-C) Microscopic validation of endogenously GFP-tagged (A) TFAM, (B) TFB2M and (C) mtRNAP. Mitochondria are labeled with MitoTracker. TFAM, TFB2M and mtRNAP protein levels were quantified with western blot analysis. Ordinary one-way ANOVA with Dunnett's multiple comparison test, * $p < 0,05$; ** $p < 0,01$; *** $p < 0.001$.

The molecular mechanisms through which anthracyclines can inhibit Topo II and induce DNA double strand breaks are well established. In contrast, the discovery that not all anthracyclines cause DNA damage, and that some variants can additionally induce histone eviction is relatively recent. The exact mechanisms by which chromatin damage leads to cell death remain unclear. Therefore, we examined the unique properties of aclarubicin, an anthracycline that does not induce DNA double-strand breaks but does evict histones, leading to chromatin damage. In **chapter 3**, through genome-wide CRISPR-Cas9 knockout screening, we identified p53 as an important regulator of cell death in response to aclarubicin.

Aclarubicin activates a p53-dependent transcriptional program that induces apoptosis, like traditional DNA-damaging anthracyclines, but in the absence of DNA lesions. Aclarubicin-induced chromatin damage resulted in relocalization and activation of p53, and subsequently in p53-dependent apoptosis. Whether p53 itself senses unpacked DNA could not be confirmed in this study. We did however observe relocalization of p53 from the cytoplasm to the nucleus, and more specifically, enhanced binding to chromatin, suggesting that p53 may be part of a DNA sensing complex in response to histone eviction.

Potential interaction partners can be speculated upon based on molecular mechanisms involved in cell death in response to another class of chromatin damaging agents: curaxins. Nucleosome collapse induced by curaxins is sensed by the histone chaperone FACT (Facilitates Chromatin Transcription), which is normally involved in maintaining nucleosome stability during replication, transcription, and DNA repair.[19] Curaxins, which are DNA intercalating agents, can trap the FACT complex on DNA, leading to CK2 activation and subsequent activation of p53.[20] Previous studies have shown that aclarubicin also induces FACT binding to DNA[21], indicating that p53 activation by aclarubicin might be mediated through FACT and CK2. However, this matter is complicated by our finding that p53 is activated through phosphorylation on different serine residues, and it is therefore likely that multiple molecular pathways are involved. The presence of multiple molecular pathways involved in sensing aclarubicin induced chromatin damage may explain why we did not identify any proteins related to the FACT pathway in our screen. This is also consistent with the observation that specific apoptosis inhibitors could not rescue aclarubicin-induced cell death. While the p53-dependent apoptosis pathway may be dominant, tumor cells may also die through alternative pathways in response to aclarubicin.

Overall, this study underscores the critical role of p53 in mediating the cytotoxic effects of aclarubicin and its implications for cancer treatment strategies. Our data demonstrates that cellular sensitivity to aclarubicin can be predicted based on p53 status in *vitro*,

indicating that assessing p53 mutation status could serve as a valuable stratification method to identify patients who would benefit from aclarubicin treatment. Additionally, our results show that aclarubicin synergizes with the BCL-2 inhibitor venetoclax, which has recently been approved for the treatment of chronic lymphocytic leukemia (CLL) and acute myeloid leukemia (AML).[22] Patients could benefit from combination therapy with limited toxicities due to the low adverse effects of both drugs.

Our screen identified p53 as a major determinant of cellular sensitivity to aclarubicin, an anthracycline that primarily causes chromatin damage. However, it is still unknown which factors are involved in the process of histone eviction and the sensing of chromatin damage. To further explore the structure-activity relationship of the molecular characteristics that may dictate histone eviction and chromatin damage, we studied various structurally closely related doxorubicin variants. We included anthracyclines that induce both DNA damage and histone eviction (doxorubicin), those that cause only DNA damage (azido-doxorubicin, hydroxy-doxorubicin, desamino-doxorubicin), and one that only induces histone eviction (*N,N*-dimethyldoxorubicin) (Figure 6).

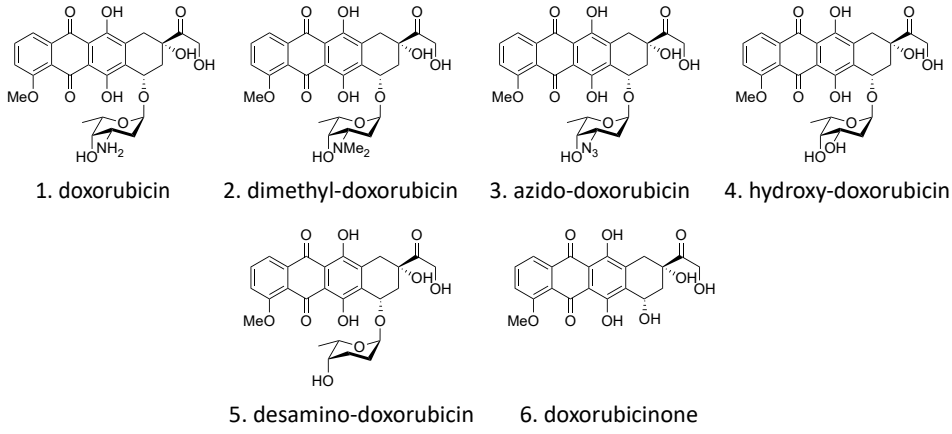

Figure 6 – Chemical structures of doxorubicin analogues.

Cells utilize various ATP-dependent nucleosome remodeling complexes to move, eject or incorporate histones, thereby guiding nucleosome assembly.[23] To determine whether anthracycline-induced histone eviction and nucleosome collapse is mediated by active processes in the nucleus, we compared histone eviction in untreated cells to that in ATP-depleted cells. We showed that histone eviction is not mediated by ATP-dependent processes, but rather occurs as an event that is probably associated with DNA intercalation and competition for space. Doxorubicin and *N,N*-dimethyldoxorubicin induced histone eviction when cells are fully depleted of ATP (Figure S1), whereas azido-doxorubicin,

hydroxy-doxorubicin, desamino-doxorubicin and doxorubinone failed to induce histone eviction altogether independent of ATP levels in the cell (Figure 7).

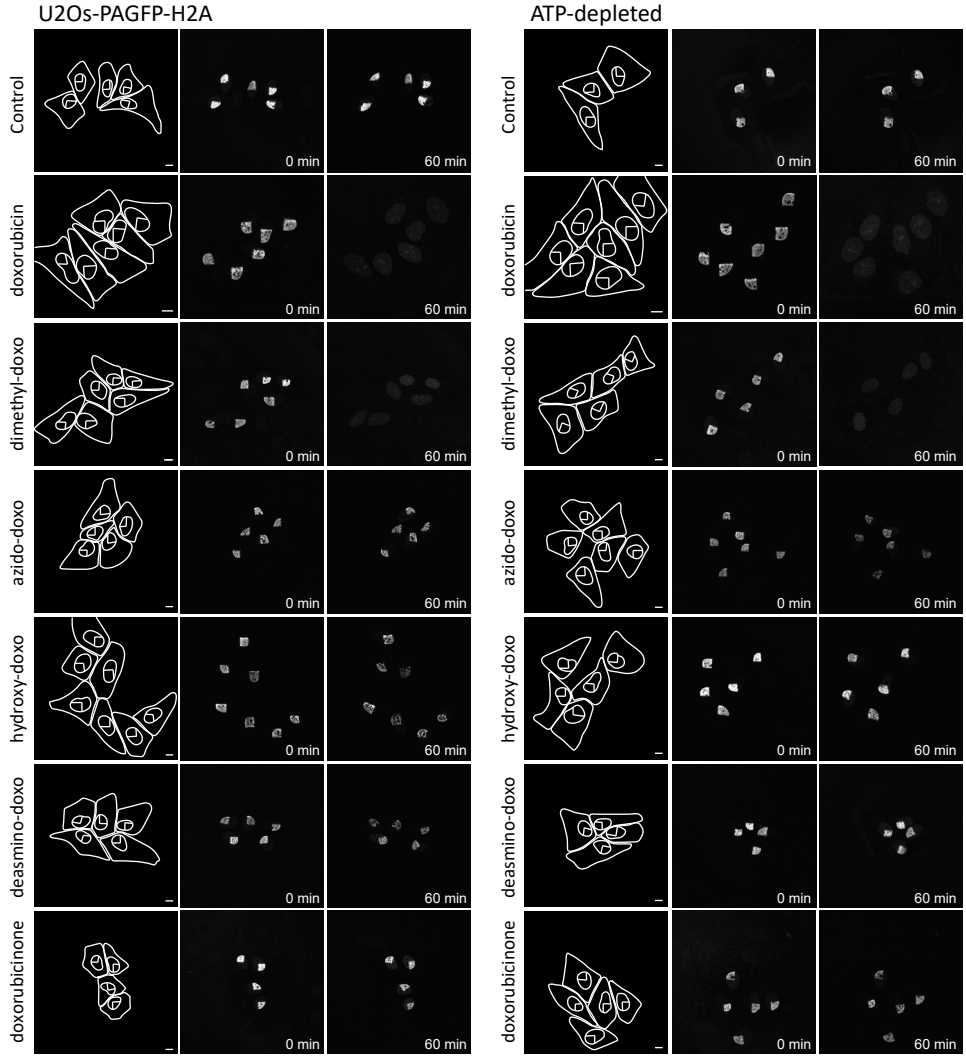

Figure 7 – Histone eviction in response to different doxorubicin analogues. Histone eviction was imaged in living U2Os-PAGFP-H2B cells and ATP-depleted cells. Left panel: cell outline and nucleus, the photoactivated part of the nucleus is indicated. Middle panel shows the photoactivated histones at the onset of the experiment after compound addition. Photo-activation was monitored by time-lapse confocal microscopy for 1 hour in the presence of the indicated compounds at 10 μM. Stills made at 60 min are shown in the right panel. Scale bar, 10 μm.

To study in detail if the intercalation and competition for space with histones is determined by structural differences, we first assessed DNA binding of these anthracyclines in a cell free setup. Here, we compared the properties of different anthracyclines in their displacement of an DNA intercalating dye (Picogreen, Figure 8A) and the displacement of a DNA minor groove binding dye (DAPI, Figure 8B).

All anthracycline variants tested intercalate into double stranded DNA and displace the Picogreen dye, albeit with different affinities. Doxorubicin displays the highest affinity for DNA intercalation in this set, and doxorubicinone the lowest. From crystal structure solution studies on the doxorubicin-DNA complex it was deduced that doxorubicin intercalates into the DNA with the sugar moiety pointing into the minor groove.[24] We performed a dye displacement assay with a minor groove binding dye, and here *N,N*-dimethyldoxorubicin showed the largest dye displacement. Remarkably, doxorubicinone, lacking the sugar moiety, displaces the minor groove binding dye DAPI like the other compounds. This could mean that the minor groove binding dye may dissociate from the DNA because of the intercalating properties that all anthracyclines used here show.

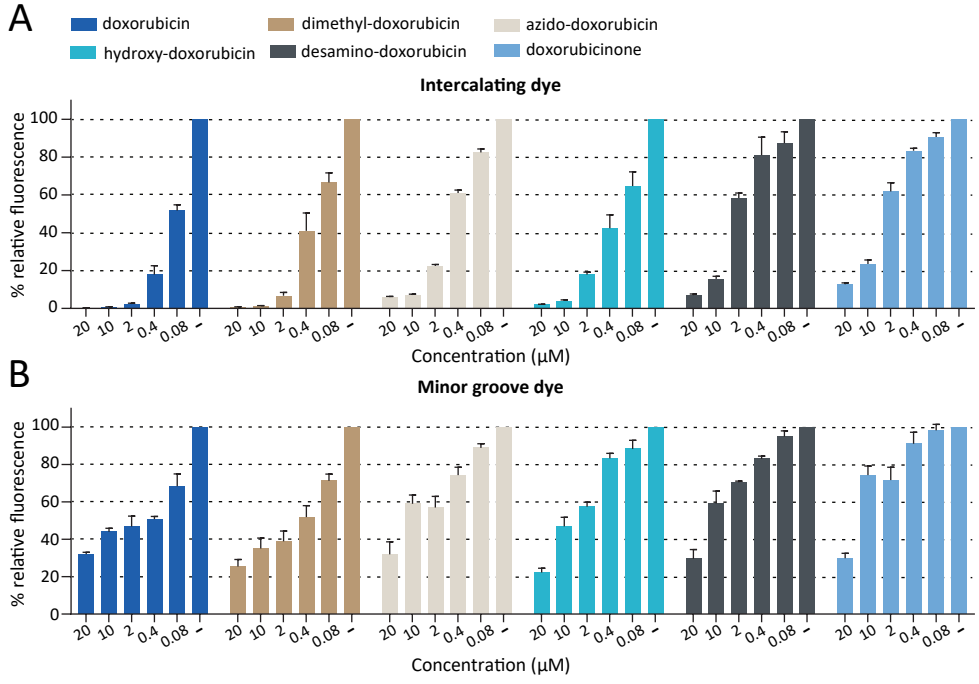

Figure 8 – DNA intercalation affinity of doxorubicin analogues. (A) The intercalation of anthracyclines was tested in a competition dye displacement assay with PicoGreen. The percentage of initial fluorescence is plotted against the concentrations of the indicated compounds. (B) The binding affinity of anthracyclines was measured with the minor-groove binding dye DAPI. The percentage of initial fluorescence is plotted against the concentrations of the indicated compounds.

In addition, we determined nucleosome collapse in cell free conditions in response to different anthracyclines. Reconstituted nucleosomes composed of the histones H2A, H2B, H3 and H4 were incubated with different concentrations of doxorubicin (Figure 9A). There is a clear dose-response relationship for doxorubicin in the disruption of nucleosomes. We compared different anthracycline variants in their capacity to cause histone dissociation, but only doxorubicin and *N,N*-dimethyldoxorubicin cause significant nucleosome collapse (Figure 9B) which is in line with the results published in **chapter 2**. Collectively, the results indicate that histone eviction is not just competition for space between anthracyclines and histones but is more likely determined by many intricate interactions. Since all doxorubicin variants intercalate into the DNA, the sugar-moiety may be a determining factor in the disruption of chromatin structures. The capacity of anthracyclines to induce histone eviction and nucleosome collapse is presumably determined by their structure, and independent of active processes within the cellular environment.

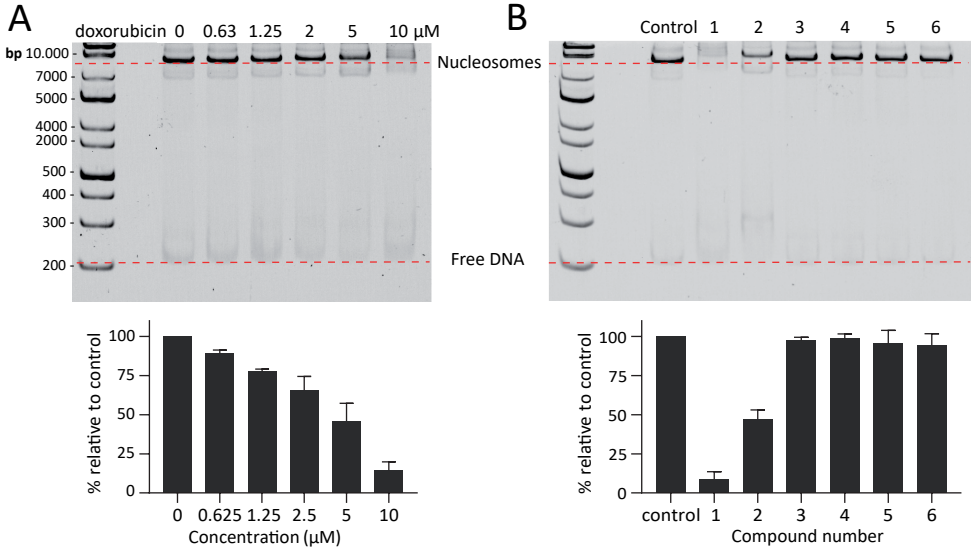

Figure 9 – Reconstituted nucleosome integrity in the presence of doxorubicin analogues. (A) Nucleosomes were incubated with different concentrations of doxorubicin. Results are quantified relative to untreated control. (B) Nucleosomes were incubated with different doxorubicin analogues at a concentration of 10µM. Results are quantified relative to untreated control. Incubation with doxorubicin or *N,N*-dimethyldoxorubicin induces nucleosome collapse.

Ultimately, higher resolution techniques are essential to study DNA intercalation and nucleosome collapse in more detail. Magnetic tweezers measurements could shed more light on the nanomechanical properties of DNA winding and unwinding in the presence

of anthracyclines. Such studies have been performed in the past for doxorubicin and daunorubicin[25,26], but larger structure-activity relationship studies with the different doxorubicin variants could greatly enhance our understanding. Recently, a very elegant method was reported to label nucleosomal DNA for nuclear magnetic resonance (NMR) spectroscopy studies. In this study, it was observed that aclarubicin binds the exposed AT-rich minor groove and, and that it is likely that the drug invades nucleosomes from the terminal ends inward, eventually resulting in histone eviction.[27] This method opens new opportunities to study the structural dynamics of nucleosomal DNA, and it may be possible to compare different anthracycline variants.

Resistance to anthracyclines presents a significant hurdle in cancer treatment and is often mediated by ATP-binding cassette (ABC) transporters that actively pump compounds across the plasma membrane, diminishing their efficacy. We previously demonstrated that the combination of DNA damage and histone eviction exerted by doxorubicin drives its associated adverse effects. However, whether the same properties dictate drug resistance is unclear.

In **chapter 4**, we evaluated a library of 40 anthracyclines on their cytotoxicity in cancer cell lines overexpressing the ABCB1 transporter or ABCG2 transporter. We identified several highly cytotoxic anthracyclines, that stand out due to their effectiveness in doxorubicin-resistant cells. We identified structural variants of the clinically used anthracyclines doxorubicin, epirubicin, daunorubicin, idarubicin and aclarubicin that outperform their respective partner compounds. We performed more in-depth analyses with these compounds, to identify how structural variations affect intracellular uptake, subcellular localization, DNA intercalation and Topo II inhibition in ABCB1-overexpressing, doxorubicin-resistant cells. Two of these anthracycline variants warrant further investigation: *N,N*-dimethyl-idarubicin and a related idarubicin variant composed of the idarubicin aglycon and the aclarubicin trisaccharide stand out, due to their histone eviction-mediated cytotoxicity toward doxorubicin-resistant cells.

This study focuses on the limitations of anthracyclines in clinical use — doxorubicin, daunorubicin, epirubicin and idarubicin — due to treatment-related toxicities and drug resistance. Previously we showed that doxorubicin and its analogues exert their anticancer effects through two independent mechanisms: inducing DNA double-strand breaks and causing chromatin damage via histone eviction. Notably, *N,N*-dimethyldoxorubicin, a compound that only induces histone eviction, showed reduced side effects compared to its clinical counterparts. We assessed a total of 40 anthracycline variants, of which their molecular mechanisms were determined in **chapter 2**, for their cytotoxicity in doxorubicin-resistant cells overexpressing ABCB1 or ABCG2. We showed that all anthracyclines that are currently in clinical use are less effective against ABCB1-

overexpressing cells, confirming their status as ABCB1 substrates. In contrast, a total of 16 of the novel anthracycline variants retained their cytotoxicity in drug- resistant cells, demonstrating potential for overcoming ABCB1 and ABCG2-mediated drug resistance. Anthracyclines featuring *N,N*-dimethyl amino sugars were shown to be less likely substrates for ABCB1, enhancing their therapeutic potential. This study highlights several promising structural variants, most notably *N,N*-dimethyl-idarubicin and *N,N*-dimethyl-idarubicin trisaccharide. The cytotoxicity of these anthracyclines is not compromised by the overexpression of drug transporters, and due to their histone-eviction mediated cytotoxic they may be less damaging than their traditional counterparts. These compounds not only bypass common resistance mechanisms but also exhibit enhanced nuclear accumulation, which correlates strongly with their efficacy.

Overall, we gained valuable insights into the design of new, safer anthracycline drugs and showed that specific structural modifications can enhance their effectiveness in drug resistant cells. Further exploration of the most promising compounds in preclinical studies is warranted. Future research should first confirm the anti-tumor efficacy of proposed *N,N*-dimethyl-idarubicin analogues in *in vivo* models. If their potency is as good as expected based on the *in vitro* results, it is of utmost importance to research if these compounds are also less cytotoxic to healthy cells and therefore may cause less side effects.

In conclusion, while anthracyclines remain cornerstone treatments in oncology due to their effectiveness, it is essential to address their associated toxicities and resistance mechanisms. Ongoing research should focus on minimizing adverse effects and improving the therapeutic use to enhance treatment outcomes and patients' quality of life.

Methods

Reagents and antibodies

Doxorubicin was obtained from Accord Healthcare Limited, UK, daunorubicin was obtained from Sanofi, aclarubicin (sc-200160) and doxorubicinone (sc-218273) were purchased from Santa Cruz Biotechnology (USA), etoposide was obtained from Pharmachemie (the Netherlands). *N,N*-dimethyl-doxorubicin, *N,N*-dimethyl daunorubicin, azido-doxorubicin, hydroxy-doxorubicin and desamino-doxorubicin were synthesized as described previously.[28]

Cell culture

AT-3 cells (provided by R. Arens, LUMC, The Netherlands), U2OS cells (ATCC, HTB-96) and H9c2 cells (provided by M. Goumans, LUMC, The Netherlands) were maintained in DMEM medium supplemented with 8% FCS. All cell lines were maintained in a humidified atmosphere of 5% CO_2 at 37 °C, regularly tested for the absence of mycoplasma and the origin of cell lines was validated using short tandem repeat (STR) analysis.

U2OS cells were endogenously GFP-tagged for TFAM, TFB2M and mtRNAP, as described previously. In short, gRNA sequences for each target protein were designed using the publicly available CRISPOR tool and subsequently cloned into the pX330/Cas9 vector. Making use of homologous recombination constructs with flanking HDRs as on the pX330 vector, both plasmids were used to co-transfect U2OS cells. Cells were single-cell FACS sorted and validated using confocal microscopy and western blot.

Flow cytometry

Cells were treated with 10 μM compound for 2 hours. Samples were washed with PBS, collected, and fixed with paraformaldehyde. Samples were analyzed by flow cytometry using BD FACS Aria II, with 561-nm laser and 610/20-nm detector. The cellular uptake of anthracyclines was quantified using FlowJo software.

Constant-Field Gel Electrophoresis (CFGE)

Cells were seeded into 12-well format (200.000 cells/well), treated with 5 μM of each compound or 200 μM of H_2O_2 for 2 hours. Subsequently, drugs were removed by extensive washing and cells were collected and processed immediately. DNA double strand breaks were quantified by constant-field gel electrophoresis as described.[29]

Long-range PCR for mitochondrial DNA damage

Cells were seeded in a 12-well plate (100.000 cells/well) and treated with 5 μM of the indicated compounds, or 100 μM H_2O_2 for 2 hours. Cells were subsequently washed and total DNA was isolated using the Isolate II Genomic DNA kit (Meridian Bioscience). Quantitative long-range PCR method was performed as described previously[30], to measure mitochondrial DNA damage. Primers used were described before, supplied by Integrated DNA Technologies: FW small (5'-CCCAGCTACTACCATCATTCAGT-3'); RV small (5'-GATGGTTTGGGAGATTGGTTGATGT-3'); FW large (5'-GCCAGCCTGACCCATAGCCATAATAT-3'); RV large (5'-GAGAGATTTTATGGGTGTAATGCGG-3'). PCR-fragments were run on agarose gels, stained with ethidium bromide, imaged using the Molecular Imager Gel Doc XR system (Bio-Rad). Images were analyzed using ImageStudio (v5.2) and relative amplification was quantified and normalized to controls.

DNA intercalation competition assay

Plasmid DNA of 17.8kb (100ng) was incubated with a concentration range indicated compounds to a final volume of 10 µL and incubated for 5 min at RT. Samples were run on a 0.8% agarose gel for 25 min on 100 V and subsequently stained using 0,5 µg/mL EtBr for 30 min followed by de-staining in ultra-pure water for 15 min. Gels were imaged with the Molecular Imager Gel Doc XR system (Bio-Rad).

RT-qPCR

U2OS or H9c2 cells were treated with 5 µM of each anthracycline or 100 µM H_2O_2 and 0,5 µg/mL EtBr for 2 hours. Subsequently, cells were washed and RNA was isolated 4 hour post treatment using the ISOLATE II RNA mini kit (Meridian Bioscience). For cDNA synthesis Transcriptor High Fidelity cDNA synthesis kit (Roche Life Science) was used. qPCR was performed with the SensiFAST SYBR No-ROX kit (Meridian Bioscience) and measured using the Bio-Rad CFX384 imager. Primers were designed and described before[31–34]. For analysis, Ct values were normalized against the expression of *GAPDH* and relative expression against the untreated control was quantified with the $2^{-\Delta\Delta CT}$ method.

Gene	Cell line	Primer Sequences
GAPDH	H9c2	FW: *CTCGTCTCATAGACAAGATGGT*
		RV: *GGGTAGAGTCATACTGGAACATG*
	U2OS	FW: *TACTAGCGGTTTTACGGGCG*
		RV: *TCGAACAGGAGGAGCAGAGAGCGA*
mt-ND1	H9c2	FW: *TCCTCCTAATAAGCGGCTCCTTCT*
		RV: *TGGTCCTGCGGCGTATTCG*
	U2OS	FW: *CCACCTCTAGCCTAGCCGTTTA*
		RV: *GGGTCATGATGGCAGGAGTAAT*
mt-CYB	H9c2	FW: *TACGCTATTCTACGCTCCATTC*
		RV: *GCCTCCGATTCATGTTAAGACTA*
	U2OS	FW: *ATCACTCGAGACGTAAATTATGGCT*
		RV: *TGAACTAGGTCTGTCCCAATGTATG*
mt-CO1	H9c2	FW: *GCCAGTATTAGCAGCAGGTATCA*
		RV: *GCCGAAGAATCAGAATAGGTGTTG*
	U2OS	FW: *GACGTAGACACACGAGCATATTTCA*
		RV: *AGGACATAGTGGAAGTGAGCTACAAC*

Western Blot

Cells were seeded (200.000 cells/well) and treated with 5 µM of each compound or 200 µM of H_2O_2 for 2 hours. For western blot, cells were washed with PBS and lysed in SDS-sample buffer (2%SDS, 10% glycerol, 5% β-mercaptoethanol, 60 mM Tris-HCl pH 6.8, and

0.01% bromophenol blue). Samples were separated by SDS-PAGE and transferred to a nitrocellulose membrane. Blocking of the filters and antibody incubations were done in PBS supplemented with 0.1% (v/v) Tween and 5% (w/v) milk powder (skim milk powder, LP0031, Oxiod). Blots were imaged by an Odyssey Classic imager (Li-Cor).

Histone eviction

For PAGFP-H2A photoactivation and time-lapse confocal imaging, U2OS-PAGFP-H2A cells were seeded in a 35 mm glass bottom petri dish (Poly-d-lysine-Coated, MatTek Corporation). Cells were treated with 10μM of the indicated compounds for 1 hour. For ATP-depletion cells were pre-incubated for 30 minutes with 0.01% NaAz and 10mM 2-deoxyglucose. Time-lapse confocal imaging was performed on a Leica SP8 confocal microscope system 63x lens, equipped with a climate chamber as described previously.

DNA Dye Competition Assay

1 μg/mL circular double-stranded DNA was incubated with Quant-iT PicoGreen dsDNA reagent (Thermo Fisher Scientific, P7581) or DAPI (Thermo Fisher Scientific, D1306) for 5 min at RT. Subsequently, indicated drug concentrations were added to the DNA/dye mixture and incubated for another 5 min at RT followed by measurement of fluorescence using a CLARIOstar plate reader (BMG Labtech) excitation 480 nm / emission 520 nm (480-20/520-10 filter) Picogreen, excitation 350nm / emission 465 nm (350-20/465-10 filter). Fluorescence was quantified relative to that of the untreated controls. Fluorescent signals of all samples were corrected for the corresponding drug concentrations in the absence of DNA.

Nucleosome assembly and collapse

Mono nucleosomes were assembled from recombinant human histones expressed in *E. coli* (two each of histones H2A, H2B, H3 and H4. Accession numbers: H2A-P04908; H2B-O60814; H3.1-P68431; H4-P62805) wrapped by provided 217 base pair DNA sequence that includes the Widom 601 sequence with an added GATC (EpiCypher, 16-1410). Mono nucleosomes were incubated with indicated compounds for 5 minutes at RT. Nucleosomes were subsequently resolved on a 8% native poly-acrylamide gel and stained with ethidium bromide. Gels were imaged with the Molecular Imager Gel Doc XR system (Bio-Rad).

References

(1) Brockmann, H. Anthracyclinones and Anthracyclines. (Rhodomycinone, Pyrromycinone and Their Glycosides). *Fortschritte der Chemie organischer Naturstoffe,* **1963,** *21*, *121-182*.

(2) van der Zanden, S. Y.; Qiao, X.; Neefjes, J. New Insights into the Activities and Toxicities of the Old Anticancer Drug Doxorubicin. *FEBS Journal*. **2021**, *288*, 6095–6111.

(3) Mattioli, R.; Ilari, A.; Colotti, B.; Mosca, L.; Fazi, F.; Colotti, G. Doxorubicin and Other Anthracyclines in Cancers: Activity, Chemoresistance and Its Overcoming. *Molecular Aspects of Medicine*. **2023**, *93*, 101205.

(4) Qiao, X.; Van Der Zanden, S. Y.; Wander, D. P. A.; Borràs, D. M.; Song, J. Y.; Li, X.; Duikeren, S. Van; Gils, N. Van; Rutten, A.; Herwaarden, T. Van; Tellingen, O. Van; Giacomelli, E.; Bellin, M.; Orlova, V.; Tertoolen, L. G. J.; Gerhardt, S.; Akkermans, J. J.; Bakker, J. M.; Zuur, C. L.; Pang, B.; Smits, A. M.; Mummery, C. L.; Smit, L.; Arens, R.; Li, J.; Overkleeft, H. S.; Neefj, J. Uncoupling DNA Damage from Chromatin Damage to Detoxify Doxorubicin. *Proceedings of the National Academy of Sciences of the United States of America*. **2020**, *117*, 15182–15192.

(5) Mortensen, S. A. Aclarubicin: Preclinical and Clinical Data Suggesting Less Chronic Cardiotoxicity Compared with Conventional Anthracyclines. *European Journal of Haematology*. **1987**, *38*, 21–31.

(6) Rothig, H. J.; Kraemer, H. P.; Sedlacek, H. H. Aclarubicin: Experimental and Clinical Experience. *Drugs under experimental and clinical research*. **1985**, *11*, 123–125.

(7) Huang, K. M.; Hu, S.; Sparreboom, A. Drug Transporters and Anthracycline-Induced Cardiotoxicity. *Pharmacogenomics*. **2018**, *19*, 883–888.

(8) Yakes, F. M.; Van Houten, B. Mitochondrial DNA Damage Is More Extensive and Persists Longer than Nuclear DNA Damage in Human Cells Following Oxidative Stress. *Proceedings of the National Academy of Sciences of the United States of America*. **1997**, *94*, 514–519.

(9) Abe, K.; Ikeda, M.; Ide, T.; Tadokoro, T.; Miyamoto, H. D.; Furusawa, S.; Tsutsui, Y.; Miyake, R.; Ishimaru, K.; Watanabe, M.; Matsushima, S.; Koumura, T.; Yamada, K. I.; Imai, H.; Tsutsui, H. Doxorubicin Causes Ferroptosis and Cardiotoxicity by Intercalating into Mitochondrial DNA and Disrupting Alas1-Dependent Heme Synthesis. *Science Signaling*. **2022**, *15*.

(10) Yin, J.; Guo, J.; Zhang, Q.; Cui, L.; Zhang, L.; Zhang, T.; Zhao, J.; Li, J.; Middleton, A.; Carmichael, P. L.; Peng, S. Doxorubicin-Induced Mitophagy and Mitochondrial Damage Is Associated with Dysregulation of the PINK1/Parkin Pathway. *Toxicology in Vitro*. **2018**, *51*, 1–10.

(11) Termini, J. Hydroperoxide-Induced DNA Damage and Mutations. *Mutation research*. **2000**, *450*, 107–124.

(12) Santos, J. H.; Meyer, J. N.; Mandavilli, B. S.; Van Houten, B. Quantitative PCR-Based Measurement of Nuclear and Mitochondrial DNA Damage and Repair in Mammalian Cells. *Methods in molecular biology (Clifton, N.J.)*. **2006**, *314*, 183–199.

(13) Yang, F.; Kemp, C. J.; Henikoff, S. Anthracyclines Induce Double-Strand DNA Breaks at Active Gene Promoters. *Mutation research*. **2015**, *773*, 9.

(14) Anderson, S.; Bankier, A. T.; Barrell, B. G.; De Bruijn, M. H. L.; Coulson, A. R.; Drouin, J.; Eperon, I. C.; Nierlich, D. P.; Roe, B. A.; Sanger, F.; Schreier, P. H.; Smith, A. J. H.; Staden, R.; Young, I. G. Sequence and Organization of the Human Mitochondrial Genome. *Nature*. **1981**, *290*, 457–465.

(15) Wu, B. Bin; Leung, K. T.; Poon, E. N. Y. Mitochondrial-Targeted Therapy for Doxorubicin-Induced Cardiotoxicity. *International Journal of Molecular Sciences*. **2022**, *23*, 1912.

(16) Pang, B.; de Jong, J.; Qiao, X.; Wessels, L. F. A.; Neefjes, J. Chemical Profiling of the Genome with Anti-Cancer Drugs Defines Target Specificities. *Nature chemical biology*. **2015**, *11*, 472–480.
(17) Taanman, J. W. The Mitochondrial Genome: Structure, Transcription, Translation and Replication. *Biochimica et biophysica acta*. **1999**, *1410*, 103–123.
(18) Chaires, J. B.; Fox, K. R.; Herrera, J. E.; Britt, M.; Waring, M. J. Site and Sequence Specificity of the Daunomycin-DNA Interaction. *Biochemistry*. **1987**, *26*, 8227–8236.
(19) Neefjes, J.; Gurova, K.; Sarthy, J.; Szabó, G.; Henikoff, S. Chromatin as an Old and New Anti-Cancer Target. *Trends in cancer*. **2024**, *10*, 696.
(20) Gasparian, A. V.; Burkhart, C. A.; Purmal, A. A.; Brodsky, L.; Pal, M.; Saranadasa, M.; Bosykh, D. A.; Commane, M.; Guryanova, O. A.; Pal, S.; Safina, A.; Sviridov, S.; Koman, I. E.; Veith, J.; Komar, A. A.; Gudkov, A. V.; Gurova, K. V. Curaxins: Anticancer Compounds That Simultaneously Suppress NF-KB and Activate P53 by Targeting FACT. *Science Translational Medicine*. **2011**, *3*.
(21) Nesher, E.; Safina, A.; Aljahdali, I.; Portwood, S.; Wang, E. S.; Koman, I.; Wang, J.; Gurova, K. V. Role of Chromatin Damage and Chromatin Trapping of FACT in Mediating the Anticancer Cytotoxicity of DNA-Binding Small-Molecule Drugs. *Cancer research*. **2018**, *78*, 1431–1443.
(22) Juárez-Salcedo, L. M.; Desai, V.; Dalia, S. Venetoclax: Evidence to Date and Clinical Potential. *Drugs in Context*. **2019**, *8*, 212574.
(23) Clapier, C. R.; Iwasa, J.; Cairns, B. R.; Peterson, C. L. Mechanisms of Action and Regulation of ATP-Dependent Chromatin-Remodelling Complexes. *Nature reviews. Molecular cell biology*. **2017**, *18*, 407.
(24) Frederick, C. A.; Williams, L. D.; Ughetto, G.; van der Marel, G. A.; van Boom, H. J.; Rich, A.; Wang, A. H. J. Structural Comparison of Anticancer Drug-DNA Complexes: Adriamycin and Daunomycin. *Biochemistry*. **1990**, *29*, 2538–2549.
(25) Liu, T.; Cai, T.; Huo, J.; Liu, H.; Li, A.; Yin, M.; Mei, Y.; Zhou, Y.; Fan, S.; Lu, Y.; Wan, L.; You, H.; Cai, X. Force-Enhanced Sensitive and Specific Detection of DNA-Intercalative Agents Directly from Microorganisms at Single-Molecule Level. *Nucleic Acids Research*. **2024**, *52*, e86–e86.
(26) Salerno, D.; Brogioli, D.; Cassina, V.; Turchi, D.; Beretta, G. L.; Seruggia, D.; Ziano, R.; Zunino, F.; Mantegazza, F. Magnetic Tweezers Measurements of the Nanomechanical Properties of DNA in the Presence of Drugs. *Nucleic Acids Research*. **2010**, *38*, 7089.
(27) van Emmerik, C. L.; Lobbia, V.; Neefjes, J.; Nelissen, F. H. T.; van Ingen, H. Monitoring Anthracycline Cancer Drug-Nucleosome Interaction by NMR Using a Specific Isotope Labeling Approach for Nucleosomal DNA. *ChemBioChem*. **2024**, *25*, e202400111.
(28) van Gelder, M. A.; van der Zanden, S. Y.; Vriends, M. B. L.; Wagensveld, R. A.; van der Marel, G. A.; Codée, J. D. C.; Overkleeft, H. S.; Wander, D. P. A.; Neefjes, J. J. C. Re-Exploring the Anthracycline Chemical Space for Better Anti-Cancer Compounds. *Journal of Medicinal Chemistry*. **2023**, *66*, 11390–11398.
(29) Wlodek, D.; Banáth, J.; Olive, P. L. Comparison between Pulsed-Field and Constant-Field Gel Electrophoresis for Measurement of DNA Double-Strand Breaks in Irradiated Chinese Hamster Ovary Cells. *International journal of radiation biology*. **1991**, *60*, 779–790.
(30) Furda, A. M.; Bess, A. S.; Meyer, J. N.; Van Houten, B. Analysis of DNA Damage and Repair in Nuclear and Mitochondrial DNA of Animal Cells Using Quantitative PCR. *Methods in molecular biology (Clifton, N.J.)*. **2012**, *920*, 111.
(31) Lei, Y.; Vanportfliet, J. J.; Chen, Y.-F.; Upton, J. W.; Li, P.; Phillip, A.; Correspondence, W.; Bryant, J. D.; Li, Y.; Fails, D.; Torres-Odio, S.; Ragan, K. B.; Deng, J.; Mohan, A.; Wang, B.; Brahms, O. N.; Yates, S. D.; Spencer, M.; Tong, C. W.; Bosenberg, M. W.; West, L. C.; Shadel, G. S.; Shutt, T. E.; West, A. P.

Cooperative Sensing of Mitochondrial DNA by ZBP1 and CGAS Promotes Cardiotoxicity. *Cell*. **2023**, *186*, 3013-3032.e22.

(32) Ferreira, A.; Cunha-Oliveira, T.; Simões, R. F.; Carvalho, F. S.; Burgeiro, A.; Nordgren, K.; Wallace, K. B.; Oliveira, P. J. Altered Mitochondrial Epigenetics Associated with Subchronic Doxorubicin Cardiotoxicity. *Toxicology*. **2017**, *390*, 63–73.

(33) Guan, G.; Yang, L.; Huang, W.; Zhang, J.; Zhang, P.; Yu, H.; Liu, S.; Gu, X. Mechanism of Interactions between Endoplasmic Reticulum Stress and Autophagy in Hypoxia/Reoxygenation-Induced Injury of H9c2 Cardiomyocytes. *Molecular Medicine Reports*. **2019**, *20*, 350.

(34) Wallace, L. S.; Mehrabi, S.; Bacanamwo, M.; Yao, X.; Aikhionbare, F. O. Expression of Mitochondrial Genes MT-ND1, MT-ND6, MT-CYB, MT-COI, MT-ATP6, and 12S/MT-RNR1 in Colorectal Adenopolyps. *Tumour biology : the journal of the International Society for Oncodevelopmental Biology and Medicine*. **2016**, *37*, 12465.

Supporting Information chapter 5

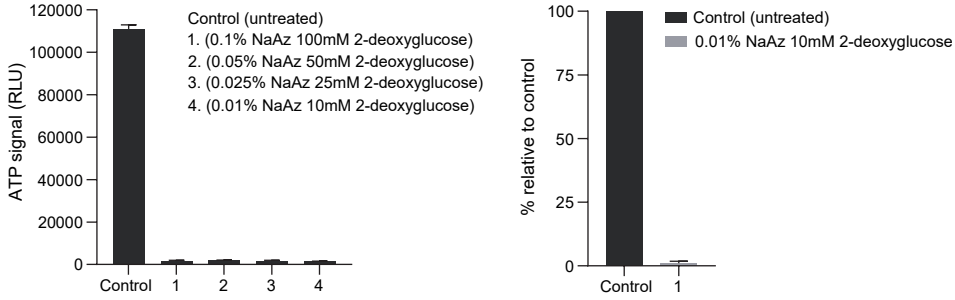

Figure S1 – ATP depletion validation for different conditions in U2OS cells. Total ATP levels were measured in U2OS cells in response to different concentrations of sodium azide and 2-deoxyglucose.

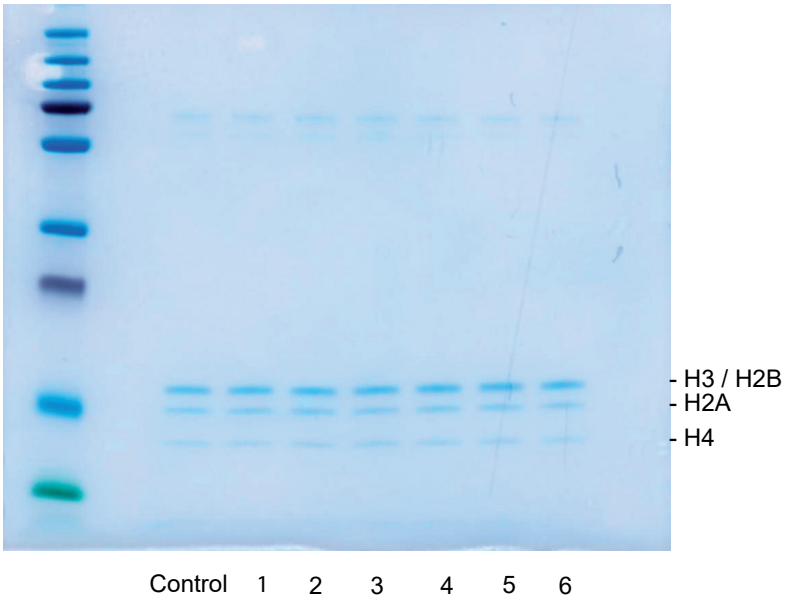

Figure S2 – Coomassie staining of mono nucleosomes. Total protein levels are shown for all treatments compared to untreated control.

Appendices

Nederlandse samenvatting
List of publications
Curriculum Vitae
Acknowledgements

Nederlandse samenvatting

Anthracyclines vormen een belangrijke klasse van chemotherapeutica en behoren tot de meest effectieve antikankermiddelen. Daunorubicine, dat voor het eerst in 1960 werd ontdekt, en doxorubicine zijn de meest prominente voorbeelden binnen deze klasse van medicijnen. Daunorubicine is vooral effectief voor de behandeling van leukemieën, terwijl doxorubicine daarentegen een bredere werkzaamheid heeft en ook wordt ingezet voor de behandeling van lymfomen, sarcomen en verschillende soorten solide tumoren. Ondanks dat deze medicijnen decennia geleden ontdekt zijn vormen ze nog steeds de basis van moderne oncologie en zijn ze essentieel voor de behandeling van verschillende kankersoorten.

De archetypische anthracyclines, zoals doxorubicine en daunorubicine, bestaan uit een tetracyclisch anthraquinone aglycon dat via een glycosidebinding is gekoppeld aan een suikergroep. De effectiviteit van de klassieke anthracyclines is zo opmerkelijk, dat er duizenden analogen zijn ontwikkeld in de hoop om vergelijkbare antikanker medicijnen te ontdekken. Tot op heden zijn er echter slechts zes anthracycline varianten die in de dagelijkse praktijk worden gebruikt. De moleculaire mechanismen waarmee anthracyclines hun anti-kankeractiviteit uitoefenen, zijn zeer complex en omvatten onder andere DNA-intercalatie, het veroorzaken van DNA-schade, de disruptie van chromatine structuren en het verstoren van de mitochondriale functie. Deze verschillende moleculaire mechanismen leiden uiteindelijk tot tumorcel dood.

Ondanks dat deze medicijnen heel effectief zijn hebben de anthracyclines zeer ernstige bijwerkingen, variërend van acute en reversibele problemen zoals misselijkheid en haaruitval tot langdurige complicaties zoals cardiotoxiciteit, vruchtbaarheidsproblemen en de ontwikkeling van secundaire tumoren. Deze bijwerkingen hebben niet alleen impact op het verloop van de behandeling van de patiënt, maar ook op hun kwaliteit van leven. Het is een uitdaging om deze bijwerkingen te voorspellen, aangezien ze afhankelijk zijn van meerdere factoren, zoals de dosis chemotherapie, het aantal behandelingscycli en individuele risicofactoren. Er zijn ontelbare pogingen gedaan om de toxiciteit van anthracyclines te verminderen, maar deze inspanningen hebben nog niet geleid tot effectieve en breed toepasbare oplossingen in de oncologie.

Een ander belangrijk probleem bij de behandeling met anthracyclines is de ontwikkeling van resistentie, wat een belangrijke hindernis vormt voor succesvolle chemotherapie. Deze resistentie wordt in het geval van anthracyclines vaak gemedieerd door een klasse membraan transporters, die zeer effectief medicijnen uit tumorcellen pompen waardoor de intracellulaire concentraties van de geneesmiddelen afnemen en de effectiviteit vermindert. Onderzoek naar nieuwe anthracycline-varianten die deze vorm van

resistentie kunnen omzeilen, is van cruciaal belang om de chemotherapie behandeling voor patiënten te verbeteren.

Dit proefschrift richt zich op de synthese en biologische evaluatie van structurele variaties van de klassieke anthracyclines. Het doel is om een beter begrip te krijgen van de structuur-activiteit relaties van deze verbindingen, zodat nieuwe varianten kunnen worden geïdentificeerd die minder bijwerkingen veroorzaken en de moleculaire mechanismen die bijdragen aan resistentie kunnen omzeilen. In **hoofdstuk 2** zijn de moleculaire mechanismen van een groot aantal verschillende anthracycline varianten in detail onderzocht. Deze informatie geeft aanknopingspunten om de zeer ernstige bijwerkingen van anthracycline behandeling te verminderen in de toekomst. Het is nog onbekend hoe sommige van deze moleculaire mechanismen leiden tot celdood. In **hoofdstuk 3** is onderzocht hoe specifiek de disruptie van chromatine structuren kan leiden tot tumorcel dood na behandeling met de anthracycline aclarubicine. In de zoektocht naar nieuwe effectieve anthracyclines is in **hoofdstuk 4** gekeken naar de manier waarop resistentie optreedt tegen verschillende varianten. De verschillende eigenschappen van anthracyclines zijn in detail verder onderzocht in **hoofdstuk 5** en op basis van deze resultaten zijn aanbevelingen geformuleerd die de huidige limitaties van anthracyclines adresseren.

Samengevat kunnen de resultaten beschreven in dit proefschrift bijdragen aan de ontwikkeling van effectievere anthracyclines die minder bijwerkingen veroorzaken voor patiënten, wat van groot belang is voor de toekomst van de behandeling van kanker.

List of publications

Re-Exploring the Anthracycline Chemical Space for Better Anti-Cancer Compounds
M.A. van Gelder*, S.Y. van der Zanden*, M.B.L. Vriends, R.A. Wagensveld, G.A. van der Marel, J.D.C. Codée, H.S. Overkleeft, D.P.A. Wander & J. J.C. Neefjes. *Journal of Medicinal Chemistry***, 2023,** *66.*

Novel *N,N*-Dimethyl-idarubicin Analogues Are Effective Cytotoxic Agents for ABCB1-Overexpressing, Doxorubicin-Resistant Cells
M.A. van Gelder, Y. Li, D.P.A. Wander, I. Berlin, H.S. Overkleeft, S.Y. van der Zanden & J.J.C. Neefjes. *Journal of Medicinal Chemistry,* **2024,** *67*.

Diversifying the anthracycline class of anti-cancer drugs identifies aclarubicin for superior survival of acute myeloid leukemia patients
X. Qiao, S.Y. van der Zanden, X. Li, M. Tan, Y. Zhang, J.Y. Song, M.A. van Gelder, F.L. Hamoen, L. Janssen, C.L. Zuur, B. Pang, O. van Tellingen, J. Li, J.J.C. Neefjes. *Molecular Cancer*, **2024**, 23.

Curriculum Vitae

Merle van Gelder completed both her Bachelor's in Neurobiology (2015) and her Master's in Biomedical Sciences (2017) at the University of Amsterdam. In 2020, she started her PhD project in the research group of Sjaak Neefjes at Leiden University Medical Center (LUMC), focusing on anthracycline biology. In 2024, she transitioned from academia to apply her enthusiasm and expertise at a non-profit research foundation.

Acknowledgements

I would like to express my gratitude to everyone who supported and guided me throughout this project.

"The more one does and sees and feels, the more one is able to do,
and the more genuine may be one's appreciation of fundamental things like
home, and love, and understanding companionship."

– Amelia Earhart